

PAST AND CURRENT MANGROVE
DYNAMICS ON THE BRAGANÇA
PENINSULA, NORTHERN BRAZIL

Dissertation zur Erlangung des Doktorgrades

Marcelo Cancela Lisboa Cohen

angefertigt am
Zentrum für Marine Tropenökologie
innerhalb des Fachbereichs 2
der Universität Bremen

2003

Erster Gutachter: PD. Dr. Hermann Behling, ZMT an der Universität Bremen
Zweiter Gutachter: Prof. Dr. Ulrich Saint-Paul, ZMT an der Universität Bremen

Acknowledgement

Special appreciation is expressed to PD Dr. Hermann Behling for supervising my thesis and to Prof. Dr. Ulrich Saint-Paul for offering excellent conditions in his working group at the Zentrum für Marine Tropenökologie (ZMT) in Bremen (Germany).

I am pleasure to acknowledge the support by PD Dr. Rubén Lara. He provided scientific assistance throughout the whole course of this work.

I like to appreciate the assistance of Dipl. Ing. Andreas Hanning during the field work and the technical maintenance of the electronic equipment in Brazil.

I also thank the members of the Center for Tropical Marine Ecology and Núcleo de Estudos Costeiros for the nice working atmosphere.

This study was carried out as a part of the Brazilian-German Cooperation Project MADAM and was financed by the Brazilian National Research Council (CNPq) and the German Ministry for Education and Research (BMBF) under the code 03F0154A. I thank the Deutscher Akademischer Austausch-Dienst (DAAD) for the scholarship support.

Contents

| | |
|------------------|------|
| Acknowledgements | i |
| List of Figures | vi |
| List of Tables | viii |
| Summary | |
| Zusammenfassung | xi |
| Resumo | |

Chapter 1

| | |
|--|-----------|
| ARE THE MANGROVES FROM BRAGANÇA PENINSULA REACTING TO THE RELATIVE SEA-LEVEL CHANGES? | 1 |
| 1.1 Introduction | 2 |
| 1.2 Objectives | 3 |
| 1.3 The Bragança Peninsula | 3 |
| 1.3.1 Location | 3 |
| 1.3.2 Geology and geomorphology | 3 |
| 1.3.3 Hydrology | 4 |
| 1.3.4 Climate | 5 |
| 1.3.5 Vegetation | 5 |
| 1.4 Methodology | 5 |
| 1.4.1 Image processing | 5 |
| 1.4.2 Elaboration of an Elevation Surface Model | 5 |
| 1.4.3 Vegetation survey | 6 |
| 1.4.4 Physicochemical parameters | 6 |
| 1.4.5 Sediment cores | 7 |
| 1.4.6 Radiocarbon data | 7 |
| 1.4.7 Pollen analysis | 7 |
| 1.5 Results | 7 |
| 1.5.1 The inundation frequency controlling the vegetation distribution on the Bragança Peninsula | 7 |
| 1.5.2 Vegetation changes in the central peninsula | 8 |
| 1.5.3 Coastline vegetation changes | 9 |
| 1.5.4 Stratigraphy and radiocarbon data from the Bragança Peninsula | 9 |
| 1.5.4.1 Estuarine mud progradational sequence (S2) | 9 |
| 1.5.5 Model of Bragança mangrove development | 10 |
| 1.5.6 RSL changes at the Bragança Peninsula between 5100 and 1000 yr BP | 11 |
| 1.5.7 RSL changes at the Bragança Peninsula during the last 1000 yr BP | 12 |
| 1.6 Conclusions | 12 |

Chapter 2

| | |
|--|-----------|
| DIGITAL ELEVATION MODEL APPLIED TO MANGROVE COAST ANALYSIS, AMAZON REGION, BRAZIL | 14 |
| Abstract | 15 |
| 2.1 Introduction | 15 |
| 2.2 Methodological considerations | 16 |

| | |
|--|-----------|
| 2.2.1 Study area | 16 |
| 2.2.2 Tidal level measures | 16 |
| 2.2.3 Topographic survey | 16 |
| 2.2.4 Elaboration of an Elevation Surface Model | 17 |
| 2.3 Results and discussion | 19 |
| 2.3.1 Tidal inundation in the “Furo do Chato” area | 19 |
| 2.3.2 Tidal inundation on the Bragança Peninsula | 20 |
| 2.4 Conclusions | 22 |

Chapter 3

| | |
|---|-----------|
| MANGROVE INUNDATION AND NUTRIENT DYNAMICS FROM A GIS PERSPECTIVE | 23 |
| Abstract | 24 |
| 3.1 Introduction | 24 |
| 3.2 Study area | 26 |
| 3.3 Material and methods | 26 |
| 3.3.1 Chemical and physicochemical parameters | 26 |
| 3.3.2 Elaboration of Surface Elevation Model | 27 |
| 3.4 Results and discussion | 28 |

Chapter 4

| | |
|---|-----------|
| TEMPORAL CHANGES OF MANGROVE VEGETATION BOUNDARIES IN AMAZÔNIA: APPLICATION OF GIS AND REMOTE SENSING TECHNIQUES | 31 |
| Abstract | 32 |
| 4.1 Introduction | 32 |
| 4.2 Material and methods | 34 |
| 4.2.1 Study area | 34 |
| 4.2.2 Field work | 34 |
| 4.2.3 Image processing | 35 |
| 4.3 Results and discussion | 35 |
| 4.3.1 Geobotanical units | 35 |
| 4.3.2 Coastline vegetation changes | 36 |
| 4.3.3 Vegetation changes in the central peninsula | 40 |
| 4.4 Conclusions | 43 |

Chapter 5

| | |
|---|-----------|
| STUDIES ON HOLOCENE MANGROVE ECOSYSTEM DYNAMICS OF THE BRAGANÇA PENINSULA IN NORTHEASTERN PARA, BRAZIL | 45 |
| Abstract | 46 |
| 5.1 Introduction | 46 |
| 5.2 Study area | 47 |
| 5.2.1 Location | 47 |
| 5.2.2. Environmental characteristics of the Bragança Peninsula | 48 |
| 5.2.3 Human impact on vegetation | 49 |

| | |
|---|-----------|
| 5.2.4 Study sites | 49 |
| 5.3 Material and methods | 50 |
| 5.3.1 Field sampling | 50 |
| 5.3.2 Pollen analysis | 50 |
| 5.4 Results | 51 |
| 5.4.1 Stratigraphy | 51 |
| 5.4.2 Radiocarbon dates and sedimentation rates | 51 |
| 5.4.3 Description of modern pollen rain | 51 |
| 5.4.4. Description of fossil pollen results | 55 |
| 5.4.4.1. Bosque de <i>Avicennia</i> | 55 |
| 5.4.4.2 Campo Salgado | 56 |
| 5.4.4.3 Furo do Chato | 60 |
| 5.5 Interpretation and discussion | 60 |
| 5.5.1 General background on Brazilian sea-level changes | 60 |
| 5.5.2 Holocene relative sea-level and the development of the mangrove ecosystem | 61 |
| 5.6 Holocene mangrove dynamics | 64 |
| 5.7 Conclusions | 65 |

Chapter 6

MODEL ON HOLOCENE MANGROVE DEVELOPMENT AND RELATIVE SEA-LEVEL CHANGES ON BRAGANÇA PENINSULA (NORTH BRAZIL) __ 67

| | |
|---|-----------|
| Abstract | 68 |
| 6.1 Introduction | 68 |
| 6.2 Study area | 69 |
| 6.3 Data sources | 69 |
| 6.3.1 Topographic survey | 69 |
| 6.3.2 Sediment cores | 69 |
| 6.3.3 Pollen analysis | 69 |
| 6.3.4 Radiocarbon data | 70 |
| 6.3.5 Modern vegetation | 70 |
| 6.3.6 Stratigraphy | 72 |
| 6.4 Results | 72 |
| 6.4.1 Modern vegetation units | 72 |
| 6.4.2 Stratigraphy and radiocarbon data from the Bragança Peninsula. | 72 |
| 6.4.2.1 Estuarine mud progradational sequence (S2) | 72 |
| 6.4.3 Model of Bragança mangrove development | 74 |
| 6.7 Discussions | 78 |
| 6.7.1 Sea-level indicated by mangrove sediments | 78 |
| 6.7.2 RSL changes from Bragança compared with data from the eastern Brazilian coast | 80 |
| 6.8 Conclusions | 82 |

Chapter 7

LATE HOLOCENE MANGROVE DYNAMICS ON THE BRAGANÇA PENINSULA (NORTHERN BRAZIL): THE RELATIVE SEA-LEVEL AND THE LITTLE ICE AGE _____ 83

| | |
|-------------------------|-----------|
| Abstract | 84 |
| 7.1 Introduction | 84 |
| 7.2 Study area | 86 |

| | |
|---|------------|
| 7.3 Methods | 86 |
| 7.3.1 Sampling and sample processing | 86 |
| 7.3.2 Radiocarbon dating | 87 |
| 7.4 Results | 89 |
| 7.4.1 Stratigraphy | 89 |
| 7.4.2 Radiocarbon age and sedimentation rates | 89 |
| 7.4.3 Pollen data | 89 |
| 7.5 Interpretation and discussion | 91 |
| 7.5.1 Climate change/Relative sea-level relation | 91 |
| 7.5.2 Relative sea-level changes at the Bragança Peninsula during the Little Ice Age chronozone | 96 |
| 7.5.3 Climate change during the last 1000 years | 97 |
| 7.6 Conclusion | 98 |
| References | 100 |

List of Figures

Chapter 1

| | |
|---|---|
| Figure 1.1 Location of the Brazilian mangrove belt. _____ | 4 |
|---|---|

Chapter 2

| | |
|------------------------------|----|
| Figure 2.1 Study area. _____ | 17 |
|------------------------------|----|

| | |
|--|----|
| Figure 2.2 Device for measuring maximal tide elevation and scheme showing their utilization. _____ | 17 |
|--|----|

| | |
|--|----|
| Figure 2.3 Combination of a) site topography with contour levels spaced at 0.5 m intervals between 0 m and 6 m relative to the bottom of the creek at the sampling site, and b) digital elevation model with percentage of the total area flooded at different high-tide levels. Low-tide phosphate concentrations corresponding to the days with high-tide levels included in each level interval were accordingly averaged for each subgroup. Inundation frequencies are calculated as the number of days in a year in which water height at high tide reached the topographic contour levels. _____ | 19 |
|--|----|

| | |
|---|----|
| Figure 2.4 Relationship between high-tide level and flooded area during one year. _____ | 20 |
|---|----|

| | |
|---|----|
| Figure 2.5 Thematic composition involving: a) satellite image with the three main morphological units; b) contour level map and c) three-dimensional relief of the Bragança Peninsula with a vertical increment of x 1000. The zero level is referred to the bottom of the tidal creek “Furo do Chato”. _____ | 21 |
|---|----|

Chapter 3

| | |
|--|----|
| Figure 3.1 Location of the study site. _____ | 26 |
|--|----|

Chapter 4

| | |
|---|----|
| Figure 4.1 Location of the study area (1a) and progression of the mangrove front (1b). ____ | 34 |
|---|----|

| | |
|--|----|
| Figure 4.2 Topographic profile of the Bragança peninsula related to mean sea-level (M.S.L.) with the vegetation units, porewater salinities (dry season) and mangrove vegetation height (2a). Temporal analysis between a RADAR (2b) and satellite images (2c) takes on 1972 and 1997, respectively. _____ | 38 |
|--|----|

| | |
|---|----|
| Figure 4.3 Evolution of coastal vegetation according to the analysis of RADAR and satellite images covering an 25-year period (1972-1997). Figures 3a, 3b, 3c, 3d and 3e: aerial photographs of the inner and outer mangrove. _____ | 39 |
|---|----|

Chapter 5

| | |
|--|----|
| Figure 5.1 Percentage summary pollen diagram showing vegetation groups, and selected accumulation rates of pollen at the five pollen trap sites: Bosque de Rhizophora/Avicennia BDR/A-(No, 1-3), Bosque de Avicennia-BDA-(No, 4-6), Campo Salgado-CS-(No, 7-10), Furo do Chato-FDC-(No, 11-12), and Restinga (No. 13-16). The average pollen accumulation rates for each vegetation type are also shown. _____ | 54 |
|--|----|

| | |
|--|----|
| Figure 5.2 Percentage summary pollen diagram of vegetation groups, percentages of the most frequent pollen taxa, total pollen sum, other taxa, concentration and accumulation rates of pollen and CONISS cluster analyses of the Bosque de Avicennia core. _____ | 57 |
|--|----|

| | |
|--|----|
| Figure 5.3 Percentage summary pollen diagram of vegetation groups, percentages of the most frequent pollen taxa, total pollen sum, other taxa, concentration and accumulation rates of Campo Salgado core. _____ | 58 |
|--|----|

| | |
|---|----|
| Figure 5.4 Percentage summary pollen diagram of vegetation groups, percentages of the most frequent pollen taxa, total pollen sum, other taxa, concentration and accumulation rates of pollen and CONISS cluster analyses of the Furo do Chato core. ____ | 59 |
|---|----|

| | |
|--|----|
| Figure 5.5 Pollen concentration and accumulation rates of Rhizophora and Avicennia from the core Bosque de Avicennia, including Rhizophora/Avicennia-ratios. _____ | 62 |
|--|----|

Chapter 6

- Figure 6.1 Location of the collected cores and the Bragança Peninsula with topographic levels. _____ 71
- Figure 6.2 Collected cores and stratigraphic profile of the Bragança Peninsula after Souza Filho (1995). _____ 75
- Figure 6.3 Mangrove development of the Bragança Peninsula. _____ 77
- Figure 6.4 Comparison between Holocene RSL curves from northeast to south Brazil. _____ 81

Chapter 7

- Figure 7.1 Topographic map from Bragança Peninsula with the sediment core position and vegetation unit. _____ 88
- Figure 7.2 Pollen records (M1 to M9) from the Bragança Peninsula. _____ 92
- Figure 7.3 Integration of stratigraphy and pollen profile. The sediment cores are named as M1 to M9 and CS. The sediment layers are C1 to C8. _____ 93
- Figure 7.4 Composition of pollen profile from study site. _____ 94
- Figure 7.5 Comparative diagram between some LIA records, and the hydrologic and paleovegetation characteristics from Bragança peninsula over the last 1000 years BP. _____ 99

List of Tables

Chapter 4

Table 4.1 Data of vegetation change in the Bragança coastline. _____ 41

Table 4.2 Data of vegetation change in the inner Bragança Peninsula. _____ 41

Chapter 5

Table 5.1 Stratigraphy from the cores Bosque de Avicennia, Campo Salgado and Furo do Chato. _____ 52

Table 5.2 List of AMS radiocarbon dates for Bosque de Avicennia, Campo Salgado and Furo do Chato. 53

Chapter 6

Table 6.1 Modern vegetation units on the Bragança Peninsula. _____ 73

Chapter 7

Table 7.1 Topographic distribution of vegetation units on the Bragança Peninsula. _____ 88

Table 7.2 AMS-Radiocarbon dates and the topographic position of the samples. _____ 90

Summary

A wide mangrove belt of about 350 km occurs along the coast between the Amazon estuary and the Gurupi River. Mangroves are of ecological relevance for their biodiversity, productivity and have a key role of material fluxes in tropical coastal regions. Furthermore, they can react with sensitivity on environmental changes in the land-ocean transition zone. Therefore, mangroves are reliable indicators and registers of present and past environmental changes. Relevant examples are changes in tidal and rain regime, inundation frequency and soil salinity.

The study of mangrove reactions to these main driving forces is important for the understanding of the past and current geobotanic framework in the North Brazilian coastal region and for the prediction of its future evolution. In this context, the main objective of this work was to identify and analyze the present effect of inundation frequency on system structure and of past changes in relative sea-level and climate, using tools such as palynology, radiocarbon dating, remote sensing and the Geographic Information Systems (GIS).

The combination of topography and tidal regime data allowed, together with GIS tools, to determine frequencies and the extent of flooded areas. This allowed the association between the topographical characteristics of the peninsula and the main vegetation types. The current mangrove dynamics, specially gain and lost of vegetation coverage at the coastline, suggest a relative sea-level (RSL) rise. The topography-dependent dynamics of this process strongly suggests an increase in inundation frequency, changes in soil salinity and the transportation of mangrove diaspores into more elevated areas.

The mangrove sediments from northern Brazil were used with success as palaeo sea-level indicator. The examined sediment cores from Bragança recorded at least two transgressive events, which defined the spatial distribution of the mangroves on that area during the Holocene.

The study area was flooded by a rapidly rising sea-level during the postglacial. The stabilization of sea-level near modern level was found around 5100 ^{14}C yr BP, and resulted in the development of mangroves on the Bragança Peninsula. Probably, between 1800 and 1400 ^{14}C yr BP occurred a maximum decrease of about 1 m below the modern RSL, following a gradual RSL rise until 1000 ^{14}C yr BP, when the RSL was re-established close to the current RSL. Between 5100 and 1000 ^{14}C yr BP the RSL at the Bragança coast probably never exceeded the current one.

The integration of stratigraphic and palynological data indicate two dry periods with relatively low inundation frequency during the last 1000 years. The first event probably extended over a period of 500 years and took place between 860 and 370 ¹⁴C yr BP. The second one started 200 ¹⁴C yr BP and probably finished about 100 years ago. These two dry events occurred during the so called “Little Ice Age” period, characterized by dry periods in South America and glacier advances.

The study also indicates that mangroves on the Bragança Peninsula have migrated to higher elevated areas during the last decades, suggesting a relative sea-level rise.

Zusammenfassung

Entlang der 350 km langen Küste zwischen dem Amazonas Ästuar und dem Gurupi Fluss befindet sich ein breiter Mangrovengürtel. Mangroven sind von grösster ökologischer Bedeutung aufgrund ihrer Biodiversität, Produktivität und haben eine Schlüsselrolle im Nährstoffflux in tropischen Küstenregionen. Darüber hinaus reagieren sie empfindlich auf Umweltveränderungen in der Land-Meer-Übergangszone. Dadurch sind Mangroven ein empfindlicher Indikator und ihre Ablagerungen ein Archiv für gegenwärtige und vergangene Umweltveränderungen. Relevante Beispiele sind Veränderungen im Gezeiten- und Niederschlagsregime, in der Inundationshäufigkeit und in der Bodensalinität.

Die Untersuchungen über die Reaktion der Mangrove auf solche Schlüsselprozesse sind wichtig für das Verständnis vergangener und gegenwärtiger geobotanischer Rahmenbedingungen der nordbrasilianischen Küste und für die Prognose über deren zukünftige Entwicklung. In diesem Zusammenhang ist es das Hauptziel der vorliegenden Studie, den gegenwärtigen Einfluss der Überflutungsfrequenz sowie vergangener Meeresspiegelschwankungen und Klimaänderungen auf das System zu identifizieren. Dies erfolgte mit Hilfe von palynologischen Methoden, Radiokarbondatierungen, Fernerkundung und unter Verwendung des Geographischen Informationssystems (GIS).

Die Kombination von Topographie und Tidenregime-Daten ermöglichte mit Hilfe von GIS Werkzeugen die Überschwemmungsgebiete zu bestimmen. Die Bestimmung der Überschwemmungsfrequenz im Mangrovegebiet erlaubte die Assoziation zwischen den topographischen Merkmalen der Halbinsel und den Hauptvegetationstypen.

Die aktuelle Dynamik der Mangroven, insbesondere der Verlust von Mangrovenwäldern an der Küste, deutet auf einen Meeresspiegelanstieg hin. Die topographieabhängige Dynamik dieser Prozesse lässt eine Zunahme in der Überschwemmungsfrequenz erkennen. Diese verändert den Salzgehalt im Boden und ermöglicht den Transport von Mangroven-Diasporen in höher gelegene Gebiete.

Die Mangrovenablagerungen aus dem nördlichen Brasilien konnten mit gutem Erfolg als Indikatoren des Paläo-Meeresspiegels benutzt werden. Die untersuchten Sedimentkerne von der Bragança-Halbinsel dokumentieren den Nachweis von wenigstens zwei marinen Transgressionen, die die räumliche Verteilung der Mangroven an der Küste während des Holozäns bestimmten.

Das Untersuchungsgebiet wurde durch einen schnell ansteigenden nacheiszeitlichen Meeresspiegel überschwemmt. Der relative Meeresspiegel (RM) erreichte um etwa 5100 ¹⁴C Jahre vor heute (Radiokarbon J.v.h.) aktuelle Werte und führte zur Entwicklung von Mangroven in diesem Gebiet. Wahrscheinlich war zwischen 1800 und 1400 ¹⁴C J.v.h. der RM maximal um einen Meter gegenüber dem heutigen RM gesunken. Danach folgte eine graduelle Zunahme des RM bis 1000 ¹⁴C J.v.h. und es wurde in etwa wieder der aktuelle RM erreicht. Der RM an der Küste von Bragança überstieg wahrscheinlich zwischen 5100 und 1000 ¹⁴C J.v.h nie den aktuellen Meeresspiegel.

Die Integration von Stratigraphie und pollenanalytischen Daten und die Zeitkontrolle durch Radiokarbondatierungen erlaubte die Identifizierung von zwei trockenen Perioden mit einer relativ niedrigen Überschwemmungsfrequenz während der letzten 1000 Jahre. Das erste Ereignis erstreckte sich wahrscheinlich über eine Periode von ~500 Jahren und fand zwischen 860 und 370 ¹⁴C J.v.h. statt. Die zweite Trockenperiode begann 200 ¹⁴C J.v.h. Aufgrund der Zunahme der globalen Temperatur und dem Abschmelzen der Gletscher, endete sie wahrscheinlich vor etwa 100 Jahren. Diese beiden Ereignisse verliefen synchron zur "Kleinen Eiszeit" Periode. Sie wurde durch ein trockenes Klima in Südamerika und durch die Ausdehnung der Gletscher charakterisiert.

Die aktuelle Wanderung der Mangroven auf der Bragança-Halbinsel zu höher gelegene Standorten deutet auf eine Zunahme des RM während der letzten Jahrzehnte hin.

Resumo

Uma faixa de manguezal ocorre ao longo de 350 km da costa entre o estuário do Rio Amazonas e o Rio Gurupi. Os manguezais são de extrema relevância ecológica pela sua biodiversidade, produtividade e papel chave no fluxo de materiais nas regiões costeiras tropicais. Além disso, eles são sensíveis às mudanças em seus ambientes e às interações continente-oceano. Portanto, representam um confiável indicador das mudanças ambientais. Relevantes exemplos disso são as mudanças no regime de maré e de chuvas, frequência de inundação e salinidade do solo.

O estudo das reações do manguezal à essas forças de controle é vital para a compreensão do arcabouço geobotânico atual e do passado no litoral Norte do Brasil e para a previsão da sua evolução futura. Neste contexto, o principal objetivo deste trabalho foi identificar e analisar o atual efeito da frequência de inundação na estrutura do sistema, usando ferramentas tais como palinologia, datações por radiocarbono, sensoriamento remoto, e sistema de informações geográficas (SIG).

A combinação de topografia e dados de regime de maré junto com técnicas de SIG permitiu determinar a frequência de inundação da península de Bragança. Esse estudo permitiu associar características topográficas da península com as unidades de vegetação. A atual dinâmica do manguezal, apresentando ganhos e perdas de cobertura vegetal na linha de costa, sugere um aumento do nível relativo do mar. Essa dinâmica, que está diretamente dependente da topografia, indica aumentos na frequência de inundação, mudanças na salinidade da água intersticial do sedimento e a transferência das sementes de mangue para áreas mais elevadas do terreno.

Os sedimentos do manguezal do norte do Brasil foram usados com sucesso como indicadores de antigos níveis de mar. A análise dos testemunhos de sedimentos revelaram dois eventos transgressivos, que definiram a distribuição espacial do manguezal nesta área durante o Holoceno.

A área de estudo foi inundada por um rápido aumento pós-glacial do nível do mar. A estabilização desse nível de mar ao redor de 5100 anos AP resultou no desenvolvimento de manguezais na Península de Bragança. Provavelmente, entre 1800 e 1400 anos AP ocorreu uma descida máxima em torno de 1 m abaixo do nível do mar atual, seguindo um gradual aumento até 1000 anos AP; quando foi restabelecido o atual nível. Entre 5100 e 1000 anos AP o nível relativo do mar em Bragança, provavelmente, nunca superou o atual.

A integração de dados estratigráficos e palinológicos indicam dois períodos secos com relativa baixa frequência de inundação durante os últimos 1000 anos. O primeiro evento provavelmente se estendeu por um período de 500 anos e ocorreu entre 860 e 370 anos AP. O segundo começou 200 anos AP e terminou provavelmente por volta de 100 anos AP. Estes dois eventos secos estão temporalmente sincronizados com "A Pequena Idade do Gelo", caracterizada por períodos secos na América do Sul e avanços de geleiras.

Esse estudo também indica que os manguezais de Bragança encontram-se migrando para zonas topograficamente mais elevadas da península durante as últimas décadas, sugerindo um aumento do nível relativo do mar.

Chapter 1
ARE THE MANGROVES FROM BRAGANÇA
PENINSULA REACTING TO THE RELATIVE SEA-
LEVEL CHANGES?

1.1 Introduction

The structure of coastal habitats is heavily influenced by inundation frequency and topographic characteristics, which to a great extent determine the configuration and dynamic of vegetation assemblages in mangrove ecosystems (Baltzer, 1970). Therefore, the mangrove ecosystem, like other wetlands, is highly susceptible to RSL fluctuations (Gornitz, 1991; Boorman, 1999), and the sediments deposited beneath mangrove vegetation provide useful indications of past sea-level stands (Scholl, 1964; Woodroffe, 1981; van de Plassche, 1986), since the development of mangroves is controlled by land-ocean interaction (Woodroffe, 1982).

One of the most significant agents of environmental transformation following climatic change is the relative sea-level (RSL) change. The increase in coastal erosion and loss of coastal habitats such as mangroves, other wetlands, and coral reef communities is probably related to the current sea-level rise, coupled with climate changes (Gable et al., 1991). Over the last 100 years, the global mean sea-level has risen approximately 1-2 mm/year (Gornitz, 1995), and recent predictions indicate a sea-level rise between 60 and 100 cm until the end of this century (Douglas et al., 2000). Hence, recent interest has arisen in the probable response of mangrove shorelines to sea-level and/or climate change (Woodroffe, 1993; Pernet, 1993; Snedaker, 1993).

In Brazil, tide gauge records obtained over the last 60 years generally show a rise in RSL (Mesquita and Harari, 1983; Mesquita and Leite, 1985; Pirazolli, 1986; Albrey et al., 1988; Silva and Neves, 1991; Silva, 1992). Beach erosion has occurred in northeastern (Muehe and Neves, 1995), southeastern (Argento, 1989; Gusmão et al., 1993; Muehe and Correa, 1989), and southern Brazil (Gomes, 1987; Muehe and Caruso Jr., 1989), while large-scale destruction of mangroves in North Brazil and French Guyana have been reported by Nittrouer et al. (1991) and Prost et al. (1988), respectively. Franzinelli (1982) described the presence of actively eroding bluffs at Atalaia Beach in Salinópolis, northern Brazil.

These changes in the geomorphology of the Brazilian coast may be related to the current trend of RSL rise (Muehe and Neves, 1995). Several studies, developed at the eastern and southern Brazilian coast, suggesting RSL changes during the Holocene (Suguio et al., 1985; Martin et al., 1988; Tomazelli, 1990; Angulo et al., 1999). In comparison, little information exists about the recent dynamic of mangrove shoreline and Holocene sea-level changes from the northern Brazilian coastline (e.g. Behling and Costa, 1997; 2001; Souza Filho and El-Robrini, 1996; 1998).

Due to that demand, an international and interdisciplinary research project, called “Mangrove Dynamics and Management (MADAM)”, was initiated in 1996 to study the mangrove ecosystem in northern Brazil. The study area of this project is located at the coastal region of Bragança City (Pará), where large mangrove areas occur.

1.2 Objectives

A main aim of this work is to recognize the distribution of current vegetation units according to inundation dynamics on the Bragança Peninsula (Chapter 2 and 3). In this context, the use of a real system property such as the flooded area should be tested as a complementary tool for the interpretation of nutrient dynamics in mangroves. Based on the relationship between flooding regime and vegetation units, possible shifts in the boundaries of these ecosystems should be identified and analysed the relation to current changes in inundation frequency (Chapter 4). The gained knowledge should help reconstruct and interpret past oscillations of the RSL during the mid (Chapter 5 and 6) and late Holocene (Chapter 7), and to propose a mangrove development model to the last 5100 yr BP (Chapter 6).

1.3 The Bragança Peninsula

1.3.1 Location

The Brazilian coast between São Caetano de Odivelas at the southern mouth of the Amazon River and Baía São Marcos measures 480 km and includes portions of the states of Pará and Maranhão. It contains the largest mangrove system in the world, with an area of 8,900 km² (Kjerfve and Lacerda, 1993).

This work was carried out on the Bragança Peninsula, in the central part of this mangrove belt (Fig. 1.1), located approximately 300 km southeast of the Amazon estuary, close to the city of Bragança (Pará State), between 46° 50' and 46° 30' W and 0° 45' and 1° 07' S, between the mouth of the Maiau and Caeté Bays (see Fig. 2.1).

1.3.2 Geology and geomorphology

According to Souza Filho and El-Robrini (1996), the Bragança coastal area is subdivided into three different geomorphologic units such as alluvial, estuarine and coastal plain. The basement of these plains, which forms the coastal plateau, is constituted by the Pirabas formation of Miocene age (Franzinelli, 1988), sediments of the Barreiras group and post-Barreiras group (Rossetti et al., 1989). The Barreiras group

is represented by conglomerates intercalated by sandy and muddy sediments. Arai et al. (1994) dated the Barreiras group to Lower Miocene. The surface of the Barreiras formation is gently undulated and decreases progressively towards the coastal plain (Costa et al., 1993).

The Bragança Peninsula mangrove is restricted to the coastal plain, which is limited to the south by inactive cliffs of 1 to 2 m height sculpted at the coastal plateau, and to the north by the estuarine plain (Souza Filho and EL-Robrini, 1996).

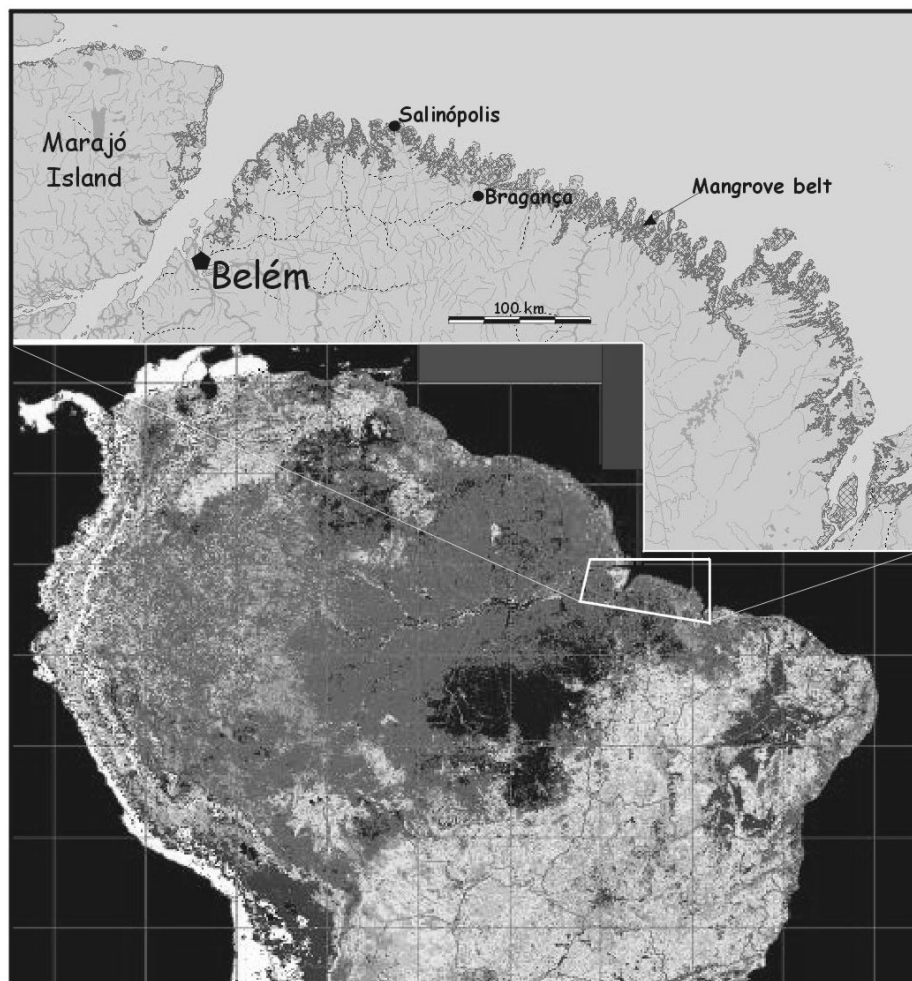


Figure 1.1 Location of the northern Brazilian mangrove belt

1.3.3 Hydrology

The system is a riverine/fringe mangrove, tide dominated with strong oscillating currents, according to the criteria of Lugo and Snedaker (1974) and Woodroffe (1992). The main hydrodynamic features are macrotides of ~4 m range and current velocities

reaching $\sim 1.5 \text{ m s}^{-1}$ for spring tides (Cohen et al., 1999). Sediment transport is highly dynamic, with areas of rapid mud erosion and deposition.

1.3.4 Climate

The coastal region of northeastern Pará is characterised by a tropical warm and humid climate. A drier period of less rainfall occurs between June to November. The coastal meteorological stations of Belém and Turiaçu (Walter and Lieth, 1967), 200 km west and 170 km east of the study area document a mean annual temperature of 25.9 and 26.4 °C, respectively. Maximum and minimum temperatures range between 31.7 and 18.1 °C (Belém) and between 33.2 and 15.2 °C (Turiaçu). The registered mean annual precipitation is 2,277 mm (Belém) and 2,134 mm (Turiaçu).

1.3.5 Vegetation

The 30 km long and up to 15 km wide peninsula is covered by 190 km² of wetlands. Isolated forests, up to 25 m tall occur on several elevated areas in the central part of the peninsula, surrounded by herbaceous and mangrove vegetation. Herbaceous vegetation are at slightly higher elevations than mangroves. The herbaceous plain is infrequently flooded and only by the highest spring tides. This vegetation unit is represented by *Eleocharis geniculata*, *Fimbristylis spadicea* (Cyperaceae) and *Sporobolus virginicus* (Poaceae).

The major part of the peninsula is covered by 10 - 25 m tall, well developed mangrove vegetation. Important species are *Rhizophora mangle*, *Avicennia germinans* and *Laguncularia racemosa* (see Table 6.1).

1.4 Methodology

1.4.1 Image processing

A mosaic of radar images taken on April 1972, and five LANDSAT images obtained on September 1990, December 1991, August 1986, 1988 and 1997 were used in the temporal analyses images. Aerial photographs and field work supported the validation of the results derived from satellite image analyses (Chapter 4).

1.4.2 Elaboration of an Elevation Surface Model

A 1:1000 topographical map of the study area was produced in 1997 as part of the MADAM Project, for an area of ~ 4 ha near the “Furo do Chato” tidal creek. Contour

levels are regularly spaced at 1 m intervals between 0 m and 6 m, relative to the bottom of the creek at the sampling site. Due to the smooth topographical gradients generally found in these mangroves, this site can be considered representative of the Bragança mangrove topography.

In order to extend the evaluation of the inundation dynamics to the entire peninsula, was installed devices for measuring the maximal high-tide elevation at 55 locations (Figure 2.2). Water levels at the respective stations were obtained during a spring tide. These values were referred and adjusted to the existing topographic map from “Furo do Chato”.

In order to enter mapped data into a digital database and calculate inundation areas, it is necessary to convert the graphic points, lines, and areas into a form based on a specific digital data structure (Jackson and Woodsford, 1991). A database containing coordinates and their corresponding elevation values was also created. These spatial data and their attributes were inputted to gridding algorithms of geographical reality (Peuquet, 1984) to create a Digital Elevation Model (Chapter 2 and 3).

1.4.3 Vegetation survey

Visual observation, photographic documentation and GPS measurements were used to determine typical plant species and characterise the main geobotanical units on the peninsula. Porewater salinities were determined (10 cm depth) in eleven topographically relevant sites. Vegetation height was estimated along 11 km of the road running the length of the peninsula. Every 100 to 300 m pictures of the forest were taken at both sides of the road and including a 6 m height gauge as reference. This was not only logistically convenient but also relevant for this work, since the road was built along a high-topography, low-inundation line. Picture digitalisation permitted precise measurement of all trees in each photographed sector (Chapter 4 and 6).

1.4.4 Physicochemical parameters

Surface water samples were taken in the middle of the creek (Figure 3.1). Dissolved phosphate was measured by standard autoanalyser methods. The water level in the creek was measured every 15 minutes with a gauge. Salinity and pH were measured “in situ” using portable instruments (Chapter 3).

1.4.5 Sediment cores

Sixteen sediment cores was sampled with vibra-core, and three were collected with the Russian sampler (Chapter 5, 6 and 7).

1.4.6 Radiocarbon data

Seven bulk samples of 1 cm³ were selected for radiocarbon dating by Accelerator Mass Spectrometry (AMS) in the Leibniz Laboratory of Isotopic Research at the Christian-Albrechts University in Kiel Germany (Cohen, unpublished). Nine radiocarbon dates were obtained by the Van der Graaff Laboratory at the Utrecht University, The Netherlands (Chapter 5, 6 and 7).

1.4.7 Pollen analysis

For pollen analysis, 0.5 or 1 cm³ samples were taken at 2.5 cm 5 cm, 10 cm or 20-cm intervals along the cores (Chapter 5 and 7). All samples were prepared using standard pollen analytical techniques and acetolysis (Faegri and Iversen, 1989).

1.5 Results

1.5.1 The inundation frequency controlling the vegetation distribution on the Bragança Peninsula

According to the Digital Elevation Model, a low-gradient intertidal zone characterises this region. In the inner part of the peninsula, salt marsh areas are higher, relative to mean tide level, than mangrove vegetated mudflats. Consequently, they are flooded much less frequently (<28 day/yr), only by the highest spring tides. This area ends smoothly in a wide extension of mudflats covered by mangroves, which extend for 3–6 km down to the mid-tide mark. These mudflats have gradients of around 1:3000, being dissected by creeks which are much deeper than those in the elevated flats. The upper mudflats are inundated only during normal spring tides (28–78 days/yr) with porewater salinity between 90 and 50 and consist mainly of *Avicennia*. At about mid-tide level, a slope break occurs and an area of relatively steep, frequently flooded (~233 days/yr) mudflats with porewater salinity around 36 and mixed mangrove forest leads down to *Rhizophora*-dominated sectors fringing the low-tide mark (Chapter 2 and 4).

Considering the topography/inundation frequency analysis to the mangrove area close to the “Furo do Chato” tidal creek, on average around 70% of the study area (Figure 3.1) is inundated at high tide during neap tides, while during spring tides more

than 92% is flooded. The mangrove topography has a steep slope, becoming relatively flat with small undulations at short distances to the channels. Above a certain tidal height, small water level variations can produce significant changes in the inundated area (Figure 2.3a). This was the case for high tide levels between 4.8 and 5.0 m, where a difference of 20 cm was enough to raise the percentage of flooded area from 54 to 82%. Thus, an increase of 4% in the tidal level caused a 51% increase in inundated area, accompanied by a decrease of 40% in the phosphate concentration in tidal creek water at low tide (Chapter 3).

Examination of the influence of topography on inundation frequency also showed remarkable patterns, particularly in the higher sectors. Between 5.4 and 6 m, increases of 10 cm in topographical height resulted in increases of inundation frequency of ~50%. Such relationships between microtopography and flooding regime can be notably relevant for the analysis of vegetation structure in infrequently inundated wetlands such as in the central part of the Bragança Peninsula. There, a topographically higher herbaceous plain, flooded only during the highest spring tides, presents evident signs of an active progression of mangrove forest into an area previously dominated by grasses and herbs, with coexistence of the grass *Sporobolus virginicus* and the herb *Sesuvium portulacastrum* and small (0.5 - 2 m height) *Avicennia* shrubs. In this and in adjacent sectors, zonation is accompanied by a clear dependence between vegetation height and flooding frequency (Chapter 4).

1.5.2 Vegetation changes in the central peninsula

Analysis of image time series indicates a significant net losses of herbaceous vegetation coverage have occurred in the elevated flats over the past 25 years. In 1972, coverage was 9.04 km², which progressively declined to values of 7.07, 6.33, 6.19, 6.15 and 5.64 km² in 1986, 1988, 1990, 1991 and 1997, respectively. For the 1972–1997 period, this was equivalent to a net coverage loss of 3.4 km², which is ~38% of the 1972 value. The average coverage loss rate was 1.6%/yr.

The central area (Figure 4.2, limit between sector A and B) shows signs of an active transition between herbaceous vegetation and mangrove forest, with coexistence of the Graminea *Sporobolus virginicus*, the Aizoaceae *Sesuvium portulacastrum* and small *Avicennia* trees (0.5-2 m). The progression of the mangrove front in this area is highly dynamic and can be clearly traced between 1972 and 1997 (Figures 4.2b and 4.2c).

Detailed coverage changes in the 1972–1986, 1986–1991 and 1991–1997 periods are shown in Table 4.2 (Chapter 4).

1.5.3 Coastline vegetation changes

The time series analysis indicates net losses of mangrove coverage along a coastline of ~166 km length, including the Bragança coastal plain and adjacent areas (Figure 4.4). Vegetation death was mainly caused by erosion and/or landward sand migration, as well as deposition on top of older mud sediments (Figure 4.3a, 4.3b, 4.3c). During the 1972–1997 period, losses were registered along ~42% of the coastline length. For the same period, no changes were observed along 39% of the coastline, while coverage gains occurred along 19%. This analysis indicated a mangrove net loss of about 3.2% during this time interval. Detailed coverage changes during the 1972–1986, 1986–1991 and 1991–1997 periods are given in Table 4.1 (Chapter 4).

1.5.4 Stratigraphy and radiocarbon data from the Bragança Peninsula

Studied landforms and sediments are located on a longitudinal transect (Figs. 6.1 and 6.2). In the Holocene stratigraphy of the Bragança Coastal Plain can be recognized three sedimentary sequences: (a) basal sand marine (shoreface) and estuarine retro gradational sequence (S₁); (b) estuarine mud progradational sequence (S₂) and; (c) upper sandy eolian (coastal dunes) and marine (barrier-beach ridges, chêniers, sandflats) retro gradational sequence (S₃) (modified of Souza Filho, 1995, Chapter 6).

1.5.4.1 Estuarine mud progradational sequence (S₂)

This sequence occur between 4 m below and 2.7 m above the present mean sea-level (Fig. 2), and extends more than 90% of the Bragança Peninsula.

Unit A

The highest elevation of the EHF sediments are 2.7 m a.m.s.l., with about 0.2 m thickness. (Fig. 1 and 2). The pollen assemblage from this unit is characterized by the increase of Poaceae (up to 15%) and Cyperaceae pollen (up to 36%), which represent the main vegetation from the EHF (Chapter 5)

Unit B

Radiocarbon data from 3 cores from the base of unit B give an age of 5115 ± 35 yr BP, 2170 yr B.P. (extrapolated) and 1437 ± 35 yr BP. (about 1.4 m amsl, 4 and 0,1 m below the mean sea-level, respectively). The ages of 1018 ± 26 yr BP (1.8 m amsl), 1830 ± 23

yr B.P. (0 m, m.s.l.) and 1265 ± 25 yr BP (0,5 m, a.m.s.l.) were obtained from the middle part of the cores, and 373 ± 25 yr BP (2.4 m amsl) was obtained from the top of this deposit (Fig. 2). The pollen record of this unit is characterized throughout by the dominance of mangrove pollen, primarily by the high pollen producer *Rhizophora* (80-97%). The low pollen producers *Avicennia* (2-7%) and *Laguncularia* (1-3%) are represented by low values (Chapter 5).

1.5.5 Model of Bragança mangrove development

Probably, the sedimentary deposits from Bragança mangroves were formed according to a models combination of lateral with vertical accretion (e.g. Woodroffe et al., 1989), following the topographic zone of mangrove development related to the RSL (Fig. 6.3, Chapter 6).

Phase 1

The phase 1 occurred when the lower elevated areas were flooded by a rapidly rising postglacial sea-level. The stabilization of sea-level around 5100 yr BP resulted in the mangrove development in this region. This phase is represented by the mangrove sediments from “Campo Salgado” core bottom, which reaches 1.4 m above the present mean sea-level. Regarding that the present Bragança mangroves developed between 1 and 2.4 m a.m.s.l. during the Holocene, the RSL during the mid Holocene, probably was close to the modern level (Fig. 6.3).

Phase 2

Palynological data indicate the presence of mangroves at the “Bosque de *Avicennia*” site during the last 2170 yr B.P (Chapter 5). At this area, around 2170 yr BP, is documented mud sediments with mangrove pollen (unit A) that overlies a marine sand layer (4 m below m.s.l.).

Two hypotheses can be proposed to interpret this data: 1) the mud with mangrove pollen would have only deposited in mangrove area. This would imply that the sea-level was at least 5 m below the current msl, and the whole sequence would have deposited by vertical accretion, or 2) the mud with mangrove pollen would have deposited mainly in the lower part of the tidal plain and in tidal channel by lateral accretion, which would not imply in a sea-level fall during this phase.

Palynological data suggest the uninterrupted presence of mangroves since 5100 until 1000 yr BP on the “Campo Salgado” area (Chapter 5), and regarding the current mangrove development zone (1-2.4 m a.m.s.l), the RSL should not have been significantly modified during this time interval in this region, or otherwise, another vegetation type (EHF or Coastal Forest) would have occurred on “Campo Salgado” site (Chapter 6)

Phase 3

From 1800 until 420 yr BP, the mud progressively filled the estuaries and mangrove forests expanded. Between 1800 and 1400 yr BP is probable a low RSL to justify the appearance of mangrove on the “Furo do Chato” (0,1 m a.m.s.l). Its relatively low sedimentation rate (0.18 cm/yr) and topographic position suggest vertical deposition instead of lateral accretion in this area. During that time, following the topographic mangrove development zone and the mangrove presence in “Campo Salgado”, probably the RSL was not lower than 1 m below the current (Fig. 6.4, Chapter 6).

Phase 4

On the “Campo Salgado” site, pollen assemblages indicate at 420 ¹⁴C yr BP a transition between mangrove dominated by *Avicennia* to herbaceous vegetation mainly occupied by Poaceae. The site changed to Cyperaceae after 200 ¹⁴C yr BP (Phase 5), under continuously low inundation frequency. In the last 400 yr BP, based on the habitat salinity zone (Table 6.1), this vegetation change suggests a gradual RSL fall or a vertical accretion of mangrove sediments that gradually eliminated the mangroves in this area (Chapter 6 and 7).

1.5.6 RSL changes at the Bragança Peninsula between 5100 and 1000 yr BP

The data presented in the chapter 5 and 6 suggest the existence of a RSL rise until 5100 yr BP, when the RSL stabilized close to the current one. Probably, between 1800 and 1400 yrs BP occurred a maximum fall of about 1 m below the modern RSL, following a gradual RSL rise until 1000 yr BP; when was re-established the current RSL. Between 5100 and 1000 yr BP the RSL at the Bragança coastline probably was never higher than 0.6 m above the current (Chapter 6).

1.5.7 RSL changes at the Bragança Peninsula during the last 1000 yr BP

The pollen and stratigraphic records from the Bragança Peninsula presented in the chapter 7 indicate two little flooded periods, which may be resulted of a relative sea-level fall associated, or not, to lower annual rainfall rates. The first event (P1), with a duration of 500 years, occurred between 880 and 370 ¹⁴C yr BP. The second one (P2) started about 200 ¹⁴C yr BP ago. The end of this period is still indefinite due to the dating limit of the ¹⁴C, but it may have finished about 100 yr BP, due to the current trend of global sea-level rise.

Between 1000 and 860 yr BP, the relative sea-level (RSL) was similar to the current, and during the following four centuries, the RSL was below the modern (756 ¹⁴C yr BP -2.5 meters below the mean sea-level (bmsl); and 450 ¹⁴C yr BP – 0.65 m bmsl). A RSL fall of about 2.5 m, about 750 yr BP, seems improbable for a time interval of ~100 years. Factors involving autocompaction (Kaye and Barghoorn, 1964) and/or lateral accretion (Woodroffe et al., 1989) may result in sea-level curve being displaced (Larcomb et al., 1995). However, the other RSL of about 0.65 m bmsl at 450 ¹⁴C yr BP, and the pollen assemblages suggest in fact that the RSL was below the present during this time interval (880 to 400 yr BP).

A RSL close to the current probably occurred about 370 ¹⁴C yr BP. Later, this region may have suffered a small RSL fall, and again a rise until to the current level (Fig. 7.5 Chapter 7).

1.6 Conclusions

The combination of topography and tidal regime data by GIS tools allowed to determine the extension of flooded sectors. Thus, it provided a solid numerical basis for the evaluation of patterns of vegetation distribution, inundation frequency and nutrients fluxes from and into well-defined sectors (Chapter 2 and 3).

This vegetation/topography relationship and time series analysis of satellite and Radar images strongly suggests an increase in inundation frequency, changes in soil salinity and the transportation of mangrove diaspores into more elevated areas over the last 25 years. Therefore, it would appear that sea-level rise may be a common forcing agent driving mangrove death in the periphery and mangrove advance into the central part of the Braganca Peninsula (Chapter 4).

During the mid Holocene, the pollen analysis and radiocarbon dating indicate that the mangrove habitats on the Bragança Peninsula probably began to develop at 5100 yr B.P. originated on the “Campo Salgado” area close at the current RSL (Chapter 5 and 6). Probably, between 1800 and 1400 yr BP this littoral suffered a maximal RSL fall of 1 meter below the modern mean sea level, following a gradual RSL rise until 1000 yr BP; when was reached the modern RSL. Between 5100 and 1000 yr BP, the RSL at the Bragança coastline probably was never higher than 0.6 m above the current (Chapter 6).

Over the last 1000 yr BP, the integration of pollen and sediment analysis, including AMS-radiocarbon dating suggests two periods of low inundation frequency (P1 and P2), which probably occurred between 875 and 370 ¹⁴C yr BP; and 200 and 100 yr BP. This alternation of dry and wet periods is coupled with relative sea-level changes. The pollen records also indicates that mangroves on the Bragança Peninsula migrate to higher elevated zones during the last decades, suggesting a relative sea-level rise (Chapter 7).

The data presented in the chapter 7 allowed to discuss the possible links between the dry/wet periods at the Bragança Peninsula and global climatic changes that occurred during the last 1000 years. The P1 and P2 events may be temporally correlated to an erosional period in the Amazon shelf, dry climate in South America and glacier advances in Europe, North America and Andes.

The present mangrove migration identified in time series analysis of satellite and Radar images (Chapter 4) and in pollen profile (Chapter 7) can be associated to the global tendency of eustatic sea-level rise, due to the increase in temperature and glaciers melting around the world during the last 150 years.

Chapter 2
DIGITAL ELEVATION MODEL APPLIED TO
MANGROVE COAST ANALYSIS, AMAZON
REGION, BRAZIL¹

¹ Cohen, M.C.L., Lara, R.J., Szlafsztein, C.F., Dittmar, T., 2001. Digital Elevation Model applied to Mangrove Coast Analysis, Amazon Region, Brazil. *Journal of International Environment Creation* 4, 1-8.

Abstract

Geographical surface data models can be created by GIS methods, which are computer-based tools for processing and displaying spatial or geo-referenced information. GIS techniques were used to process and visualise topography and tidal regime data, focusing on the inundation of a mangrove ecosystem (Bragança, North Brazil). As part of the MADAM Project, a 1:1000 topographical map covering about 4 ha near the “Furo do Chato” tidal creek was produced. Contour levels were regularly spaced at 1 m intervals between 0 and 6m, relative to the bottom of the creek at the sampling site. Due to the smooth topographical gradients found in these mangroves, this site can be considered representative of the Bragança mangrove topography. Another topographical map of the whole peninsula was prepared using simple devices for measuring tide elevation simultaneously at several location in an area of ~190 km². During average neap and spring tides, ~70% and ~90% of the mangrove is flooded, respectively. The topographical features of the study area cause that small water level variations can produce significant changes in the inundation area. The used model approach realistically reflects geomorphology-dependent processes. It showed relationships between vegetation assemblages and topographically defined habitats, providing numerical basis for the evaluation of vegetation distribution patterns and nutrients dynamics in well-defined catchment areas. Further, it provided a link to sediment-water interactions not previously evaluated in our own investigations on creek water chemistry

Keywords: GIS, mangroves, topography, inundation

2.1 Introduction

The complexity of the marine environment, especially in coastal regions, requires a variety of data analysis techniques and models to identify and explain the diversity associated with physical, biological and chemical processes. Frequently, the integrated examination of multidisciplinary data sets is complicated by different terminology and approaches. Geographical Information Systems can be used to re-elaborate and synthesise data sets of diverse origins, thus also facilitating process analysis and the elaboration of coastal management policies.

The structure of coastal habitats is heavily influenced by inundation frequency and topographic characteristics, which to a great extent determine the configuration and

dynamic of vegetation assemblages in mangrove ecosystems (Baltzer, 1970). Besides, tidal flooding regime can strongly vary with slight topographic variations and significantly influence the chemical reactions involved in the retention and release of nutrients in sediments (Silva and Sampaio, 1998).

The geographical distributions of such features are inherently complex; therefore, it may be necessary to develop "Geographical Data Models", involving a process of simplification that converts geographical reality into a finite number of database records (Mandelbrot, 1982). One of the results of the Geographical Data Model, the Surface Model, represents the spatial variations of a single variable using a collection of discrete objects.

The present work was performed in the frame of the MADAM Project (Mangrove Dynamic and Management). This paper deals with the application of a Surface Data Model to the study of vegetation distribution and geochemical processes in the mangroves of Bragança, Pará.

2.2 Methodological considerations

2.2.1 Study area

This work was conducted on the "Furo do Chato" tidal creek and later expanded to the whole Bragança peninsula. (Figures 2.1 and 3.1).

2.2.2 Tidal level measures

The water level in the creek was measured with a gauge every 15 minutes over 24 hours and each three weeks during a year, for a total of 18 campaigns from June 1996 to August 1997.

2.2.3 Topographic survey

A 1:1000 scale topographic map of the tidal creek "Furo do Chato" was produced in 1997 as part of the MADAM Project, for an area of around 4 ha near the "Furo do Chato" tidal creek. Contour levels are regularly spaced at 1 m intervals between 0 m and 6 m, relative to the bottom of the creek at the sampling site. This site can be considered as representative of the general topography of the mangrove forest, as indicated by field work, regional maps, and geomorphologic analysis using satellite images and aerials photographs.

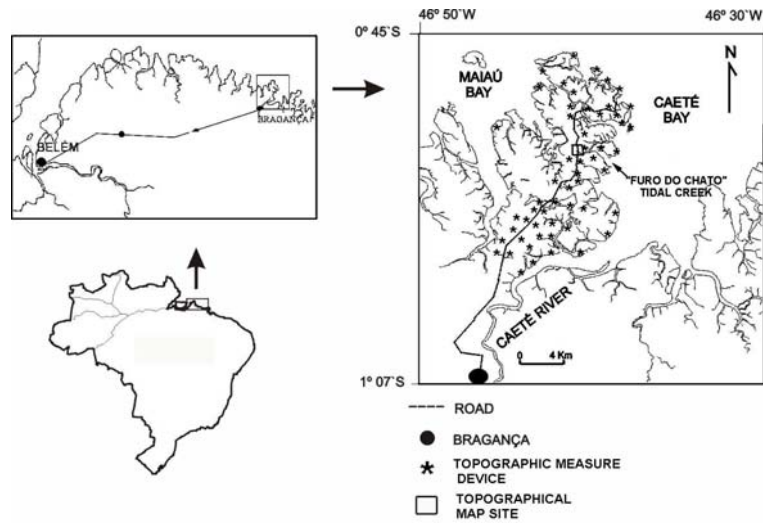


Figure 2.1 Study area

In order to extend the evaluation of the inundation dynamics to the entire peninsula, we installed devices designed by U. Berger for measuring the maximal high-tide elevation at 55 locations (Figure 2.2). Water levels at the respective stations were obtained during a spring tide. These values were referred and adjusted to the existing topographic map from “Furo do Chato”.

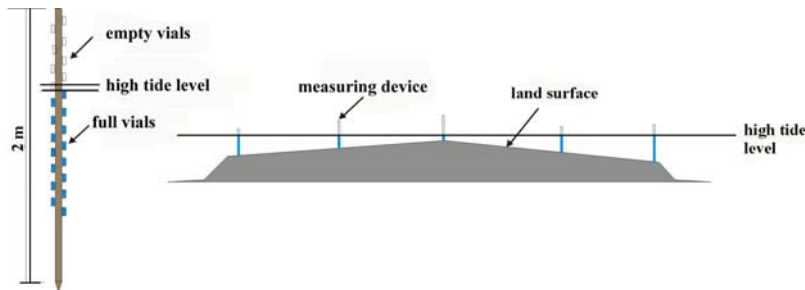


Figure 2.2 Device for measuring maximal tide elevation and scheme showing their utilisation.

2.2.4 Elaboration of an Elevation Surface Model

In order to enter mapped data into a digital database and calculate inundation areas, it is necessary to convert the graphic points, lines, and areas into a form based on a specific digital data structure (Jackson and Woodsford, 1991). A digital georeferenced (20 UTM data co-ordinates obtained by GPS) vector model of the map was produced using AutoCAD V.14 (Autodesk) software. A database containing co-ordinates and their corresponding elevation values was also created. These spatial data and their attributes were inputted to gridding algorithms of geographical reality (Peuquet, 1984) to create a

special surface model, the Digital Elevation Model (DEM). Gridding methods produce a regularly spaced array of Z values from irregularly spaced x , y , z data (topographical level data), that it means they fill the "no data" areas by extrapolating or interpolating Z values at those locations. The two gridding methods adopted in this work are:

1) *Cell Grid*: the area is partitioned into a regular cells; the variable value attached to each cell is assumed to represent all locations within the cell (e.g. remote sensing image). Grid structures, obtained using the software IDRISI 2.0 (Clark University) are used for the analysis in GIS-raster systems, becoming a very good means of representing the topography of land surface (Jenson and Domingue, 1988).

2) *Regular Point Sampling*: the database contains a set of tuples (x , y , z) representing sampled values of the irregularly arrayed variable, which are interpolated to a regularly spaced grid, using the program SURFER (Golden Software).

Grid method parameters control the interpolation procedure. In this work we used the Kriging method, which is a linear unbiased spatial interpolation method that provides minimum mean-squared error estimates at unsampled locations. While kriged surfaces may be good estimators, they are also unrealistically smooth and continuous.

These methods were used to elaborate a Digital Elevation Model (DEM) represented as contour map and surface grid cell formats. A contour map is a set of lines each consisting of an ordered set of x , y pairs having associated z value, created from gridded data. The contour levels are regularly spaced using intervals of 0.5 and 0.2 m between the smallest (0) and largest (6) Z values (Figures 2.3a and 2.3b, respectively).

The calculations of tidal inundation areas were derived from the DEM by reclassification operations. This comprises the repackaging of information on a single overlay, applying a generalised reclassification function, such as "level slicing" which splits a continuous range of map category values into discrete intervals (e.g. Star and Estes, 1990).

The inundation frequency was based on the height of the daily high tides of the Guaras Island (distant 100 km from Bragança) obtained in the 1997 tide chart, and adjusted referring to 24 hours tide gauge measurements performed every three weeks during one year in the study area. Afterwards, the times that the tides reached each topographical quota of the Bragança peninsula into one year period were quantified.

2.3 Results and discussion

2.3.1 Tidal inundation in the “Furo do Chato” area

This was obtained by reclassification of the DEM values. Tidal levels tidal creek registered between June 1996 and August 1997 were used, corresponding half of them to spring tide and half to neap tide situations. A 3D orthographic projection of the DEM, combined with a map showing the flooded areas at different water heights is shown in Figure 2.3.

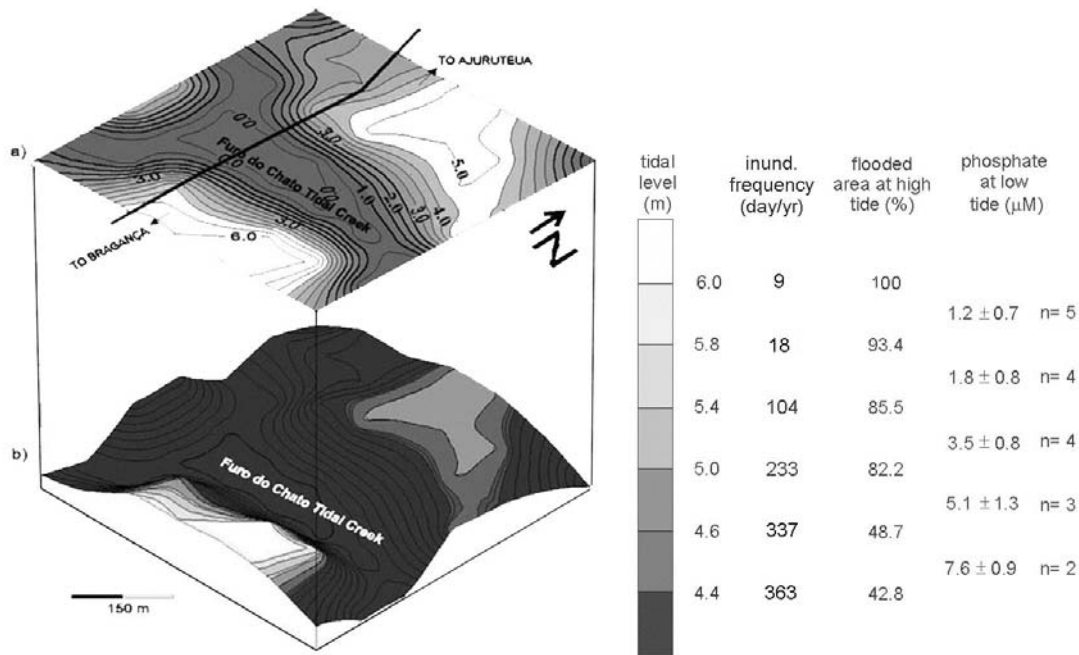


Figure 2.3 Combination of a) site topography with contour levels spaced at 0.5 m intervals between 0 m and 6 m relative to the bottom of the creek at the sampling site, and b) digital elevation model with percentage of the total area flooded at different high-tide levels. Low-tide phosphate concentrations corresponding to the days with high-tide levels included in each level interval were accordingly averaged for each subgroup. Inundation frequencies are calculated as the number of days in a year in which water height at high tide reached the topographic contour levels.

According to the DEM, around ~70% of this area is inundated during neap tides at high-tide (~4.9 m) on average, while during spring tides (~5.7m) more than 92% is flooded. The creek’s bank has a steep slope, becoming relatively flat with small undulations at short distances to the channels (Figure 2.3a). Above a certain tidal height, small level variations can cause significant changes in the inundation area. For levels between 4.8 and 5.0 m a difference of 20 cm raised the percentage of flooded area from 54 to 82% (Figure 2.4). Thus, an increase of 4% in the tidal level caused a 51% increase in the inundated area.

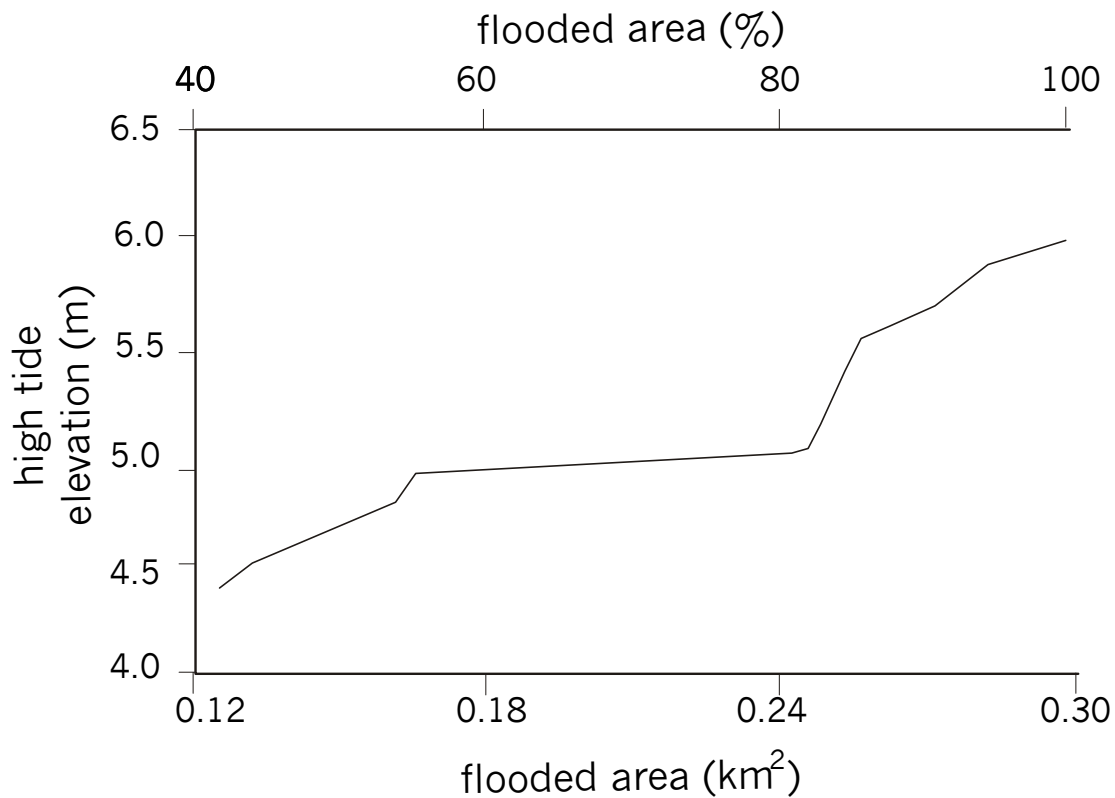


Figure 2.4 Relationship between high-tide level and flooded area during one year.

These data have been used (Cohen et al, in press) to analyse sediment/water interactions in the creek. Significant correlations were found between inundation area at high tide and dissolved phosphate and calcium in low tide water, when the proportion of groundwater in the creek is maximum. Low-tide phosphate was inversely proportional to the flooded area. There was also an inverse relationship between the low-tide/high-tide pH ratios of creek water and the inundation area. During highest and lowest inundation events, calcium was inversely proportional to the flooded area. These findings suggest that mangrove inundation may cause a pH increase of sediment porewater, favouring the phosphorus retention in form of calcium compounds.

2.3.2 Tidal inundation on the Bragança Peninsula

For logistic reasons it was not possible to extend topographic field work to the Maiiau Bay. The development of approximate contour levels was based mainly on the analysis of the drainage network under consideration of the topographical configuration of the opposite side to the peninsula. This was done by examination of satellite images (Cohen et al., in press) aided by the tidal elevation data obtained as described in Figure 2.2.

This procedure was combined with field observations to tentatively outline topographically defined habitats on the Bragança Coastal Plain (Figure 2.5).

A low-gradient intertidal zone characterises this region. In the inner part of the peninsula, salt marsh areas are higher, relative to mean tide level, than mangrove vegetated mudflats. Consequently, they are flooded much less frequently (<28 day/yr), only by the highest spring tides.

The salt marshes end smoothly in a wide extension of mudflats covered by mangroves, which extend for 3 to 6 km down to the mid-tide mark. These mudflats have slopes of around 1:3000 (0.033%), being dissected by creeks which are deeper than those in the marshes.

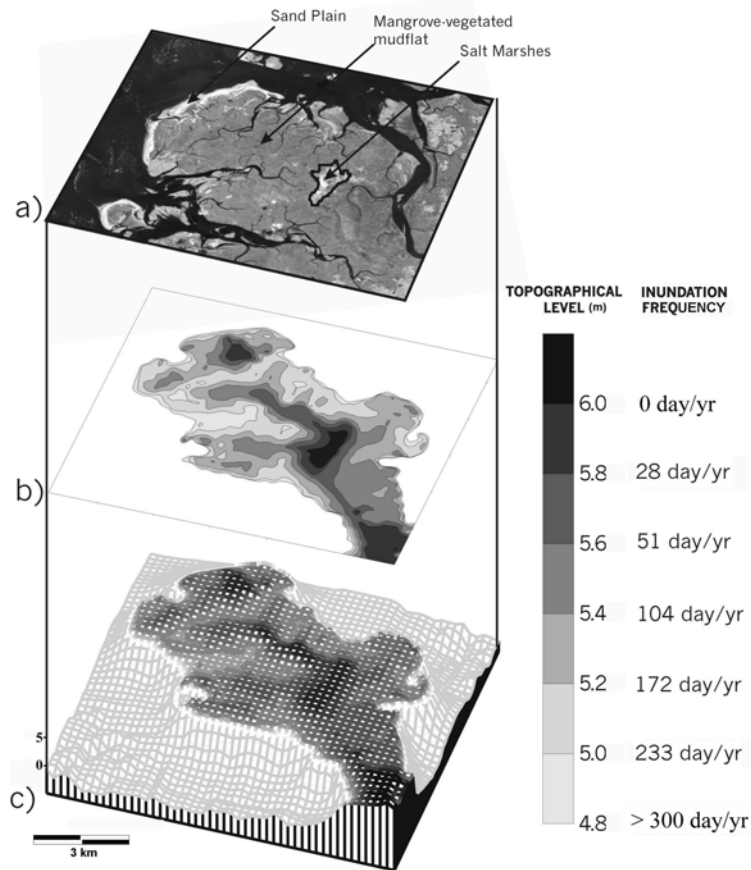


Figure 2.5 Thematic composition involving: a) satellite image with the three main morphological units; b) contour level map and c) three-dimensional relief of the Bragança peninsula with a vertical increment of x 1000. The zero level is referred to the bottom of the tidal creek “Furo do Chato”.

The upper mangrove-vegetated mudflats bordering the salt marsh zone are relatively high, being only inundated during normal spring tides (28-78 day/yr). At slightly lower level inner sand plains are found, which extend to about mid-tide level. There, a slope break occurs and an area of relatively steep mangrove-vegetated mudflats, frequently flooded (~233 day/yr), lead down to sandier material which fringes the low-tide mark.

The present habitat assignment is reinforced by further field work on species distribution (Menezes, unpublished), which documents a clear influence of environmental gradients directly or indirectly determined by landform patterns and associated physical processes.

2.4 Conclusions

The combination of topography and tidal regime data by GIS tools allowed to determine the extension of flooded sectors. Thus, it provided a solid numerical basis for the evaluation of patterns of vegetation distribution and nutrients fluxes from and into well-defined sectors. It also generated a link between sediment and water geochemical processes not jointly evaluated in the respective original studies (Cohen et al., 1999; Lara and Dittmar, 1999). The mesoscale appraisal of the inundation frequency of the Bragança coastal plain allowed the assignment of main vegetation assemblages to the topographical features of the peninsula.

The present approach is presently being expanded to other peninsulas of the Pará State for analysing the spatial distribution of sub-environments within the mangrove ecosystem as described by topography and vegetation zonation.

Chapter 3
MANGROVE INUNDATION AND NUTRIENT
DYNAMICS FROM A GIS PERSPECTIVE²

² Cohen, M.C.L., Lara, R.J., Szlafsztein, C.F., Dittmar, T. Mangrove inundation and nutrient dynamics from a GIS perspective. *Wetlands, Ecology and Management* (in press).

Abstract

A digital elevation model describing topography, tide elevation and inundation degree and frequency of a mangrove forest in North Brazil is discussed in relation to existing phosphate and physicochemical data in waters of an adjacent tidal creek. Due to smooth topography, an increase of 20 cm in tidal height above average neap tides increases flooded area from about 50 to 80%. Analysis of the relationship between microtopography, tidal height and flooding rate showed that in the upper 60 cm of the mangrove forest, increases of 20 cm in topographical height resulted in a doubling of the inundation frequency. This can be particularly relevant for the analysis of nutrient mobilization and vegetation structure of infrequently inundated wetlands. Throughout the year, low-tide phosphate in creek water was inversely proportional to the maximum area flooded during high tide, this correlation being higher during the dry season. Similarly, the inverse relationship between flooded areas and low-tide/high-tide pH ratios was highly significant during the dry season and the beginning of the rainy season. Although the high correlations obtained are based on data pairs obtained at high and low tide, it has to be clarified whether the association between inundation degree and creek water pH is relevant for the stability of P compounds in sediment on the short scale of a tidal cycle.

Key words: geographical data model, flooding frequency, topography, phosphate, porewater

3.1 Introduction

Inundation regimes can significantly influence nutrient dynamics in mangroves and other wetlands. For example, variations in tidal inundation frequency influenced porewater phosphate influence concentrations in sediments beneath mangrove communities in the Indian River (Carlson et al., 1983). Silva and Sampaio (1998) indicated that the mechanisms involved in the retention and release of phosphate in the soil of Combu Island (North Brazil) were related to an inundation gradient caused by slight topographic differences. Due to its dependence on tidal height, phosphorus can become limiting in elevated mangrove forest areas (Boto and Wellington, 1983). Concentration of dissolved inorganic phosphorus in mangroves is generally low (Alongi et al., 1992; Lara and Dittmar, 1999).

Several investigations on nutrient dynamics have been carried out recently in the mangrove region near Bragança, North Brazil. The diel variability of silicate

concentrations in creek water was, to a large extent, explained by hydrodynamical calculations (Lara and Dittmar, 1999). Mangrove inundation produced not only this simple tidal mixing, but also influenced porewater input of phosphate and DOC from the upper forest sediment layers (Dittmar and Lara, 2001) due to the hydrostatic gradient between creek water and sediment water table. This was investigated by correlating solute concentration at low tide with the number of hours per day during which tidal height was below a determined level. While the resulting highly significant correlations strongly support the influence of hydraulic gradient on phosphate dynamics, time itself is not a system-intrinsic parameter which can be used in a process-oriented analysis of sediment-water interactions.

Most cited works use inundation height or duration in correlations with solute concentrations. However, the evaluation of physicochemical processes at the sediment surface as well as the fluxes between sediment and water or between catchments areas, can also require the determination of the area of exposed and inundated sediment sectors. These can include complex topographic settings such as curved creeks and irregular wetland substrate surfaces.

Quantification of the extent and frequency of surface inundation as a function of tidal level and regime, as well as their influence on mobilization or retention of nutrients, represents a necessary but difficult combination of topographic, hydrographic and chemical studies. The spatial distribution of such parameters is inherently complex, and may therefore necessitate developing a “Geographical Data Model” involving a description process that converts geographical reality into a finite number of database records (Mandelbrot, 1982). The purpose of such a surface model is to represent the spatial variations of a single parameter using a collection of discrete objects.

In the present work, a Digital Elevation Model describing topography, tide elevation and inundation degree and frequency of a mangrove forest in North Brazil is discussed in relation to existing phosphate and physicochemical data for an adjacent tidal creek (Dittmar and Lara, 2001). The main goal is to test the feasibility of such an approach, as a complementary tool for the interpretation of nutrient dynamics in mangroves by the use of a real system property such as the flooded area. A similar approach has been applied to relate GIS-based studies on inundation dynamics to other ecosystem characteristics in floodplains (Townsend and Walsh, 1998; Slavich et al., 1999), but to our knowledge, similar studies on mangroves do not yet exist.

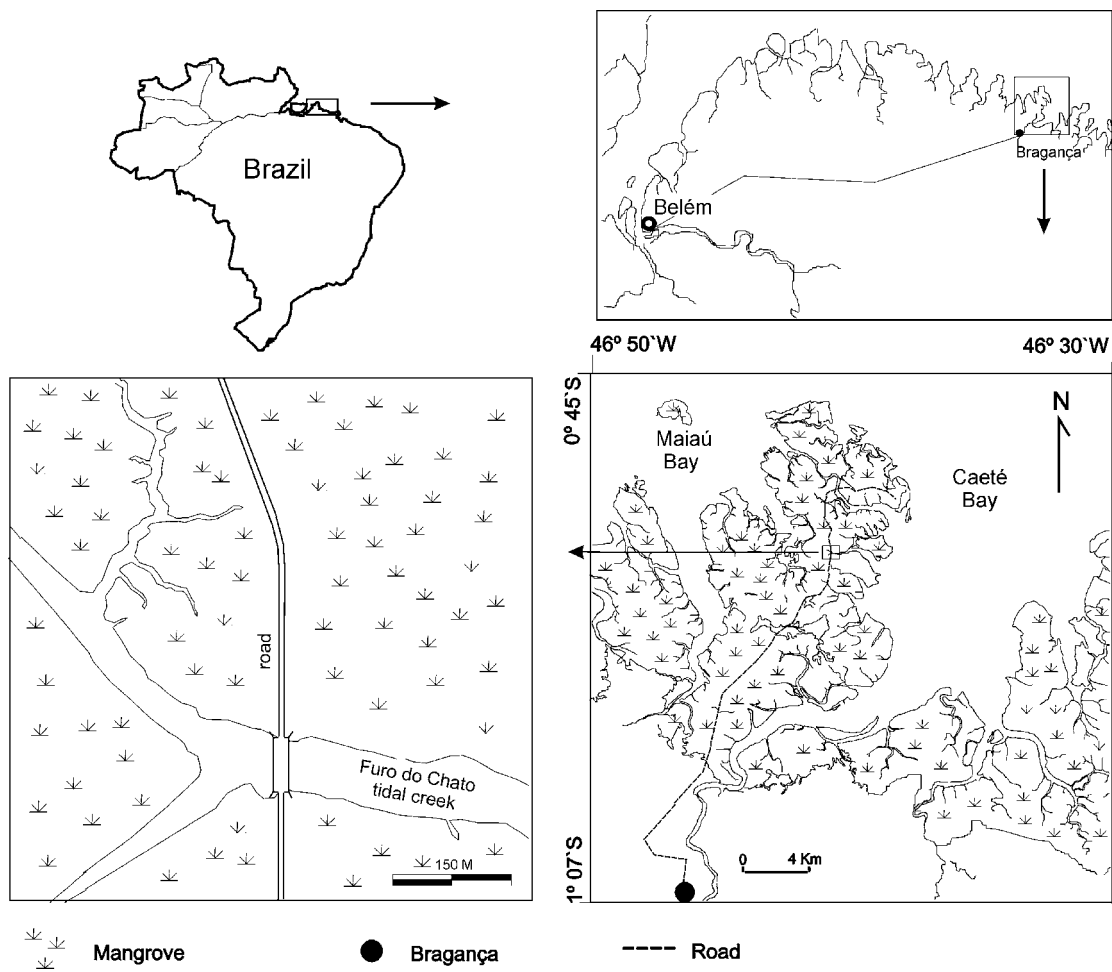


Figure 3.1 Location of the study site.

3.2 Study area

This work was developed on the “Furo do Chato” tidal creek is situated in Bragança Peninsula between $46^{\circ}50'$ and $46^{\circ}30'$ W and $0^{\circ}45'$ and $1^{\circ}07'$ S (Figure 3.1).

3.3 Material and methods

3.3.1 Chemical and physicochemical parameters

Data sources used in this work are cited below. Briefly, surface water samples were taken in the middle of the creek, at hourly intervals over 24 hours and every three weeks during a year, in a total of 18 campaigns from June 1996 to August 1997. Dissolved phosphate was measured by standard autoanalyser methods (Lara and Dittmar, 1999). The water level in the creek was measured every 15 minutes with a gauge. Salinity and pH were measured “in situ” using portable instruments (Cohen et al., 1999; Lara and

Dittmar, 1999). Phosphate values measured at low tide, one hour before flood onset were used, in order to deal with a state of high, accumulated porewater input (Lara and Dittmar, 1999).

3.3.2 Elaboration of Surface Elevation Model

A 1:1000 topographical map of the study area was produced in 1997 as part of the MADAM Project, for an area of ~4 ha near the “Furo do Chato” tidal creek. Contour levels are regularly spaced at 1 m intervals between 0 m and 6 m, relative to the bottom of the creek at the sampling site. Due to the smooth topographical gradients generally found in these mangroves, this site can be considered representative of the Bragança mangrove topography.

In order to enter mapped data into a digital database and calculate inundation areas, it is necessary to convert the graphic points, lines, and areas into a form based on a specific digital data structure (Jackson and Woodsford, 1991). A georeferenced vector model of the map (20 UTM data coordinates obtained by GPS) was produced using AutoCAD 14 (Autodesk) software. A database containing coordinates and their corresponding elevation values was also created. These spatial data and their attributes were inputted to gridding algorithms of geographical reality (Peuquet, 1984) to create a Digital Elevation Model (DEM). Grid structures, obtained using IDRISI 2.0 software (Clark University) are the basis for analysis in raster GIS systems and a very good means of representing land surface topography (Jenson and Dominguez, 1988). The database contains a set of tuples (x, y, z) representing sampled values of the variable, irregularly arrayed, which are then interpolated onto a regularly spaced grid using SURFER (Golden Software). Three-dimensional topographic representations of a grid file were produced as surface plots, connecting each grid node or cell with z values proportional to surface height.

For the calculation of tidal inundation areas, contour maps were derived from a map of topographic elevations by reclassification operations. This comprises the repackaging of information on a single overlay, applying a generalized reclassification function, such as “level slicing” which splits a continuous range of map category values into discrete intervals (e.g. Star and Estes, 1990). The distribution of inundation frequencies of the system surface was determined for contour levels regularly spaced at 0.1 m intervals between 4.6 m and 6 m relative to the bottom of the creek at the sampling site. This was carried out by analysis of the frequency distribution of tide gauge registers from the

study site, determining how many times in a year high-tide levels reached the above-mentioned contour levels.

3.4 Results and discussion

Mangrove flooded areas were calculated for the registered high tide levels ($n = 18$), about half of them corresponding to spring tide and the other half to neap tide situations. An orthographic projection of the DEM, combined with a map showing the flooded areas at different water heights, is shown in Figure 2.3. For better visualization, inundation data were reclassified and divided in six subgroups. Phosphate concentrations at low tide on the respective sampling day were accordingly redistributed and averaged for each subgroup.

According to the DEM, on average around 70% of the study area is inundated at high tide during neap tides (~4.9 m), while during spring tides (~5.7 m) more than 92% is flooded. The mangrove topography close to the creek has a steep slope, becoming relatively flat with small undulations at short distances to the channels. Above a certain tidal height, small water level variations can produce significant changes in the inundated area (Figure 2.3a). This was the case for high tide levels between 4.8 and 5.0 m, where a difference of 20 cm was enough to raise the percentage of flooded area from 54 to 82%. Thus, an increase of 4% in the tidal level caused a 51% increase in inundated area, accompanied by a decrease of 40% in the phosphate concentration in tidal creek water at low tide. Further water level increments of 20 cm produced increases in the flooded area of about 5%, as well as average phosphate concentration decreases of about 30%. At a water level of 6 m, 100% area coverage and the lowest phosphate values in the low-tide water are reached.

Examination of the influence of topography on inundation frequency also showed remarkable patterns, particularly in the higher sectors. Between 5.4 and 6 m, increases of 10 cm in topographical height resulted in increases of inundation frequency of ~50%. Such relationships between microtopography and flooding regime can be notably relevant for the analysis of vegetation structure in infrequently inundated wetlands such as in the central part of the Bragança peninsula. There, a topographically higher herbaceous plain, flooded only during the highest spring tides, presents evident signs of an active progression of mangrove forest into an area previously dominated by grasses and herbs, with coexistence of the grass *Sporobolus virginicus* and the herb *Sesuvium portulacastrum* and small (0.5 - 2 m height) *Avicennia* trees (Cohen et al., in press). In

this and in adjacent sectors, zonation is accompanied by a clear dependence between vegetation height and flooding frequency. It is still unclear whether this is primarily due to the measured salinity gradients, nutrient availability, or inundation-dependent redox conditions (Lara, unpublished).

The covariation of inundated area and low-tide phosphate concentration was particularly marked during the dry season, with a highly significant correlation ($r = -0.96$, $n = 8$, $p < 0.001$) for the relationship between both parameters. During the wet season, this correlation was lower ($r = -0.85$, $n = 10$, $p < 0.001$). For the whole year the correlation was also highly significant, with $r = -0.92$, $n = 18$, $p < 0.001$. The different relationships we obtained for each season might be caused by the distinct characteristics of the creek water flooding the system during the rainy season. The range of salinities in the creek is 14.8 to 38.5 and 8.9 to 32 in the dry and the rainy season, respectively. However, the different correlations might be within natural variability: all phosphate data were grouped according to the inundation intervals used for Figure 1.3, and the concentrations in each subgroup were averaged. The correlation between the centered value of the respective water level intervals and the corresponding averaged phosphate values was highly significant and about as high as for the dry season ($r = -0.99$, $n = 5$, $p < 0.001$).

Several non-excluding factors may explain the inverse correlations between flooded area and low-tide phosphate. The larger volume of low-phosphate seawater that would be moved during a higher tide would cause a greater dilution of phosphate-enriched porewaters. Besides this, hydrostatic pressure would increase with the inundated area, probably reducing the input of groundwater or crab hole water from the sediment (Dittmar and Lara, 2001).

The extent of inundated area also showed a highly significant correlation with pH in creek water. Throughout the year, creek water pH was consistently higher at high tide (mean 7.9) than at low tide (mean 7.2) due to the more buffered inflowing estuarine water. To test the influence of inundation on porewater pH and to circumvent the influence of oscillations in the background signal of high-tide pH on low-tide pH, the data were treated as follows. Instead of comparing raw pH values, we calculated the ratio between creek water pH at low tide and high tide and correlated this quotient with the values of the mangrove flooded area. For the pooled data of dry and rainy season, both parameters showed a weak correlation ($r = -0.34$, $n = 18$), most probably due to the effect of rain during the wet season, which significantly modifies the physicochemical

characteristics of creek waters. However, during the dry season and the beginning of the wet season this relationship was highly significant ($r = -0.87$ $n = 10$), suggesting that the waters flooding the mangroves, with a pH higher than in porewater, receive hydrogen ions from the latter, becoming more acidic with increasing flooded area.

Schwendenmann (1998) reported extreme pH values from 4.5 to 7.5 for porewater surface sediments at Furo do Chato creek, where most values were consistently slightly acidic throughout the year, mostly in the range 5.6 - 6.6. In coastal profiles on Combu Island, Silva and Sampaio (1998) studied the influence of pH on the retention and release of phosphate. At depths from 0 to 0.4 m, sediment pH was in the range 4.5 - 5.1, accompanied by low mean concentrations of calcium-bound phosphate compounds. According to Bromfield (1960), in this range of pH some compounds of calcium phosphate are unstable. In our study area, the infiltration of high-tide water through crab holes and other macropores is probably followed by an increase in porewater pH. Salomons and Gerretse (1981), Fabre (1992), Maine et al. (1992) and Silva and Sampaio (1998), found higher P concentration in the soils with largest inundation periods. However, it is uncertain to what extent the relationship between inundation degree and creek water pH reported in the present work may be relevant for the stability of P compounds in sediment on the short scale of a tidal cycle.

The approach used in the present work for calculating inundation frequencies provides an accurate proxy of the average flood history (Slavich et al., 1999) of well determined sectors. Thus, through their dependence on both topography and tidal regime, flooding frequencies could probably typify exchange processes between sediment and flood water more realistically than tidal height alone and help clarify uncertainties related to the time scale in which these interactions affect nutrient mobilization in wetlands.

Chapter 4
TEMPORAL CHANGES OF MANGROVE
VEGETATION BOUNDARIES IN AMAZÔNIA:
APPLICATION OF GIS AND REMOTE SENSING
TECHNIQUES³

³ Cohen, M.C.L., Lara., R.J. Temporal changes of mangrove vegetation boundaries in Amazônia: application of GIS and remote sensing techniques. Wetlands Ecology and Management. (in press)

Abstract

The present work analyses a 25-year time series of radar and satellite images, identifies areas with losses and gains of vegetation coverage in the inner parts of the Bragança peninsula and along the coastline of Pará (North Brazil). The geomorphology of this region has significantly changed in recent years. A result of these changes has been retreat of the mangrove vegetation along the coastline, mainly due to landward sand migration, which covers the mudflat and asphyxiates the vegetation. Image analysis suggests that loss of vegetation coverage has been the dominating process in the last 25 years, occurring at ~42% of the Bragança coastline and adjacent areas. Vegetation has remained stable along ~39% of the coastline, while mud sedimentation has allowed mangrove development along ~19% of it. On the other hand, the mangroves invaded 3,4 km² of the elevated herbaceous flats in the highest portion of Bragança peninsula. Despite other possible causes for mangrove death along the coastline, such as littoral drift currents or cyclical changes in coastal sediment dynamics, the invasion of mangrove into herbaceous elevated flats in the central peninsula cannot be attributed to these factors. The current dynamics of vegetation coverage change seem to be compatible with a long-term trend related to the predicted rates of sea-level rise.

Key words: coastline evolution, herbaceous flat, inundation frequency, mangrove, salinity, satellite.

4.1 Introduction

The Brazilian coast contains the world's second largest unitary mangrove region, estimated to cover a total area of 1.38 million hectares, along a coastline of approximately 6800 km (Kjerve and Lacerda, 1993). The most luxuriant mangrove habitats are found in North Brazil, where similar geomorphological features caused the development of analogous biological units with common fauna and flora and similar patterns of resource exploitation (Szlafsztein et al., 2000).

Coastal wetlands are considered highly susceptible to sea-level rise (Gornitz, 1991; Boorman, 1999). These systems are often the final steps in the levelling and filling of coastal depressions (Frey and Basan, 1985), and depend on the balance between sea level and tidal sediment accumulation, which in turn is governed by tidal exposure (Chapman, 1960). Thus, a relative sea-level rise may result in mangrove retreat near the

shoreline and landward migration due to higher inundation frequency. Similarly, internal vegetation domains on elevated mudflats will be subject to boundary adjustments, since mangroves would migrate to higher locations and could invade these areas.

Global mean sea level has risen approximately 1-2 mm/year over the last 100 years (Gornitz, 1995). There is a 1:1 possibility that greenhouse gases will raise sea level at least 15 cm more by the year 2050, 35 cm by 2100, and 80 cm by 2200. Moreover, there is a 1:40 chance that climate change will cause sea level to rise 35 cm by 2050, 80 cm by 2100 and 300 cm by 2200 (Titus and Narayanan, 1995).

These rises may be causing mangrove shorelines in Western Australia to erode and retreat (Semeniuk, 1980). Despite broad Holocene progradational plains with chenier ridges (Jennings and Coventry, 1973; Jennings, 1975), the dominant trend at present is erosional, with retreat through sheet erosion, cliff erosion and tidal creek extension (Semeniuk, 1981).

In Brazil, tidal records obtained over the last 50 years show a general rise in relative sea level; Pirazolli (1986) reported a rising trend at four locations for the period 1950-1970. Studies conducted at Cananéia and Rio de Janeiro in the Southeast region also indicate a rise since 1960 (Mesquita and Harari, 1983; Mesquita and Leite, 1985; Silva and Neves, 1991; Silva, 1992). Based on a time span of about 20 years ending in 1968, Aubrey et al. (1988) reported rates of relative sea-level rise along the Brazilian coast from 0.3 to 3.6 mm/year.

Large-scale destruction of mangroves at the oceanic front in North Brazil and French Guyana has been reported by Nittrouer et al. (1991) and Proust et al. (1988), respectively. Extensive shore erosion along the Brazilian coast has been reported (Muehe and Neves, 1995 and references therein). Since there is still insufficient evidence to relate these observations to sea-level changes, these authors have recommended intensive monitoring of certain coastline sectors identified as vulnerable. One of the locations suggested is Salinópolis (Pará), which suffers the effects of severe erosion, as already described by Franzinelli (1982). This site is situated at ~100 km from the Bragança region, where the present study was carried out. The general characteristics of this area make it representative of the extensive mangrove belt near the Amazon mouth (Szlafsztein et al., 2000).

This paper analyses a time series of satellite and aerial images covering a 25-year period from 1972 to 1997, focusing on the identification and quantification of areas with

vegetation coverage losses or gains in mangroves and elevated mudflats. The main goals were to assess the recent evolution of coastal vegetation on a regional scale and to identify local indicators for tracing this process in these and other mangroves of North Brazil.

4.2 Material and Methods

4.2.1 Study area

This work was conducted on the Bragança peninsula (Figure 4.1a), between $46^{\circ} 50'$ – $46^{\circ} 38'$ W and $00^{\circ} 05'$ – $01^{\circ} 00'$ S and adjacent areas (Figure 4.3), between $47^{\circ} 05'$ – $46^{\circ} 30'$ and $0^{\circ} 40'$ – $1^{\circ} 00'$ S in 1999 during the dry season.

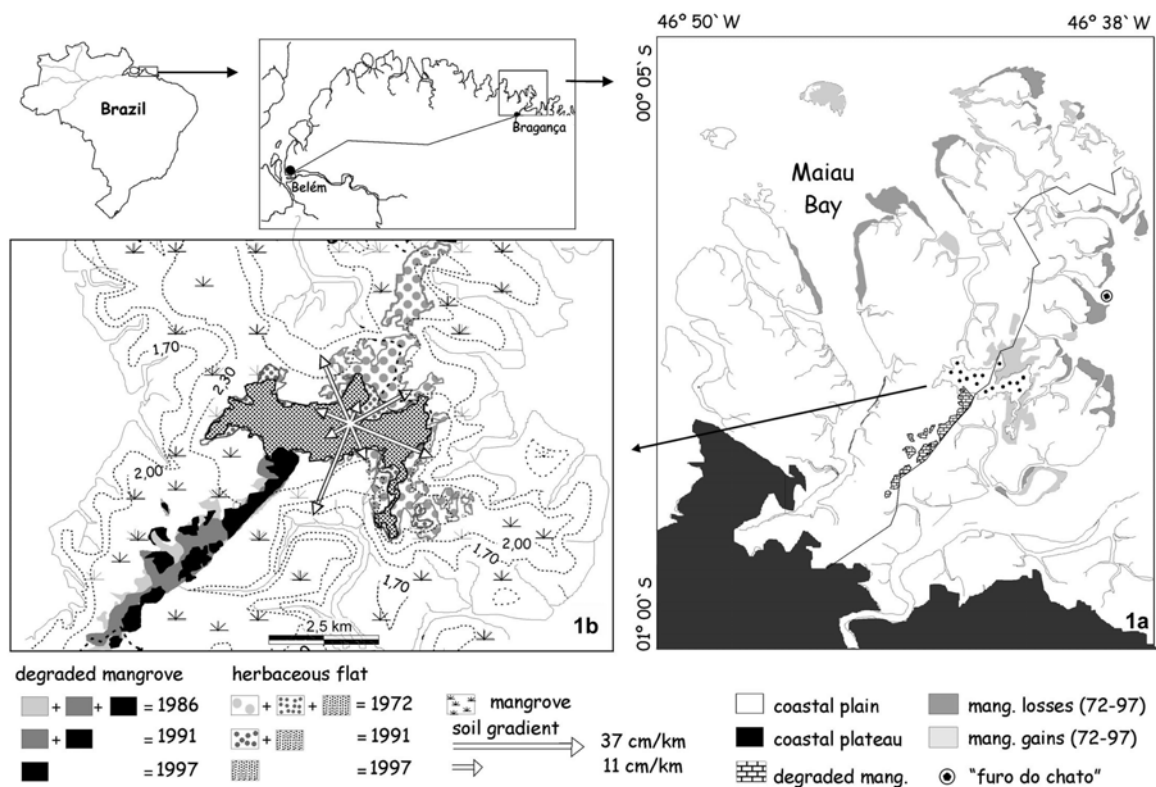


Figure 4.1 Location of the study area (1a) and progression of the mangrove front (1b).

4.2.2 Field work

Visual observation, photographic documentation and GPS measurements were used to determine typical plant species and characterise the main geobotanical units in the peninsula. Porewater salinities were determined (10 cm depth) in eleven topographically relevant sites. Vegetation height was estimated along 11 km of the road running the length of the peninsula. Every 100 to 300 m pictures of the forest were taken at both

sides of the road and including a 6 m height gauge as reference. This was not only logistically convenient but also relevant for this work, since the road was built along a high-topography, low-inundation line. Picture digitalisation permitted precise measurement of all trees in each photographed sector. Topographic surveys complemented elevation data from Cohen et al. (2000) and provided the information for elaborating a topographic map and calculating inundation frequencies using tidal data from the DHN (Hydrographic Division of the Brazilian Navy, 1999).

4.2.3 Image processing

A mosaic of airborne radar images (Band X) taken on April 1972 was released by the Federal University of Pará. Radar images allow discrimination of areas with different vegetation coverage due to the sensitivity of radar signals to target roughness. Five LANDSAT images obtained on September 1990, December 1991, August 1986, 1988 and 1997 were obtained from INPE (National Institute of Space Research, Brazil). A three-colour band composition (RGB 543) image was created and processed using the ERMAPER 5.5 image processing system. Further processing included:

- 1) Digitalisation of vegetation cover limits of individual images and posterior layer overlap using georeferenced points to develop a time-series. Image texture, object size and shape features allowed a clear delimitation of the dense mangrove areas, due to its contrast with other adjacent vegetation types. Coverage losses and gains were identified and quantified.
- 2) Acquisition of aerial photographs (April 1999). Twenty sites were checked to validate the classification of vegetation cover derived from satellite image analyses.
- 3) Selection of areas for field validation of satellite and aerial images and for more detailed evaluation of changes in vegetation coverage. Internal elevated flats and degraded mangrove areas in central and peripheral sectors of the peninsula were chosen.

4.3 Results and discussion

4.3.1 Geobotanical units

Figure 4.2a shows a longitudinal transect across the peninsula with the main topographical features and vegetation units. Elevated flats in the inner part of the peninsula are flooded much less frequently (<28 days/yr) than mangrove vegetated areas, and only by the highest spring tides. These flats constitute a hypersaline habitat, at least during the dry season, with porewater salinities reaching 90 and 100 (Figure

4.2a). Vegetation in the elevated flats is dominated in the dry season by the Gramineae *Sporobolus virginicus* and in the rainy season by the Cyperaceae *Eleocharis geniculata* and *Fimbristylis spadicea*.

This area ends smoothly in a wide extension of mudflats covered by mangroves, which extend for 3–6 km down to the mid-tide mark. These mudflats have gradients of around 1:3000, being dissected by creeks which are much deeper than those in the elevated flats. The upper mudflats are inundated only during normal spring tides (28–78 days/yr) with porewater salinity between 90 and 50 and consist mainly of *Avicennia*. At about mid-tide level, a slope break occurs and an area of relatively steep, frequently flooded (~233 days/yr) mudflats with porewater salinity around 36 and mixed mangrove forest leads down to *Rhizophora*-dominated sectors fringing the low-tide mark.

Similar patterns were identified by Santos et al. (1997) in the mangrove of Maranhão (Northern Brazil) with porewater salinities between 35 and 50 around the mean high tide level. Exceptionally occur a hypersaline small *Avicennia germinans* zone with porewater salinities around 80, positioned between the mean high tide level and the mean spring tide level, limited by a hypersaline tropical salt marsh communities with porewater salinities between 90 and 100 and close to the mean spring tide level.

In Braganca peninsula, tree heights did not exhibit any major differences on the two sides of the road and were therefore averaged for each measuring point along the investigated transect. There was a clear inverse correlation between tree height and topography, reflecting a close correlation between inundation frequency and vegetation structure (Figure 4.2a).

4.3.2 Coastline vegetation changes

Analysis of image time series indicates net losses of mangrove coverage along a coastline of ~166 km length, including the Bragança coastal plain and adjacent areas (Figure 4.4). Vegetation death was mainly caused by erosion and/or landward sand migration, as well as deposition on top of older mud sediments (Figure 4.3a, 4.3b, 4.3c). During the 1972–1997 period, losses were registered along ~42% of the coastline length. For the same period, no changes were observed along 39% of the coastline, while coverage gains occurred along 19%. Detailed coverage changes during the 1972–1986, 1986–1991 and 1991–1997 periods are given in Table 4.1.

In 1972, the study area had mangrove vegetation coverage over an area of about 592 km², which progressively declined to 585, 583 and 573 km² in 1986, 1991 and 1997,

respectively. Local tendencies in respect of coverage gain or loss were consistent for almost the whole studied area during the investigated period. In the 1972–1997 period, the overall net loss of vegetation coverage was 19 km², representing a total net loss of 3.19%, which is ~0.76 km²/yr. On average, about 0.13% of the coverage was lost per annum, but the trend seems to have intensified in the 1991–1997 span (Table 4.1).

Gross coverage loss increased from 0.22 to 0.30 to 0.32%/yr during the three periods assessed from 1972 to 1997 (Table 4.1). The overall annual rate of gross coverage gain increased from 0.13%/yr in 1972–1986 to 0.24%/yr in 1986–1991, decreasing sharply to 0.046%/yr in 1991–1997. This indicates that during the last period, in addition to an increase in gross loss, vegetation expansion had also stopped, even in the areas with previous gross gains where abiotic conditions should be more favourable for vegetation growth. This is the case, for example, on the west coast of Boiuçucanga Island (Figure 4.3a), which had a gross coverage gain of 0.55 km² between 1972 and 1986, presenting no gains but gross losses in the last two periods. At the mouth of the Furo do Chato tidal creek, gross gains decreased throughout the three investigated periods from 0.15 to 0.063 to 0 km².

At the present rates, mangrove vegetation on some islands may soon disappear. For example Maiiau Island (Figure 4.3c) presented insignificant gross gains over the last 25 years, while the annual rate of net loss has increased (Table 4.1). An extrapolation of these trends suggests that all the mangrove vegetation on this island may perish within the next 15 years, perhaps sooner.

If the rate of net coverage loss – 3.19% in 25 years – persists, the mangroves in the studied region will disappear almost entirely in approximately 750 years. However, this may be a conservative estimate. The global mean sea level has risen approximately 1–2 mm y⁻¹ during the past 100 years (Gornitz, 1995), and this rate is predicted to increase 2–5 fold by the year 2100 (Titus and Narayanan, 1995; Biljsma, 1996). The sea level could rise about 80 cm by the year 2100 or 2200 (Titus and Narayanan, 1995). In the Bragança coastal plain, mangroves occur within a topographical range of ~1.0 m between their boundaries and the inner peninsula. Thus, in this scenario, the distribution of mangroves would be restricted in 100–200 years to narrow bands along the estuary, which would retreat landward, leaving only small, mangrove-covered islands with more elevated topography.

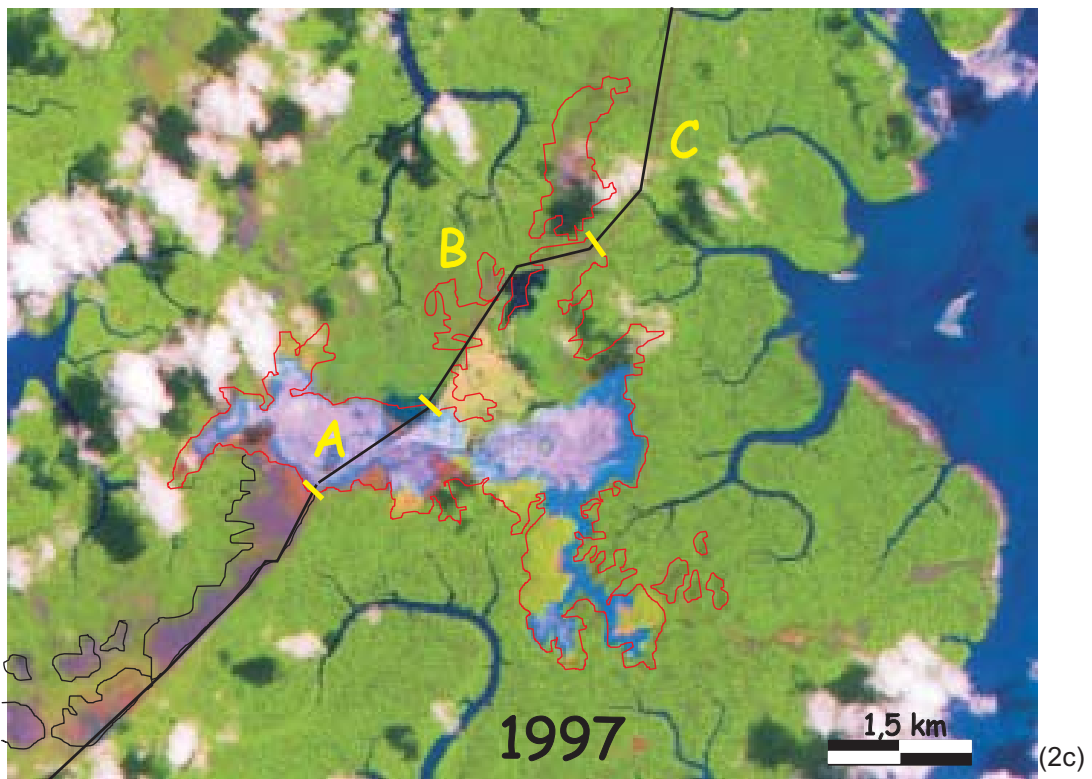
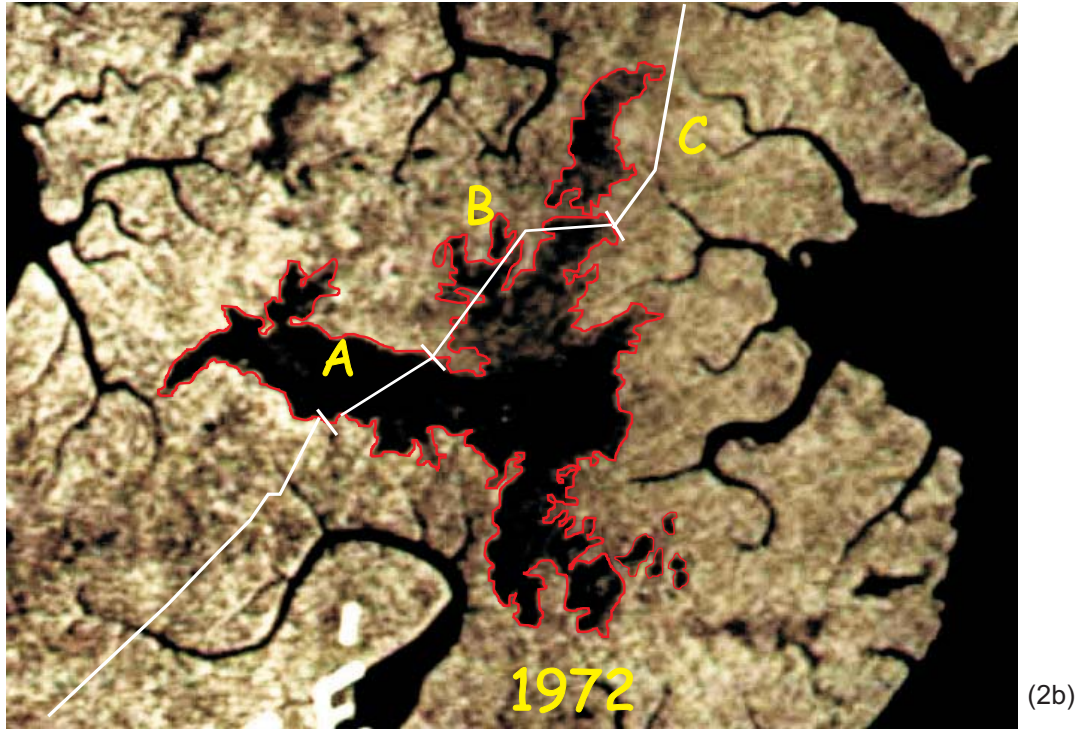
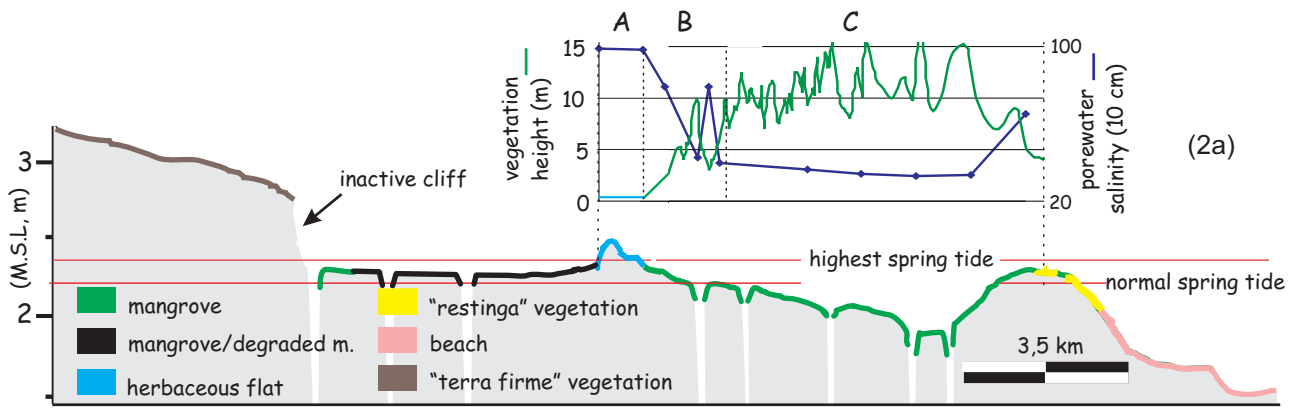


Figure 4.2 Topographic profile of the Bragança Peninsula related to mean sea-level (MSL) with the vegetation units, porewater salinities (dry season) and mangrove vegetation height (2a). Temporal analysis between a RADAR (2b) and satellite images (2c) takes on 1972 and 1997, respectively.

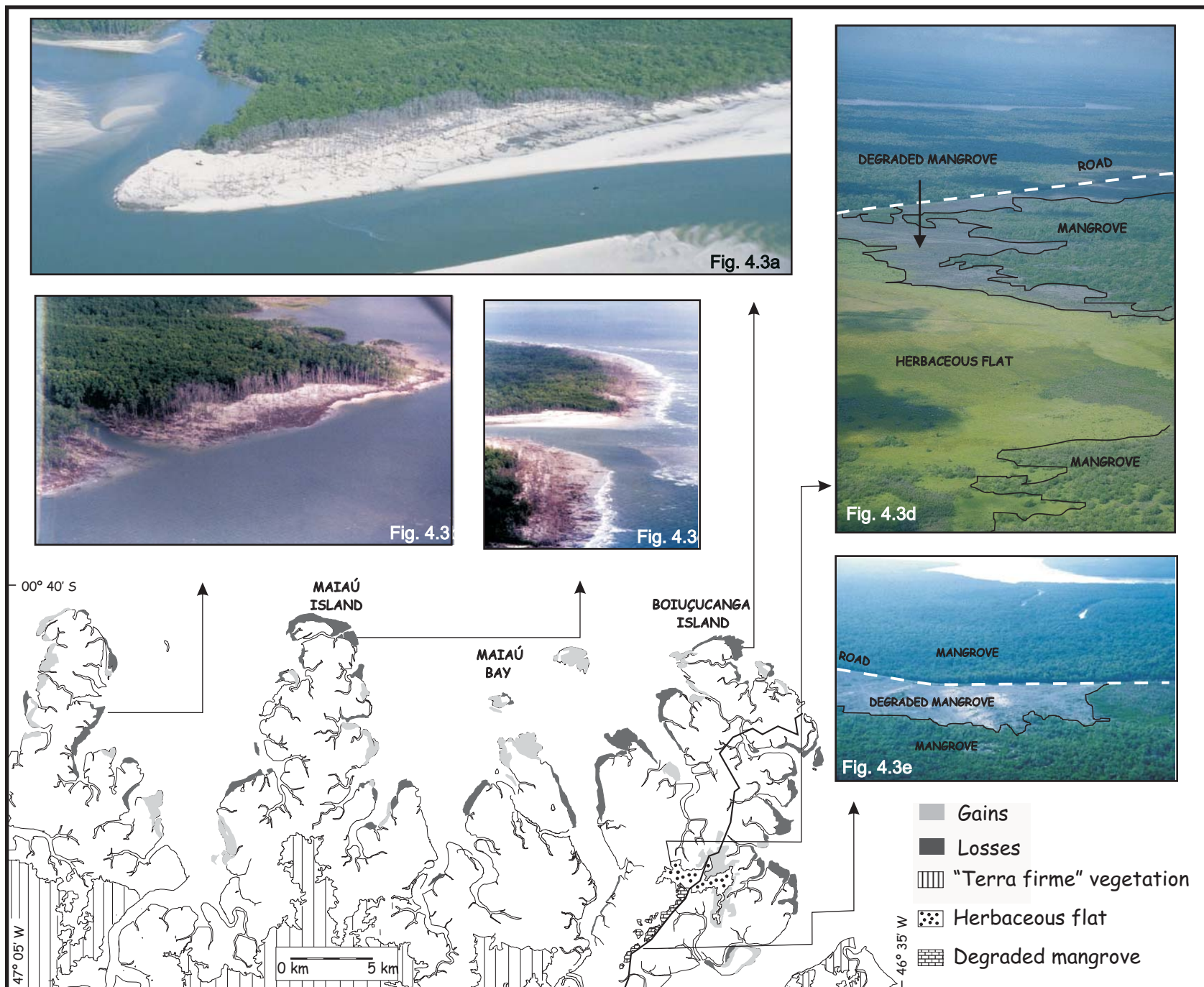


Figure 4.3 Evolution of coastal vegetation according to the analysis of RADAR and satellite images covering an 25-year period (1972-1997). Figures 3a, 3b, 3c, 3d and 3e: aerial photographs of the inner and outer mangrove.

Nevertheless, loss rates should be interpreted with caution, since the driving forces of this process may be multiple and interrelated. Sand deposition causing mangrove death may be caused not only by transgression, but also by littoral drift currents generated by waves (Suguio et al., 1985). Furthermore, the Pará-Amazon-Orinoco plain is characterised by chernier formation (Price, 1955), which is induced by the dominant winds and currents and could cause cyclical, increased sand migration. The coasts of Suriname have extensive, shore-oblique mudshoals separated by troughs, considered as giant mudwaves with a migration period of ~30 years. The cheniers may grow between the mudflats (Augustinus, 1980). Until now, there have been no investigations dealing with the periodicity of formation of such geofoms in our study region. It is possible that recurrent, large-scale oscillations of wind or current regimes generate modifications in local sediment dynamics, inducing periods of prevailing gains or losses in the mangrove coverage along the coastline.

If this phenomenon is merely a periodic oscillation, there must be evidence for cycles of death and recolonisation at the marginal zones of the ecosystem. The satellite images used in this work show the presence of several paleo-cheniers or beach ridges partially covered by vegetation on this and neighbouring peninsulas (Szlafsztein, unpublished). Thus, it is unclear to what extent the observed vegetation losses represent a short-term oscillation around 'steady state' conditions, or whether it is consequence of a long-term, more generalised phenomenon, such as sea-level rise.

4.3.3 *Vegetation changes* in the central peninsula

Significant net losses of herbaceous vegetation coverage have occurred in the elevated flats over the past 25 years. In 1972, coverage was 9.04 km², which progressively declined to values of 7.07, 6.33, 6.19, 6.15 and 5.64 km² in 1986, 1988, 1990, 1991 and 1997, respectively. For the 1972–1997 period, this was equivalent to a net coverage loss of 3.4 km², which is ~38% of the 1972 value. The average coverage loss rate was 1.6%/yr. Detailed coverage changes in the 1972–1986, 1986–1991 and 1991–1997 periods are shown in Table 4.2.

The central area (Figure 4.2, limit between sector A and B) shows signs of an active transition between herbaceous vegetation and mangrove forest, with coexistence of the Graminea *Sporobolus virginicus*, the Aizoaceaea *Sesuvium portulacastrum* and small *Avicennia* trees (0.5-2 m). The progression of the mangrove front in this area is highly dynamic and can be clearly traced between 1972 and 1997 (Figures 4.2b and 4.2c).

Table 4.1 Data of vegetation change in the Bragança coastline.

| Overall | 72-86 | 86-91 | 91-97 | 72-97 |
|--|--------------|--------------|--------------|--------------|
| Initial mangrove area (km ²) | 592 | 585 | 583 | 592 |
| Loss along coastline (%) | 37 | 40 | 42 | 42 |
| Gain along coastline (%) | 19 | 16 | 5 | 19 |
| Stable coastline (%) | 44 | 44 | 53 | 39 |
| Gross loss (km ²) | 18 | 9 | 11 | 38 |
| Gross gain (km ²) | 11 | 7 | 2 | 20 |
| Net loss (km ²) | 7 | 2 | 10 | 19 |
| Net loss rate (km ² /yr) | 0,5 | 0,4 | 1,6 | 0,8 |
| Percentage of net loss (%) | 1,2 | 0,3 | 1,6 | 3,2 |
| Gross loss rate (%/yr) | 0,2 | 0,3 | 0,3 | 0,3 |
| Gross gain rate (%/yr) | 0,1 | 0,2 | 0,0 | 0,1 |
| Net loss rate (%/yr) | 0,1 | 0,1 | 0,3 | 0,1 |
| Maiiau Island | | | | |
| Initial mangrove area (km ²) | 5,2 | 3,2 | 2,5 | 5,2 |
| Gross loss (km ²) | 2,0 | 0,7 | 0,9 | 3,5 |
| Gross gain (km ²) | 0 | 0 | 0,1 | 0,1 |
| Net loss (km ²) | 2,0 | 0,7 | 0,8 | 3,4 |
| Boiuçucanga Island | | | | |
| Initial mangrove area (km ²) | 3,9 | 3,9 | 3,5 | 3,9 |
| Gross loss (km ²) | 0,6 | 0,3 | 0,6 | 1,5 |
| Gross gain (km ²) | 0,5 | 0 | 0 | 0,5 |
| Net loss (km ²) | 0,0 | 0,3 | 0,6 | 1,0 |
| T. Creek "Furo do Chato" | | | | |
| Initial mangrove area (km ²) | 1,8 | 1,7 | 1,6 | 1,8 |
| Gross loss (km ²) | 0,3 | 0,1 | 0,3 | 0,7 |
| Gross gain (km ²) | 0,1 | 0,1 | 0,0 | 0,2 |
| Net loss (km ²) | 0,1 | 0,0 | 0,3 | 0,5 |

Table 4.2: Data of vegetation change in the inner Bragança peninsula.

| | 72-86 | 86-88 | 88-90 | 90-91 | 91-97 | 72(86*)-97 |
|--|--------------|--------------|--------------|--------------|--------------|-------------------|
| Initial herbaceous flat (km ²) | 9,9 | 7,1 | 6,3 | 6,2 | 6,2 | 9,9 |
| Net loss (km ²) | 2,9 | 1,7 | 0,2 | 0,0 | 0,5 | 4,3 |
| Net loss rate (%/yr) | 2,1 | 5,2 | 0,3 | 0,0 | 1,5 | 1,7 |
| Initial degraded area* (km ²) | 0 | 3,8 | 3,3 | 3,1 | 3,0 | 3,8 |
| Net loss (km ²) | | 0,5 | 0,3 | 0,1 | 0,0 | 0,9 |
| Net loss rate (%/yr) | | 0,9 | 4,0 | 0,5 | 0,3 | 2,1 |

A similar process seems to have occurred before 1972 in the dark areas in the northern part of the central peninsula (Figure 4.2b, sector B and beginning of C, left road side). Topographically, this zone is the extension of the low-gradient, rapid-colonisation sector (central and upper part of Figure 4.1b) and may have been previously affected by increasing flooding frequencies. This possibility seems to be corroborated by a regular increase in tree height in a forest dominated by *Avicennia*,

which exhibits a smooth gradient extending from 0.5 m where it meets with herbaceous vegetation, and 10 m close to the channel and the older mangrove (Figure 4.2a, sector B). Ongoing pollen analysis and ^{14}C -dating on sediments along this transect will help assess the former boundaries of the herbaceous flats and the dynamics of invasion by a transgressive mangrove.

The low tree heights may be mostly due to the fact that trees have established relatively recently. Nevertheless, at several sites along the mangrove expansion front, trees seem to be growing under higher salinity stress (Figure 4.2a). Therefore, it is probable that salt leaching as a result of increasing inundation frequency is displacing the boundaries of high soil salinity areas, expanding the area where mangroves can grow.

A similar effect caused by a sustained trend of increasing rainfall seems unlikely. The analysis of a 25-year rainfall data set from a neighbouring meteorological station (Traquateua) did not reveal such a pattern for the investigated period, but instead a clear inverse relationship to the intensity of El Niño events (Lara, unpublished). Vetter and Botosso (1989) reported correlations between rainfall, El Niño strength and growth ring thickness in trees of Central Amazonian trees. However, to our knowledge, this kind of dependence has not been investigated for mangrove forests as yet.

Degraded areas are found close to the centre of the peninsula (Figure 4.1a), consisting of almost dry mudflats with remains of what are mainly *Avicennia* trees. The 1972 image does not show any signs of mangrove degradation, so these areas most likely originated after the road connecting the city of Bragança with the beaches in the north of the peninsula (Ajurutea) was constructed in 1974. In these areas, the low inundation frequency must have determined the existence of a mangrove ecosystem that probably subsists near tolerance limits under flooding conditions and is therefore particularly sensitive to hydrological perturbations.

In the period from 1986 to 1997, the size of the degraded area decreased by about 24% (Table 4.2) due to the growth of new mangrove trees. Degraded areas are found only on the west side of the road (Figures 4.3d, 4.3e), which suggests it was mainly the tide reaching the area from the east side that maintained inundation conditions, thus permitting mangrove survival in the period before the road was built. Thus, recolonisation may have been favoured by an increase in the frequency with which tides flood the area from the west side. Recolonisation currently seems to be levelling off, as suggested by the annual percentage decline in degraded area. These rates decreased

progressively from 6.3%/yr in 1986–1988 to 0.06%/yr in 1991–1997 (Table 4.2). In the 1988–1991 period, mangrove advance into the elevated flats also slowed down. These rate decreases in both study areas may be related to the slightly steeper topography in the central part of the peninsula, which would prevent an significant increase of inundation frequency until a determined topographic threshold is exceeded.

The vegetation distribution on the Bragança peninsula follows well-known patterns, including close links between plant assemblages and topographically defined habitats (Baltzer, 1970), where salinity excludes competing, intolerant species (Snedaker, 1978). Soil salinity is basically controlled by flooding frequency and position along the estuarine gradient (Lara, unpublished), leading to characteristic patterns of species zonation and predictable types of community structure (Menezes, unpublished). Thus, the observed adjustment of the new limits of the mangrove habitat in the inner peninsula are coherent with the postulated increase in inundation frequency. This is further supported by the existence of zones of rapid and slow change, which are related to different topographic features. The most significant mangrove progression occurred in the northeast and east portions of the elevated flats, where the topographical gradients are smoother than in the west part (Figure 3.1b). In the case of the degraded area, the more substantial recolonisation occurred in the central portion, which has a lower topography combined with smooth gradients. If the rate of net coverage loss of $\sim 3.39 \text{ km}^2$ (37.53%) in 25 years persists, the herbaceous elevated flats in the Bragança peninsula would disappear in ~ 65 years, with probable substitution by low *Avicennia* forests.

The increase in mangrove coverage in the inner peninsula cannot compensate the losses registered at the coastline, since low-topography areas are more extensive than high ones. In 25 years, losses at the coastline reached $\sim 7.7 \text{ km}^2$, while gains in the internal area were only $\sim 3.4 \text{ km}^2$. Landward mangrove migration will probably be obstructed by a line of inactive cliffs of ~ 1 m height at ~ 25 km from the modern coastline and sculpted at the coastal plateau. This has been described by Souza Filho (1995) as remainder of the highest Holocene sea level.

4.4 Conclusions

The current dynamics of vegetation coverage loss seem to be compatible with a long-term trend related to the predicted rates of sea-level rise usually found in the literature. Despite other possible causes for mangrove death along the coastline, such as littoral

drift currents or cyclical changes in coastal sediment dynamics, the invasion of mangrove into herbaceous elevated flats in the central peninsula cannot be attributed to these factors. The topography-dependent dynamics of this process strongly suggests an increase in inundation frequency, changes in soil salinity and the transportation of mangrove seeds into more elevated areas. Therefore, it would appear that sea-level rise may be a common forcing agent driving mangrove death in the periphery and mangrove advance into the central part of the Braganca peninsula. A strong correlation between tree height and topography-dependent inundation frequency may help mid-term monitoring of this process.

Chapter 5
STUDIES ON HOLOCENE MANGROVE
ECOSYSTEM DYNAMICS OF THE BRAGANÇA
PENINSULA IN NORTHEASTERN PARÁ, BRAZIL⁴

⁴ Behling, H., Cohen, M. C. L., Lara, R. J., 2001. Studies on Holocene mangrove ecosystem development and dynamics of the Bragança Peninsula in northeastern Pará, Brazil. *Palaeogeography, Palaeoclimatology, Palaeoecology* 167, 225-242.

Abstract

Three sediment cores from the Bragança Peninsula located in the coastal region in the north-eastern portion of Pará State have been studied by pollen analysis to reconstruct Holocene environmental changes and dynamics of the mangrove ecosystem.

The cores were taken from an *Avicennia* forest (Bosque de *Avicennia* (BDA)), a salt marsh area (Campo Salgado (CS)) and a *Rhizophora* dominated area (Furo do Chato). Pollen traps were installed in five different areas of the peninsula to study modern pollen deposition. Nine accelerator mass spectrometry radiocarbon dates provide time control and show that sediment deposits accumulated relatively undisturbed. Mangrove vegetation started to develop at different times at the three sites: at 5120 14C yr BP at the CS site, at 2170 14C yr BP at the BDA site and at 1440 14C yr BP at the FDC site. Since mid Holocene times, the mangroves covered even the most elevated area on the peninsula, which is today a salt marsh, suggesting somewhat higher relative sea-levels. The pollen concentration in relatively undisturbed deposits seems to be an indicator for the frequency of inundation. The tidal inundation frequency decreased, probably related to lower sea-levels, during the Late Holocene around 1770 14C yr BP at BDA, around 910 14C yr BP at FDC and around 750 14C yr BP at CS. The change from a mangrove ecosystem to a salt marsh on the higher elevation, around 420 14C yr BP is probably natural and not due to an anthropogenic impact. Modern pollen rain from different mangrove types show different ratios between *Rhizophora* and *Avicennia* pollen, which can be used to reconstruct past composition of the mangrove. In spite of bioturbation and especially tidal inundation, which change the local pollen deposition within the mangrove zone, past mangrove dynamics can be reconstructed. The pollen record for BDA indicates a mixed *Rhizophora/Avicennia* mangrove vegetation between 2170 and 1770 14C yr BP. Later *Rhizophora* trees became more frequent and since ca. 200 14C yr BP *Avicennia* dominated in the forest.

Keywords: Holocene; Pollen analysis; Mangrove dynamics; Salt marshes; Coastal evolution; Sea-level; North Brazil

5.1 Introduction

The Brazilian coastal region holds, with ca. 13 800 km² (Kjerve and Lacerda, 1993) one of the world's largest mangrove areas. Mangroves grow on intertidal mudflats and form a linkage between terrestrial and marine environments. The ecosystem is highly productive and an important economic resource for people living in the coastal region.

Future natural and/or human related changes of the mangrove ecosystem might substantially impact the economy and society of the coastal region. Background information on the natural history is important to understand modern environmental changes and dynamics of mangroves.

The Holocene development of mangrove ecosystems is not well known and their dynamics are poorly understood. An important factor affecting the development and dynamics of mangrove belts are past and recent sea-level changes. Many studies on Holocene relative sea-level changes focused on the east Brazilian coastal region (e.g. Angulo and Lessa, 1998; Martin et al., 1988; Suguio et al., 1985; Pirazolli, 1986; Mesquita and Leite, 1985; Silva and Neves, 1991; Silva, 1992; Muehe and Neves, 1990). However, little information exists on Holocene relative sea-level changes and coastal evolution for the north Brazilian coast (e.g. Behling and da Costa, 1997, 2001; Souza Filho, 1995).

To study the mangrove ecosystem in northern Brazil, an international and interdisciplinary research project, “Mangrove Dynamics and Management (MADAM)” has been initiated in 1996. The study area of this project is located at the coastal region of Bragança City in north-eastern Pará State, where large mangrove areas occur. This study deals with past environmental changes, such as coastal evolution, sea-level oscillations, development and dynamics of the mangrove ecosystem. Several sediment cores were collected from the Bragança Peninsula for pollen analysis and radiocarbon dating. Studies on past environmental changes using biomarkers will be published elsewhere. Studies of modern pollen rain from different vegetation types were also carried out. Although disturbance of sediment deposits by bioturbation and inundation could complicate the interpretation of the pollen analyses. This study shows that sedimentary deposits from within the mangrove zone can be used to reconstruct the dynamics of mangrove ecosystems.

5.2 Study area

5.2.1 Location

The study region is situated on the Bragança coastal plain, which is part of the mangrove belt along more than 370 km of coastline between the city of Belém and the Gurupi River in north-eastern Pará State (Figure. 6.1).

5.2.2. Environmental characteristics of the Bragança Peninsula

The relatively plain surface of the peninsula is deeply dissected by mangrove-lined channels. Several vegetational units are found on the peninsula:

1. small “islands” of unflooded forests;
2. salt marshes;
3. several different mangrove types;
4. restinga;
5. coastal grassland (campo de dunas), stable and movable dune vegetation.

The distribution of these units is related to topography, physical processes and other environmental factors such as inundation frequency and salinity.

1. Isolated forests, up to 25 m tall occur on several elevated areas in the central part of the peninsula, surrounded by salt marshes and mangroves. The species composition of these forest islands has not been studied, but it seems to relate to both Amazon terra firme forest and restinga vegetation.

2. The non-forested salt marsh areas of the central peninsula region cover ca. 3 - 4 km² and occur on slightly lower elevations than the forest islands. Salt marshes are at slightly higher elevations than mangroves. Marshes are infrequently flooded and only by the highest spring tides. Salt marsh species are *Eleocharis geniculata*, *Fimbristylis spadicea* (Cyperaceae) and *Sporobolus virginicus* (Poaceae) (Moirah P.M. Menezes, personal communication).

3. The major part of the peninsula is covered by 10 - 25 m tall, well developed mangrove vegetation. Important species are *Rhizophora mangle*, *Avicennia germinans* and *Laguncularia racemosa*. There are distinct mangrove types. On relatively high elevated areas in central parts of the peninsula *Avicennia* dominates. In intermediate areas *Rhizophora* and *Avicennia* co-occur, while on lower lying areas, including the borders of tidal creeks and channels, *Rhizophora* dominates. Shrubby 2 - 3 m tall scattered *Avicennia* stands occur in transition zones to the higher elevated salt marsh area. *Laguncularia* occurs everywhere in the mangroves, but dominates only in disturbed sites, e.g. channel borders (Thüllen and Berger, 2001). The composition and distribution of the mangrove species is related to several environmental factors such as the salinity, which depends on the frequency of inundation. A decreased frequency of inundation provokes an increase of salinity. Studies show an increase in salinity from *Rhizophora* dominated forests to *Avicennia* dominated forests and to salt marshes (Cohen et al., 2001; Reise, 1999).

4. Restinga and 5. Coastal grassland vegetation (campo de dunas) occur on sand plains and on stable and movable dunes in the form of small patches in the northern part of the peninsula close to the shore line. Studies of the floristic composition of these species-rich vegetation types are in progress. Published floristic data on the restinga are available from other coastal regions of northeastern Pará and indicate the predominance of Cyperaceae, Poaceae, *Humiria balsamifera*, *Byrsonima crassifolia*, *Chrysobalanus icaco*, *Anacardium occidentale* and others (Bastos, 1988; Santos and Rosário, 1988).

5.2.3 Human impact on vegetation

The major impact on the mangrove ecosystem, occurred since 1986, related to the construction of a 35 km long road connecting Bragança with the small fishing village Ajuruteua in the northernmost part of the peninsula. It is unclear whether the central salt marsh can be considered a natural vegetation, because at least since 1986 the area has been used for cattle grazing. Strong evidence for human impact is found near the central part of the peninsula (west of the road) where many *Avicennia* trees were cut in the last a few years, resulting in a strongly degraded mangrove area (Fig. 6.1).

5.2.4 Study sites

Three different areas were selected for collecting sediment cores (Fig. 6.1). The first site, “Bosque de *Avicennia* (BDA)” (00° 55’65” S, 46° 40’ 09” W, 2.4 m a.s.l), is located on the relatively high central southern part of the peninsula. Tidal creeks and channels are at least 500 m distant from core site, and the area seems to be little disturbed by tidal inundations. Only *Avicennia* trees form the mangrove forest. A high number of dead trees are found in this area. The second site, “Campo Salgado (CS)” (00° 54’ 46” S, 46° 40’63” W, 2.7 m a.s.l), is in Cyperaceae-dominated open salt marsh in of the central part of the peninsula. The area is about 3 - 4 km² large and at a slightly higher elevation than the first site. The third site, “Furo do Chato (FDC)” (00° 52’25” S, 46° 39’ 00” W, 1.9 m a.s.l), is in the northern part of the study area and at lower elevation than the two other sites. Here *Rhizophora* trees dominate in the mangrove, but *Avicennia* trees occur close to the site. The core site is near tidal channels and is more influenced by inundations than the other two sites. The frequency of tidal inundations for the three sites is 74 days/yr for BDA, 28 days/yr for CS and .233 days/yr for FDC (Cohen et al., 2001). For collection of modern pollen rain data, pollen traps were installed in five different vegetation types of the Bragança Peninsula (Figure 6.1): (A) in

the tall *Rhizophora* and *Avicennia* mixed forest area called “Bosque de *Rhizophora/Avicennia* (BDR/A)” (00° 56’91” S, 46° 44’ 15” W), (B) in the *Avicennia* dominated forest “BDA” (00° 55’65” S, 46° 40’09” W), (C) in the salt marsh “CS” (00° 54’ 46” S, 46° 40’63” W), (D) in the *Rhizophora* dominated forest “FDC” (00° 52’25” S, 46° 39’00”W), and (E) in the restinga vegetation called “Restinga” (00° 51’40” S, 46° 36’37” W).

5.3 Material and methods

5.3.1 Field sampling

Three sediment cores were collected in 50 cm long sections, using a Russian Sampler. The core ‘BDA’ is 640 cm long. The core ‘CS’ is 134 cm long and the core ‘FDC’ is 180 cm long. After stratigraphic description, and sub-sampling for pollen analysis and radiocarbon dates, core sections were stored in the refrigerator. For collection of modern pollen rain data, 25 plastic tube pollen traps were installed in the field in five different regions. The distance between the five traps set up in each region was ca. 10 m. The plastic tubes, 11.5 cm high and 2.7 cm in diameter, were filled with 5 cm³ of glycerine and covered with a nylon mesh. In the mangrove and salt marsh area, pollen traps were installed between 30 and 100 cm height above the surface to avoid inundation. In the restinga area, traps were put at 10 cm height above the surface. The collecting period was one year, from November 1998 to November 1999.

5.3.2 Pollen analysis

For pollen analysis, 0.5 or 1 cm³ sediment samples were taken at 5 cm, 10 cm or 20 cm intervals along the cores. Prior to processing sediment and pollen rain samples, one tablet of exotic *Lycopodium* spores was added to each sample for calculation of pollen concentration (grains/cm³) and pollen accumulation rate (grains/cm²/yr). All samples were prepared using standard pollen analytical techniques including acetolysis (Faegri and Iversen, 1989). Sample residues were mounted in a glycerin gelatin medium. For identification of pollen grains and spores published pollen morphological descriptions were consulted (Behling, 1993; Herrera and Urrego, 1996; Roubik and Moreno, 1991), as well as the first author's own reference collection. A minimum of 300 pollen grains were counted. In a few cases only 200 grains were counted. The total pollen sum excludes fern spores, fungal spores, algae and micro-foraminifers. Pollen and spore data are presented in pollen diagrams as percentages of the total pollen sum. Taxa were

grouped into mangrove, palms, other shrubs and trees, herbs, aquatics, fern spores, fungal spores, algae and micro-foraminifera. The software Tiliagraph was used to plot the pollen diagrams. Tilia was used for calculations and Coniss was used for the cluster analysis of terrestrial pollen taxa (Grimm, 1987).

5.4 Results

5.4.1 Stratigraphy

The stratigraphic description of the three cores is shown in Table 1. The sediments of the cores BDA and FDC consist of relatively homogenous deposits rich in organic matter, while the sediments of the core CS are mainly composed of silt deposits.

5.4.2 Radiocarbon dates and sedimentation rates

From each core, three samples of 1 cm thickness were taken and dated by accelerator mass spectrometry (AMS) at the Van der Graaff Laboratory of the University of Utrecht. The dates, shown in Table 2, provide time control and indicate that the studied sediment deposits accumulated relatively continuously. Bioturbation was apparently less significant than assumed. The base of the core BDA dates 2170 14C yr BP (extrapolated). Radiocarbon dates, as well as pollen concentrations, indicate that the lower core section (640-175 cm) has been deposited within 400 years, while the upper core section (175-0 cm) has been accumulated during the last 1770 years. The calculated sedimentation rates for either interval are 1.16 cm^3/yr and 0.1 cm^3/yr , respectively. The bottom of the core CS is dated 5115 - 35 14C yr BP. The base of core FDC has an age of 1437 - 35 14C yr BP. The lower part of this core (180-87.5 cm) has accumulated in 530 years, while the upper part (87.5-0 cm) has been deposited within 910 years. The calculated sedimentation rates for both intervals are 0.18 cm^3/yr and 0.1 cm^3/yr , respectively.

5.4.3 Description of modern pollen rain

Sixteen of the 25 installed pollen traps were used for the pollen analysis. A few traps were lost or were inundated by high spring tides. The results from the five different vegetation types on the Bragança Peninsula provide insights on modern annual pollen rain. Percentages of the most frequent pollen taxa and the pollen accumulation rate are shown in Figure 5.2. The total pollen accumulation rates show marked variations between the five different sites. Very high accumulation rates are from the mixed

Rhizophora/Avicennia (site BDR/A) and from the *Rhizophora* dominated forest area (site FDC) (average 15,370 and 14,040 grains/cm²/yr, respectively). Markedly lower are the rates from the *Avicennia* dominated forest area (site BDA) (average 2500 grains/cm²/yr), the salt marsh area (site CS) (average 1050 grains/cm²/yr), and the restinga area (average 1380 grains/cm²/yr).

Table 5.1 Stratigraphy from the cores Bosque de *Avicennia*, Campo Salgado and Furo do Chato

| | |
|----------------------------|---|
| Bosque de <i>Avicennia</i> | Grey-greenish organic material, compact, some plant remains and rootlets |
| 0-620 cm | Grey-greenish organic material, compact, some plant remains and rootlets |
| 620-640 cm | Grey organic material, fine sandy with some fine sandy layers and lens, compact |
| Campo Salgado | |
| 0-3 cm | Brown organic material, many sedge fragments |
| 3-12 cm | Black organic material with silt |
| 12-34 cm | Grey silt, compact, with a few plant remains |
| 34-64 cm | Light grey silt, compact, with a few plant remains, and spots of mottled material |
| 64-134 cm | Grey silt, somewhat fine sandy, compact, with a few plant remains and spots of mottled material |
| 134- | Grey fine sandy silt, very compact |
| Furo do Chato | |
| 0-35 cm | Light grey organic material, somewhat fine sandy and silty, several small spots of oxidised organic material (0.5 cm in diameter), with a few oxidised channels, very few rootlets and root fragments |
| 35-83 cm | Grey organic material, somewhat fine sandy and silty, compact |
| 83-175 cm | Light grey organic material, somewhat fine sandy, compact, rootlets, root fragments |
| 132-175 cm depth | very few root fragments |
| 175-180 cm | Grey organic material with several small layers of fine sand, silty, very compact |

Table 5.2 List of AMS radiocarbon dates for Bosque de *Avicennia*, Campo Salgado and Furo do Chato records

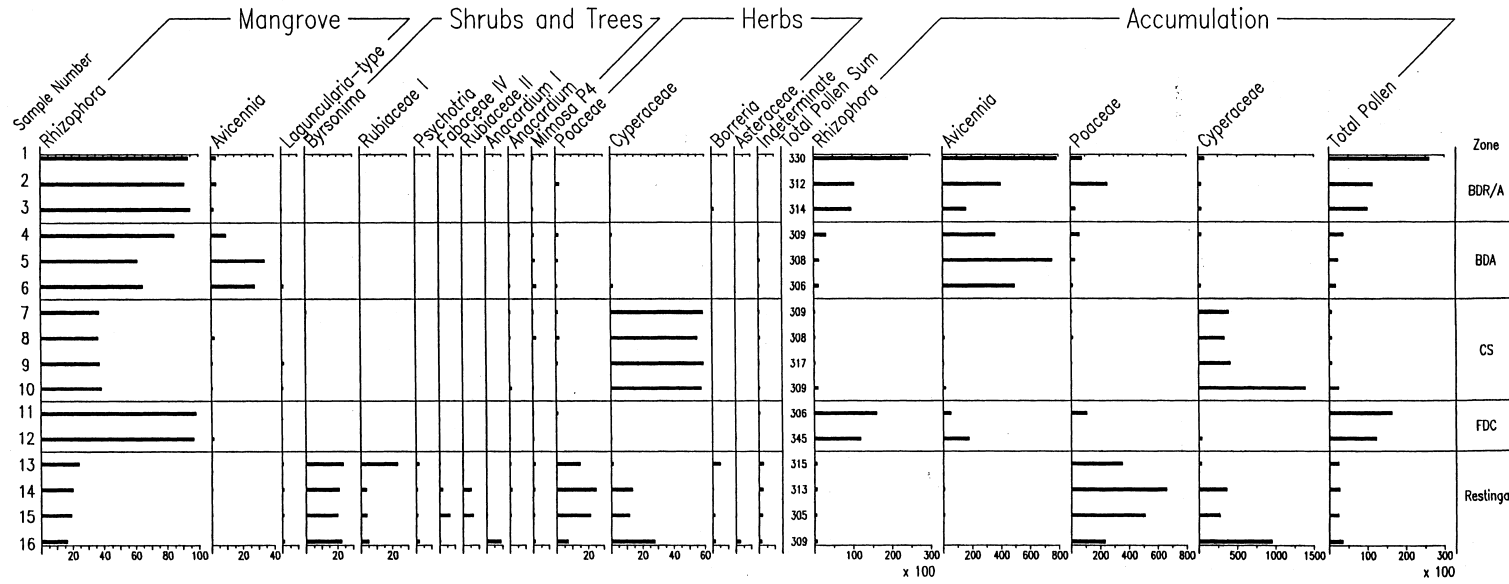
| Lab. number | Depth (cm) | 14C yr BP | 13C/12C (‰) | Calendar age (cal BP) |
|-----------------------------------|------------|-----------|-------------|-----------------------|
| Bosque de <i>Avicennia</i> | | | | |
| UtC-8722 | 40 | -15 ± 41 | -25.8 | Modern |
| UtC-8723 | 240 | 1830 ± 23 | -26.0 | 1818-1713 |
| UtC-8724 | 540 | 2088 ± 39 | -257.2 | 2119-1994 |
| Campo Salgado | | | | |
| UtC-8724 | 30 | 373 ± 25 | -26.9 | 483-434, 352-333 |
| UtC-8725 | 90 | 1018 ± 26 | -26.5 | 952-927 |
| UtC-8737 | 135 | 5115 ± 35 | -26.0 | 5913-5888, 5806-5764 |
| Furo do Chato | | | | |
| UtC-8719 | 30 | 2482 ± 23 | -28.5 | Modern |
| UtC-8720 | 120 | 1265 ± 25 | -25.3 | 1260-1196, 1193-1173 |
| UtC-8721 | 179 | 1437 ± 35 | -27.9 | 1349-1297 |

Highest percentage values of *Rhizophora* pollen grains are found in the mixed *Rhizophora/Avicennia* and on the *Rhizophora* (site FDC) dominated forest area (90-100%). Markedly lower are the percentages from the *Avicennia* dominated forest area (60-85%), the salt marsh area (35-40%) and the restinga area (15-25%). Pollen accumulation rate of *Rhizophora* is very high in the mixed *Rhizophora/Avicennia* forest area (average 14,750 grains/cm²/yr) and slightly lower in the *Rhizophora* dominated forest area (average 13,850 grains/cm²/yr). Accumulation rates from the *Avicennia* dominated area (average 1890 grains/cm²/yr), the salt marsh area (average 410 grains/cm²/yr) and the restinga area (average 530 grains/cm²/yr) are markedly lower.

Percentages of *Avicennia* pollen are high in the *Avicennia* dominated forest area (15-35%), and low in the mixed *Rhizophora/Avicennia* area (2-5%). Pollen traps of the other three sites show in average less than 1%. Accumulation rates of *Avicennia* pollen is high in the mixed *Rhizophora/Avicennia* forest area (average 450 grains/cm²/yr) and in the *Avicennia* dominated forest area (average 540 grains/cm²/yr), while rates are very low in the *Rhizophora* dominated forest area (average 120 grains/cm²/yr), the salt marsh area (average 8 grains/cm²/yr) and in the restinga area (average 4 grains/cm²/yr).

Results on modern pollen accumulation rates indicate that among the mangrove taxa *Rhizophora* is a high pollen producer, while *Avicennia* and *Laguncularia* are low pollen producers. This is plausible, because *Rhizophora* is wind pollinated whereas *Avicennia* and *Laguncularia* are insect pollinated (Menezes, 1997; Tomlinson, 1986). The pollen traps from the CS site, which are located at least 1-2 km distant from the closest

Braganca Peninsula
 Modern Pollen Rain (Nov. 1998 – Nov. 1999)
 Percentage pollen diagram



Rhizophora trees and 100 m distant from *Avicennia* shrubs, document an average of 410 *Rhizophora* grains/cm²/yr and an average of 8 *Avicennia* grains/cm²/yr. This indicates that a certain amount of *Rhizophora* pollen grains can be transported by wind, while wind transportation of *Avicennia* pollen is very low.

Traps from the CS site are primarily dominated by Cyperaceae pollen (55-60%), while the pollen rain from the restinga vegetation is mainly dominated by pollen grains of Rubiaceae I, *Byrsonima*, Poaceae, and Cyperaceae.

The proportions of *Avicennia* and *Rhizophora* pollen from the three mangrove sites are interesting. The *Rhizophora/Avicennia*-ratio (R/A-ratio) from the *Avicennia* dominated forest is 4:1, from the mixed *Rhizophora/Avicennia* forest 33:1, and from the *Rhizophora* dominated forest 115:1. These different R/A-ratios can be used to interpret past mangrove dynamics between the most important species *Rhizophora* and *Avicennia*.

5.4.4. Description of fossil pollen results

5.4.4.1. Bosque de *Avicennia*

In the pollen percentage diagram from the 640-cm long core of the *Avicennia* dominated area (Fig. 5.3) shows pollen sums of different groups and the most abundant pollen taxa out of the 80 different types which were identified. Six pollen types are unknown. Marked changes in the pollen assemblages, also illustrated by cluster analysis (Coniss), 3 pollen zones were recognised in the pollen record: zone BDA-I (640-175 cm: 2170-1770 14C yr BP, 24 samples), zone BDA-IIa (175-55 cm: 1770-180 14C yr BP, 12 samples), and zone BDA-IIb (55-0 cm: 180 14C yr BP-modern, 10 samples). Pollen concentration values are low in zone BDA-I (around 15,000 grains/cm³) high in zone BDA-IIa (around 40,000 grains/cm³) and even higher in zone BDA-IIb (around 70,000 grains/cm³). Pollen accumulation rates are higher in zone BDA-I (around 16,000 grains/cm²/yr) than in zone BDA-IIb (around 5000 grains/cm²/yr) and in zone BDA-IIa (around 7000 grains/cm²/yr). The pollen record of BDA is characterised throughout by the dominance of mangrove pollen, primarily by the high pollen producer *Rhizophora* (80-90%). The low pollen producers *Avicennia* (2-5%) and *Laguncularia* (1-2%) are represented by low values. Minor fluctuations occur between the frequency of *Rhizophora* and *Avicennia* pollen during the last 2170 14C yr BP. Percentages of *Avicennia* pollen are relatively high in zone BDA-I, lower in zone BDA-IIa and higher again in zone BDA-IIb. The calculated average *Rhizophora/Avicennia*-ratio for each

pollen zone is 41:1 (zone BDA-I), 64:1 (zone BDA-IIa) and 27:1 (zone BDA-IIb) (Fig. 5.5).

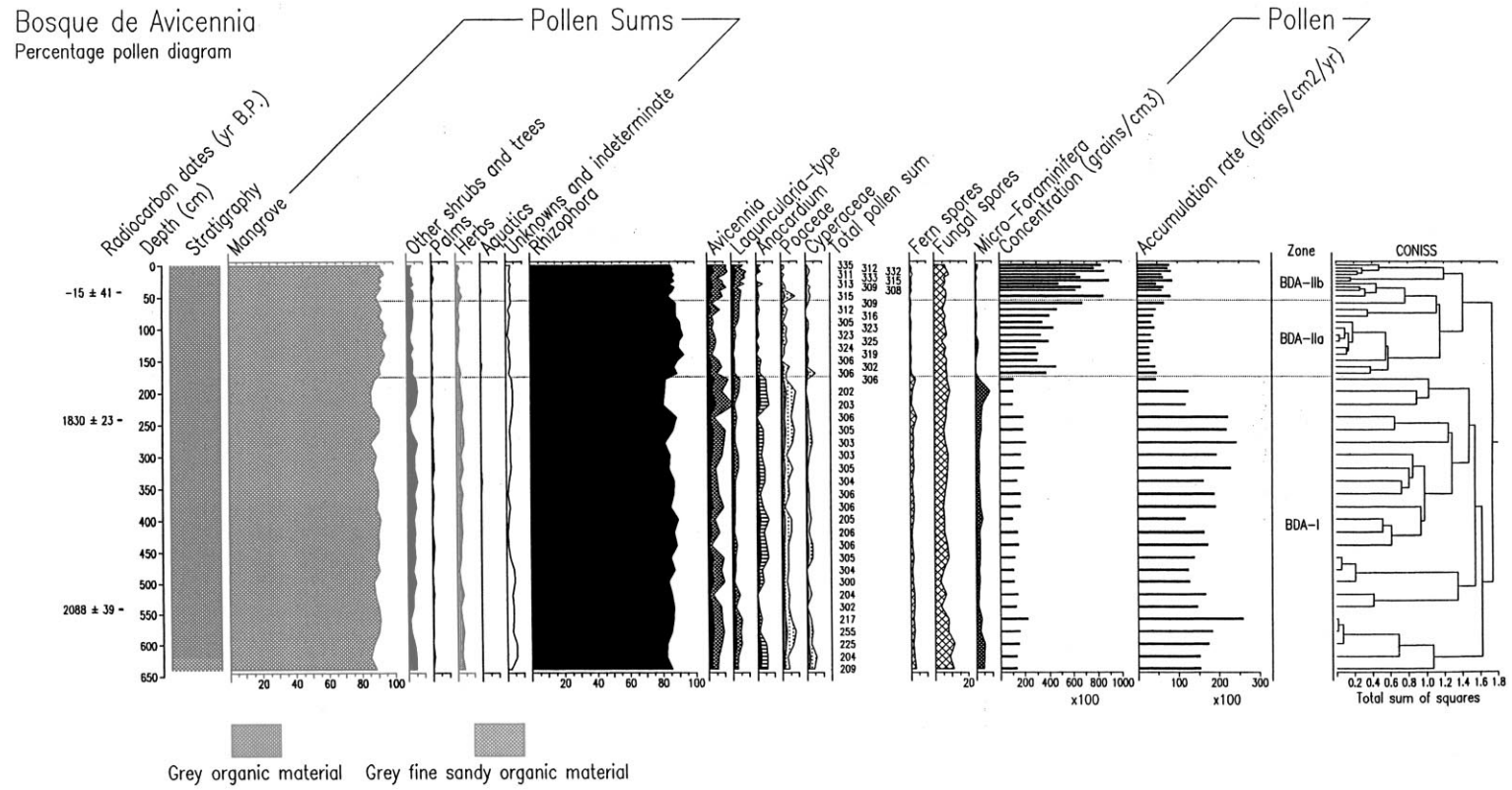
There are a high number of other different shrub and tree taxa, such as *Anacardium*, Moraceae/Urticaceae, Myrtaceae, *Virola*, Malpighiaceae, *Mimosa*, Fabaceae, *Didymopanax*, Symphonia, palms such as *Euterpe/Geonoma*-type, *Orbignya*-type, and herb taxa, e.g. Poaceae, Cyperaceae, Amaranthaceae/Chenopodiaceae, *Gomphrena/Pfaffia*, *Alternanthera* and *Borreria*. Most of these taxa are represented only by single pollen grains or less than 1%. Some taxa, such as *Anacardium*, *Mimosa*, Poaceae, Cyperaceae and *Borreria* and *Alternanthera* are somewhat more frequent. The presence of different pollen grains from other shrubs and trees (3-6%), palms (0-2%), herbs (2-4%), aquatics (,1%) and fern spores (1-3%) is relatively stable, but slightly lower in the zone BDA-II. Interesting is the markedly higher occurrence of marine micro-foraminifers in the sediment deposits of zone BDA-I (3-9%) than in zone BDA-II (1-2%).

The pollen percentage diagram from the 135-cm long core of the salt marsh site (Fig. 5.4) shows pollen sums of different groups and the most abundant pollen taxa out of 61 different types identified. Six types are unknown. Samples between 64 and 34 cm core depth (light grey silt deposits) contain pollen and spores mostly destroyed and are not included in the pollen diagram. Four pollen zones were recognised: zone CS-Ia (135-120 cm: 5120-3750 14C yr BP, 2 samples), zone CS-Ib (120-64 cm: 3750-750 14C yr BP, 9 samples), zone CS-II (34-17.5 cm: 420-200 14C yr BP, 3 samples), zone CS-III (17.5-0 cm: 200 14C yr BP-modern, 4 samples).

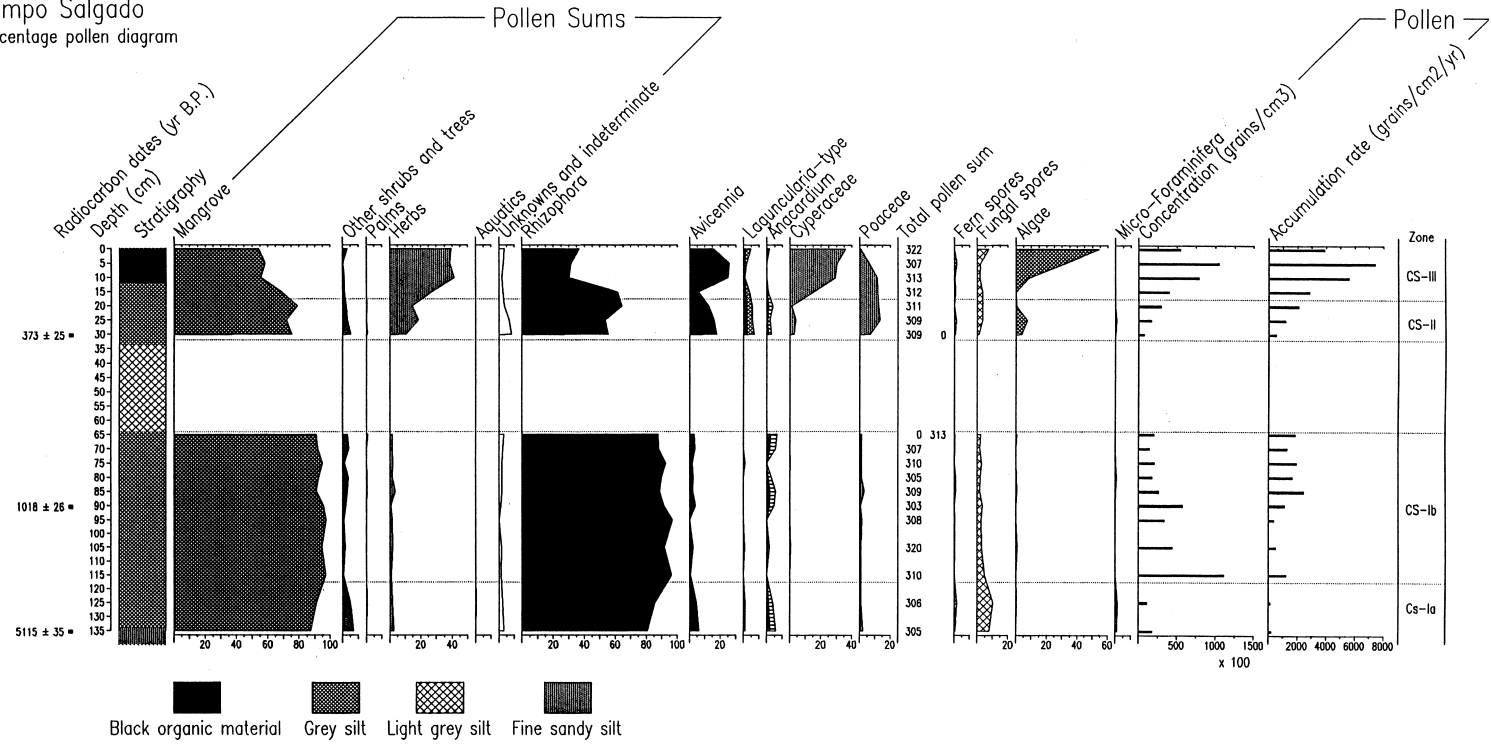
5.4.4.2 Campo Salgado

Pollen concentration and accumulation values are variable in the analyzed sediment samples. Highest average values are found in zone CS-III with ca. 45,000 grains/cm³ and ca. 5000 grains/cm²/yr, respectively.

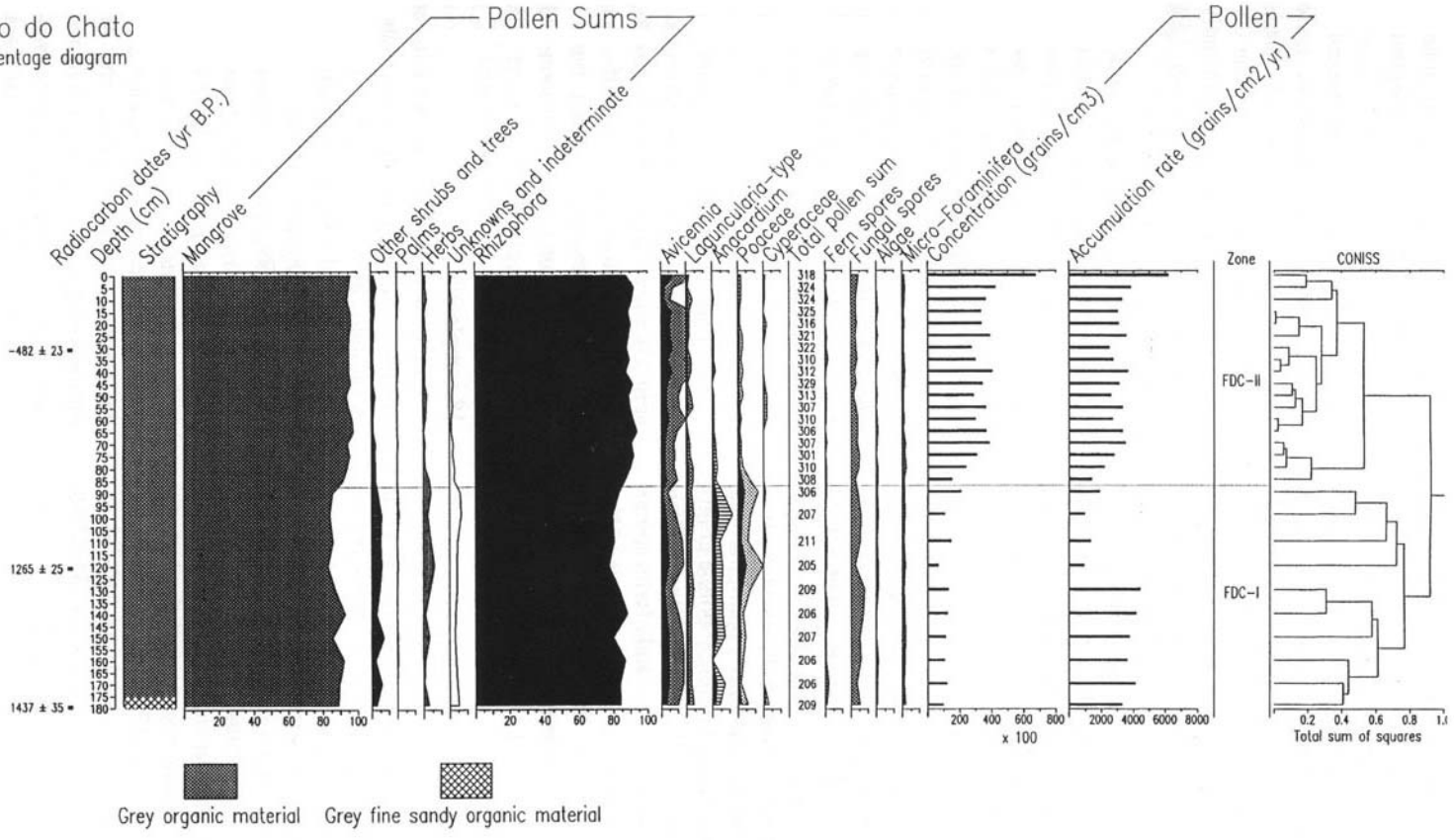
Zone CS-Ia and CS-Ib in the pollen record of CS shows high percent mangrove pollen *Rhizophora* (85-95%), *Avicennia* (1-6%) and *Laguncularia* (1-3%). Above the hiatus in zone CS-II and CS-III, these percentages change significantly related to the decrease of *Rhizophora* pollen (to 55%) and increase of *Avicennia* pollen (to 27%). Pollen grains from other shrubs and trees show relatively low values in the record (3-5%), but higher percentages (7-8%) occur in zone CS-Ia. Pollen of palm trees, aquatics and fern spores are rare.



Campo Salgado
Percentage pollen diagram



Furo do Chato
Percentage diagram



Herb pollen grains are low in zone CS-I (1-3%), but Poaceae increase markedly (up to 15%) in zone CSII and Cyperaceae (up to 36%) in zone CS-III. Percentages of Poaceae pollen decrease strongly and certain algae increase markedly at the end of zone CS-III. Only a few micro-foraminifers (1%) were found in the sediment samples.

5.4.4.3 Furo do Chato

The pollen percentage diagram from the 180-cm long core from the *Rhizophora* dominated area (Fig. 5.4) shows different plant groups and the most abundant pollen taxa out of the 56 different identified types. Four pollen types are unknown. Two pollen zones were distinguished: zone FDC-I (180-87.5 cm: 1440-910 14C yr BP, 10 samples) and zone FDC-II (87.5-0 cm: 910 14C yr BP-modern, 18 samples).

Pollen concentration values are lower in zone FDCI (around 10,000 grains/cm³) and higher in zone FDCII (around 30,000 grains/cm³). Pollen accumulation rates show in the record fluctuations mostly between 1000 and 4000 grains/cm²/yr.

The pollen percentage diagram of the FDC record is characterised by the dominance of mangrove pollen, mainly by *Rhizophora* (85-97%), and low percentages of *Avicennia* (3-7%) and *Laguncularia* (1-2%). There are some minor fluctuations between the frequency of *Rhizophora* and *Avicennia* pollen throughout the 1440 14C yr BP long record. The calculated average *Rhizophora/Avicennia*-ratio for each pollen zone is 28:1 (zone FDC-I) and 25:1 (zone FDC-II).

The presence of different pollen grains from other shrubs and trees (2-6%), palms (0-1%), herbs (1-5%), and fern spores (1-2%) are relatively stable throughout the record. Percentages of other trees and shrubs and herbs are slightly lower in zone FDC-II. Marine micro-foraminifers are relatively stable, represented by around 2% in both zones.

5.5 Interpretation and discussion

5.5.1 General background on Brazilian sea-level changes

During the Last Glacial Maximum period the Atlantic sea-level was around 120 m lower than today (e.g. Shackleton and Opdyke, 1973). The Late Pleistocene/Early Holocene sea-level rise reached modern levels in northern Brazil at the Caxiuanã region, 330 km west of Belém, between 8000 and 7000 14C yr BP (Behling and da Costa, 2000). Approximate modern sea-level was reached in the Lago do Aquiri record from Maranhão State, 450 km south-east of Belém, at 7450 14C yr BP (Behling and da Costa,

1997) and in the Lago Crispim, 130 km north-east of Belém, at 7330 14C yr BP (Behling and Costa, 2001). The occurrence of some *Rhizophora* pollen grains at the beginning of the Holocene in the Lagoa Curuçá record (Behling, 1996), which is located 100 km north-east of Belém and 110 km west of the study area, may be related to long distance wind transport.

Information on past sea-levels from the north-eastern Brazilian coast (Suguio et al., 1985) shows that the relative sea-level ca. 7000 to 5500 yr BP. was about 1-2 m higher than present. The maximum Holocene transgression occurred between 5500 and 5000 yr BP when sea-level was 4-5 m higher than today. The Early Holocene and strong mid-Holocene transgression is not documented in the Rio Curuçá record of the Caxiuanã region (Behling and da Costa, 2000). The reconstructed palaeoenvironment indicates a continuous rise of water level at the study site between 6000 and 2500 14C yr BP. About 2500 14C yr BP water reached the modern level. This conflicts with data from the north-eastern Brazilian coast where the relative sea-level remained ca. 2 m higher than present (including two sea-level regressions ca. 3900 and 2800 yr BP), and then decreased after 2500 yr BP, continuously, to the modern level (Suguio et al., 1985). However, interpretations on the Brazilian sea-level data are still under discussion (Angulo and Lessa, 1998). If and how far Late Quaternary tectonic activity may have played a role here also, is still unclear.

5.5.2 Holocene relative sea-level and the development of the mangrove ecosystem

Sea-level changes play an important role in the development and the dynamics of mangrove ecosystems. Huge areas of probably former mangroves, coastal vegetation and terra firme forest on the northern Brazilian continental shelf (at the study site ca. 170-200 km seawards) were flooded during the Late Quaternary Atlantic sea-level rise. Following the shifting coastline new mangrove areas developed on intertidal higher elevated areas.

The radiocarbon dates indicate that the development of the mangroves started at the three sites on the Bragança Peninsula at different times: at the CS site at around 5120 14C yr BP, BDA at around 2170 14C yr BP (extrapolated), and FDC at around 1440 14C yr BP. At these three different ages, the surface of the three sites relative to modern sea-level was at CS 1.35 m a.s.l. (modern 2.7 m a.s.l.), at BDA 2.4 m b.s.l. (modern 2.4 m a.s.l.) and at FDC 0.1 m a.s.l. (modern 1.9 m a.s.l.).

The presence of mangroves since 5120 14C yr BP at the highest elevated site of CS, which is today a salt marsh, suggests relatively high sea-levels during mid Holocene times. The highest representation of other different shrub and tree pollen taxa in the basal samples suggests that mangroves replaced an earlier coastal forest ecosystem prior to 5200 14C yr BP. Compared with other sites from northern Brazil, it appears that the mid Holocene isostatic sea-level was at that time only slightly higher than today. Results from the site Lago do Crispim (Behling and da Costa, 2001), which is located next to the modern coastline and only 1-2 m a.s.l., was never flooded during the Holocene. The about 4-5 m higher mid Holocene relative sea-level stand, as reported from north-eastern Brazil (Suguio et al., 1985), cannot be confirmed from the Lago do Crispim record. How far tectonic activity may have played a role during Holocene times is still unclear.

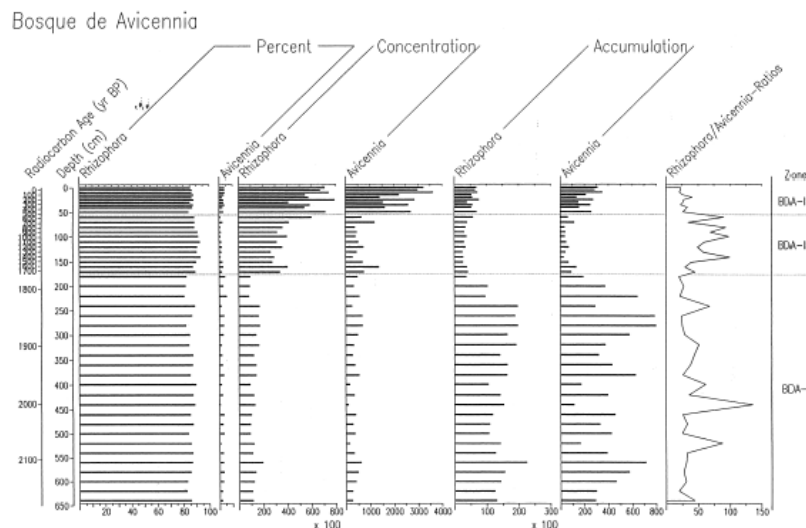


Fig. 5.5 Pollen concentration and accumulation rates of *Rhizophora* and *Avicennia* from the core Bosque de *Avicennia*, including *Rhizophora/Avicennia*-ratios.

However, a relatively high mid Holocene sea-level lead to mangrove expansion at the CS area. Poor pollen preservation in the light grey silt sediments between 64 and 34 cm depth, between 750 and 420 14C yr BP, indicate that mangrove deposits were exposed and the area was relatively dry. The frequency of inundation must have been lower in response to lower sea-levels. Pollen assemblages indicate that after the hiatus at 420 14C yr BP an open Poaceae dominated salt marsh with *Avicennia* shrubs developed. The site changed to a Cyperaceae dominated salt marsh after 200 14C yr BP, and flooding was infrequent.

The very high sedimentation rate in the core BDA of 465 cm within 400 years between 2170 and 1770 14C yr BP (1.16 cm/yr.), and the low concentration of pollen grains indicate rapid deposition. Tidal inundation must have been frequent resulting in higher sedimentation rates during that time. The relatively high number of marine micro-foraminifers and the slightly higher presence of herbs and other forest shrubs and trees, which were probably mostly transported from the inland by rivers, support this interpretation. After 1770 14C yr BP, the sedimentation rate changed to 0.1 cm/yr, pollen concentration increased and the presence of micro-foraminifers decreased markedly. The frequency of inundations probably was reduced. It also has to be considered that the base level at the core location at 1770 14C yr BP was already close to the present, having filled up with sediments. High pollen concentrations during the last 180 14C yr BP, suggest a further reduction of sedimentation and inundation frequency.

The pollen concentration in relatively undisturbed mangrove deposits, such as Bosque de *Avicennia* (Fig. 5.5), seems to be a good indicator of the frequency of inundations. This relationship has to be tested by in future studies. The modern relationship of pollen concentration from the BDA site (average of 70 000 grains/cm³ in zone BDA-IIb) and the present-day frequency of inundation (74 days/yr) can be used to calculate past inundation frequency. Using this correlation, the average concentration of 40,000 grains/cm³ in zone BDA-IIa would correspond to an inundation frequency of 130 days/yr and 15 000 grains/cm³ in zone BDA-I to a frequency of 345 days/yr.

Mangrove expansion at the FDC site at around 1440 14C yr BP began relatively late. According to the elevation of the site at 1.9 m a.s.l., and the earlier occurrence of mangroves at the CS area, mangroves should have been present much earlier at this site as well. The location of the site close to a tidal creek, may explain the age discrepancy. Lower sedimentation rates (0.18 cm/yr) and lower pollen concentrations in the lower core section (180-87.5 cm) compared to the upper core section, indicate a higher frequency of inundation before 910 14C yr BP. The accumulation rate of 0.1 cm/yr for the last 1770 14C yr BP is similar to the BDA site.

According to the radiocarbon dates, the inundation frequency decreased markedly at 1770 14C yr BP (BDA), at 910 14C yr BP (FDC) and at 750 14C yr BP (CS), suggesting that the relative sea-level fell around this time (Fig.5.6). There temporal difference between the sites is minor and might be explained by difference in location and elevation of the sites at that time. The high *Avicennia* pollen concentrations in the

sediments from BDA during the last 180 14C yr BP, suggest a regression of sea-level. The change from a Poaceae dominated to a Cyperaceae dominated modern saltmarsh at the CS site during the last 200 14C yr BP may also be related to a lower relative sea-level.

5.6 Holocene mangrove dynamics

When studying Holocene mangrove dynamics, using deposits within modern mangrove stands one has to consider bioturbation problems. Crabs can move mangrove sediments from .40 cm depth to the surface (Rademacher, 1998). Tidal inundation may mix local mangrove pollen assemblages with those from surrounding areas. Because of its length and favourable location with respect to distance to tidal creeks and channels, the BDA core is optimal to reconstruct Holocene mangrove dynamics.

Mangrove dynamics can be reconstructed using changes in the proportions of both major tree taxa, *Rhizophora* and *Avicennia*. Annual modern pollen rain data from three different mangrove sites show an interesting proportional relationship between the high pollen producing *Rhizophora* and the low pollen producing *Avicennia*. The calculated average ratio of *Rhizophora/Avicennia* (R/A-ratio) is 4:1 for the *Avicennia* forest (BDA), 33:1 for the mixed *Rhizophora/Avicennia* forest (BDR/A), and 115:1 for the *Rhizophora* dominated forest (FDC). Increases in the R/A-ratio indicates increases in *Rhizophora* trees in the mangroves.

Comparison of mangrove pollen ratios in annual modern pollen rain with surface samples from the mangrove site BDA shows marked differences. The modern pollen rain R/A-ratio is 4:1 compared to 22:1 in the surface sample. The difference of the R/A-ratios is probably the result of tidal inundation, leading to over representation of *Rhizophora* pollen.

In the fossil samples the calculated average R/A-ratios are 41:1 in zone BDA-I (2170-1770 14C yr BP), 64:1 in zone BDA-IIa (1770-180 14C yr BP) and 27:1 in zone BDA-IIb (180 14C yr BP-present) (Fig. 5.5). These R/A-ratios indicate that *Rhizophora* was abundant until 180 14C yr BP. When the *Rhizophora/Avicennia* mixed mangrove changed to an *Avicennia* dominated forest. The high concentration of *Avicennia* (proportional significantly higher than the *Rhizophora* concentration) during the last 180 14C yr BP (Fig. 5.5), indicates also, the almost *Avicennia* dominated mangrove. Presence of dead *Avicennia* trees at this study site today, seems to be the consequence of a lower inundation frequency. These changes seem to be a natural change from an

Avicennia forest to salt marsh vegetation. The change from a mangrove to a salt marsh ecosystem occurred on the somewhat higher elevated CS site about 240 years earlier. This suggests that the present-day salt marsh, which is at the core site CS ca. 420 14C yr BP old, is natural and not the result of anthropogenic perturbation. The construction of the road in 1986, forming a dam, probably reduced the frequency of inundation even more on the distal side of the road than on the proximal side where the BDA site is located. It is suggested that the road construction favoured the reduction of inundation frequency and as consequence an increase in salinity, which supported the formation of a degraded area.

5.7 Conclusions

The development of mangrove on the Bragança peninsula in the north Brazilian coastal region occurred at the CS site around 5120 14C yr BP, at the BDA site around 2170 14C yr BP (extrapolated), and at the FDC site around 1440 14C yr BP. The location and elevation of the three sites are important aspects determining the timing of the formation of the mangrove ecosystem. The decrease of the frequency of tidal inundations at the BDA site around 1770 14C yr BP, at the FDC site around 910 14C yr BP and at the CS site around 750 14C yr BP, suggests that the relative sea-level decreased during the late Holocene.

Pollen concentration in relatively undisturbed mangrove sediments seems to be an indicator of inundation frequency. This correlation allows us to estimate past tidal inundation frequency, but has to be tested in future studies. Using modern analogues, the inundation frequency at the BDA site could have averaged 345 days/yr between 2170 and 1770 14C yr BP and 130 days/yr between 1770 and 180 14C yr BP. During the last ca. 180 14C yr BP the tidal inundation frequency was on average 74 days/yr (modern value).

Modern pollen rain analogues from different mangrove vegetation types show a distinct pollen ratio for the high pollen producing *Rhizophora* and the low pollen producing *Avicennia*. The R/A-ratio can be used to reconstruct mangrove dynamics of the two most important mangrove trees *Rhizophora* and *Avicennia*. Studying mangrove dynamics in detail by using mangrove deposits is somewhat limited, because of bioturbation and tidal inundation, which affect pollen deposition of the local mangrove. The dates suggest that at the BDA site a *Rhizophora-Avicennia* mixed mangrove dominated between 2170 and 1770 14C yr BP. Between 1770 and 180 14C yr BP,

Rhizophora was more frequent than before. Since around 180 14C yr BP, an almost pure *Avicennia* stand formed the mangrove.

The mangrove ecosystem in the central area of the peninsula (site CS), changed to a salt marsh at about 420 14C yr BP. The present-day salt marsh, which is used as cattle land, is probably natural and not formed by human activity.

Chapter 6
MODEL ON HOLOCENE MANGROVE
DEVELOPMENT AND RELATIVE SEA-LEVEL
CHANGES ON BRAGANÇA PENINSULA (NORTH
BRAZIL)⁵

⁵Cohen, M.C.L., Souza Filho, P.W.M., Lara, R.J., Behling, H., Angulo, R.J. Model on Holocene mangrove development and relative sea-level changes on Bragança Peninsula (North Brazil). In preparation.

Abstract

Based on the integration of the geologic information, pollen records, radiocarbon data, and modern mangrove distribution, this paper proposes a model for the Bragança peninsula development according to relative sea-level changes for the mid and late Holocene. Two transgressive events defined the space distribution of the mangroves on that area during the Holocene. The first mangrove habitats on the Bragança Peninsula probably began to develop at 5100 yr BP, originated on the middle of the peninsula, close at the current relative sea-level (RSL). As sea-level stabilized, occurred a widespread mangrove phase. Between 1800 and 1400 yr BP, the data suggests a maximum fall of about 1 meter below the current RSL. After that, occurred a gradual RSL rise until 1000 years B.P; when again was reached the current mean sea level. Between 5100 and 1000 yr BP, the RSL at the Bragança coastline probably was never higher than 0.6 m above the current. The first mangrove forest (5100 yr BP) from this region disappeared from the plains as vertical accretion continued and/or a RSL fall, and were replaced by herbaceous vegetation (Cyperaceae and Poaceae).

Keywords: Inundation frequency, mangrove, palynology, relative sea-level, topography

6.1 Introduction

The North Brazilian littoral is formed by one of the world's largest mangrove area of 8,900 km² (Kjerve and Lacerda, 1993). The development of mangrove is controlled by land-ocean interaction, and its expansion is determined by the topography of the pre-Holocene sediment surface and prevailing wave and current energy conditions (Woodroffe, 1982).

In Australia, rising sea-level invaded the rather shallow and broad valleys towards the end of the postglacial transgression (Chappell and Polach, 1991). Mangrove facies composed of organic muds containing mangrove pollen commonly overlies the prior valley floors, recording the inundation of the valley by the rising sea-level around 7000-8000 yrs BP. Transgressive basal sediments pass upwards into mangrove facies showing that these macrotidal estuaries became areas of vertical accretion under widespread mangrove forest, which has been termed the "big swamp", throughout the last 8 m or more of sea-level rise (Woodroffe et al., 1987).

Therefore, the mangrove ecosystem is considered as highly susceptible to sea-level changes, and the sediments deposited beneath mangrove vegetation provide useful indications of old sea-level (Scholl, 1964; Woodroffe, 1981; van de Plassche, 1986).

Studies on Holocene sea-level changes of the eastern and southern Brazilian coast suggest several sea-level curves for the Holocene (Suguio et al., 1985; Martin et al., 1988; Tomazelli, 1990; Angulo and Lessa 1997, Angulo et al., 1999) based on sea level indicators (e.g. shell middens, marine and lagoonal terraces and vermetid). These indicators have contribute to elucidate the history of the eastern and southern coastal region. In comparison, little information exists about the dynamic of mangrove ecosystems and Holocene sea-level changes from the northern Brazilian coast (e.g. Behling et al. 2001; Behling and Costa, 1997, 2001; Souza Filho and El-Robrini, 1996, 1998).

Seeking to contribute to the mangrove research in North Brazil, an international research project “Mangrove Dynamics and Management (MADAM)” was initiated in 1996.

Based on the integration of the geologic information, pollen record, radiocarbon data, and modern mangrove distribution, this paper proposes a evolutionary model for the Bragança Peninsula during the mid and late Holocene.

6.2 Study area

The study site is located on Bragança Peninsula, between the bays of Maiaú and Caeté (00° 46' - 1° 00' S and 46° 36' – 46° 44' W, Fig. 6.1).

6.3 Data sources

6.3.1 Topographic survey

The topographic limits of the wetlands on the Bragança Peninsula (Tab. 1 and Fig. 1) were identified by 55 hydro-topography devices distributed on 190 km² (Cohen et al., 2001).

6.3.2 Sediment cores

Eleven vibracores performed by Souza Filho and El-Robrini, (1998) were used to aid in the selection of the eight new core position. Three cores were collected with the Russian sampler (Behling et al., 2001) and five were obtained by vibracore.

6.3.3 Pollen analysis

Pollen analysis have been carried out on the sediment cores: “Bosque de *Avicennia*” (BDA), “Campo Salgado” (CS) and “Furo do Chato” (FDC). For pollen analysis, 0.5 or 1 cm³ samples were taken at 5-cm, 10-cm or 20-cm intervals along the cores (Behling et al., 2001). Prior to processing of sediment and pollen rain samples, one tablet of exotic *Lycopodium* spores was added to each sample for calculation of pollen concentration (grains/cm³) and pollen accumulation rate (grains/cm²/yr). All samples were prepared using standard pollen analytical techniques and acetolysis (Faegri and Iversen, 1989).

6.3.4 Radiocarbon data

Three sediment cores: “Campo Salgado” (the highest part of the Bragança peninsula with a herbaceous vegetation, 2.7 m above mean sea level, a.m.s.l.); “Bosque de *Avicennia*” (the highest part of the mangrove area, 2.4 m a.m.s.l.); “Furo do Chato” area, (1.9 m a.m.s.l., Fig. 1 and 2) have been dated at the Van der Graaff Laboratory at the University of Utrecht by Accelerator Mass Spectrometry (Behling et al., 2001).

6.3.5 Modern vegetation

A descriptive characterization of the main vegetation units was carried out by satellite image interpretation. The image LANDSAT TM5 WRS 222/061 purchased from National Institute of Space Researches-Brazil (INPE) was used for the study area. The image was processed to Level 6 (map oriented, precision corrected and resampled with a cubic convolution to 30 m pixels) acquired on December 1991.

The fieldwork was carried out from acquisition of oblique aerial photographs (April 1998) and satellite image analysis of the coastal region. Ground control points were checked to validate the classification of vegetation types. The typical plant species in each unit was determined with photographic documentation and GPS measurements of the forest. Using texture, features size and shape as identification parameters, the dense mangrove areas were easily classified, contrasting sharply with the adjacent Elevated Herbaceous Flat (EHF), degraded mangrove area and restinga. These sites were located by Global Positional System (GPS) in a Geographic Information System (GIS) by matching and distinguishing coastal features. The resulting vegetation map, supported by the geomorphologic map of the Souza Filho (1995), was arranged with a topographical map obtained from Cohen et al. (2001, Fig. 6.1).

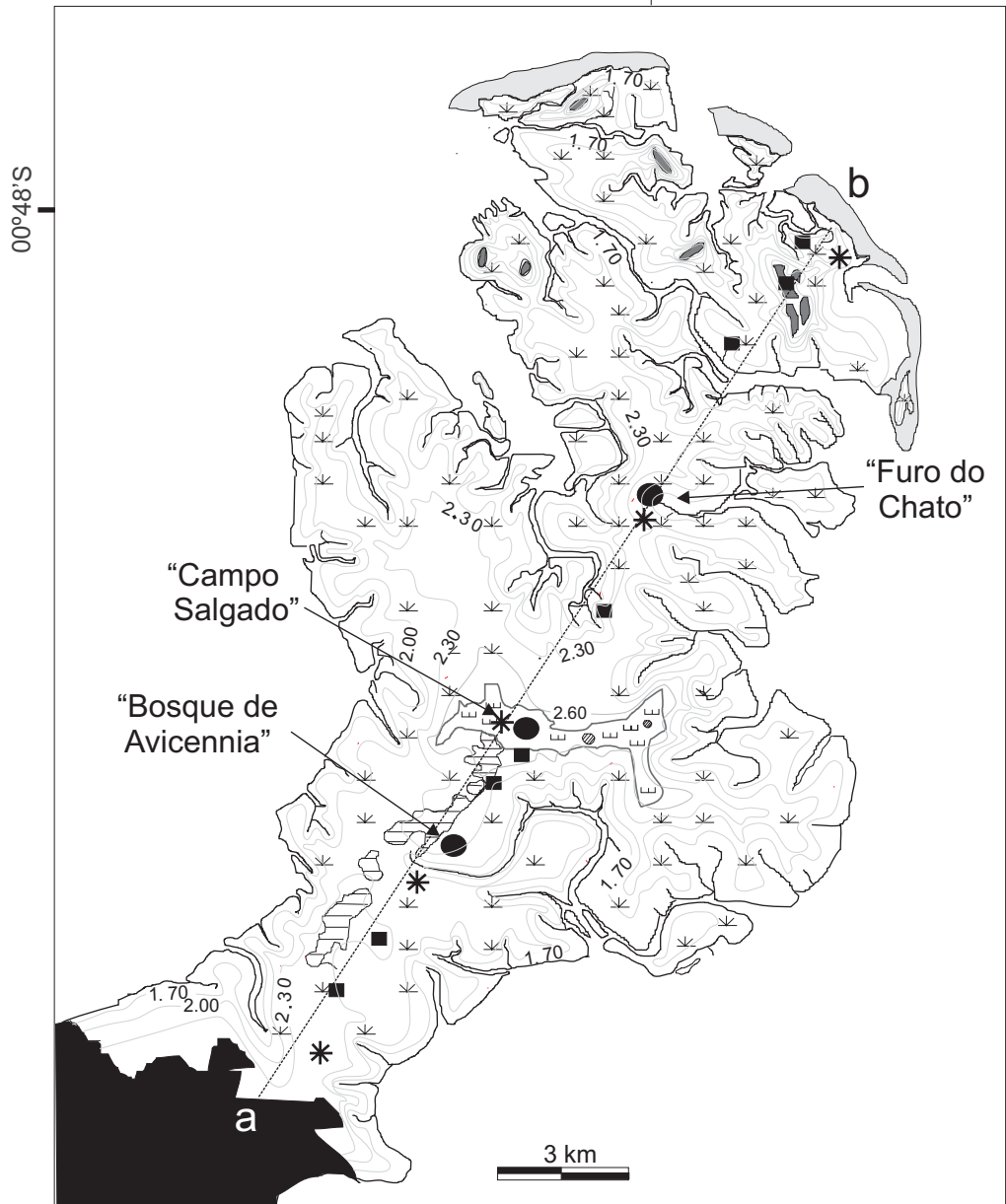
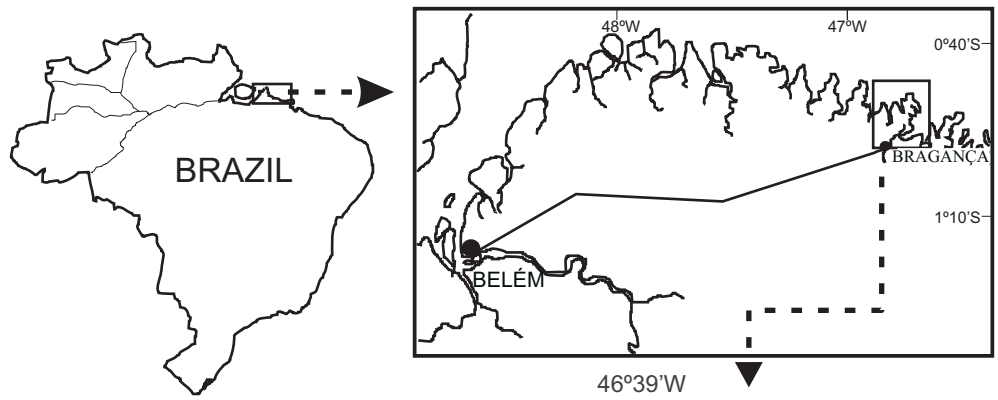


Figure 6.1 Location of the collected cores and the Bragança Peninsula with topographic levels.

6.3.6 Stratigraphy

Based on geomorphologic map and modern vegetation units, several sites were chosen to collect eight sediment cores. The sediment cores were taken and topographically positioned in a longitudinal transect across the peninsula. Regarding the stratigraphy presented by Souza Filho (1995), the integration of the sediment cores allow modifications of the stratigraphic profile from the Bragança Peninsula (Fig. 6.2).

6.4 Results

6.4.1 Modern vegetation units

The vegetation of the Bragança Peninsula are represented by the following units: Amazon coastal forest, Elevated Herbaceous Flats (EHF), Mangroves, Degraded Mangroves and Restinga. Details of those vegetation units are described in Table 6.1 and Figure 6.1.

6.4.2 Stratigraphy and radiocarbon data from the Bragança Peninsula.

Studied landforms and sediments are located on a longitudinal transect (Figs. 6.1 and 6.2). In the Holocene stratigraphy of the Bragança Coastal Plain can be recognized three sedimentary sequences: (a) basal sand marine (shoreface) and estuarine retro gradational sequence (S_1); (b) estuarine mud progradational sequence (S_2) and; (c) upper sandy eolian (coastal dunes) and marine (barrier-beach ridges, *chêniers*, sandflats) retro gradational sequence (S_3) (modified of Souza Filho, 1995).

6.4.2.1 Estuarine mud progradational sequence (S_2)

This sequence occur between 4 m below and 2.7 m above the present mean sea-level (Fig. 2), and extends more than 90% of the Bragança Peninsula.

Unit A

The highest elevation of the EHF sediments are 2.7 m a.m.s.l., with about 0.2 m thick. (Fig. 1 and 2). The pollen assemblage from this unit is characterized by the increase of Poaceae (up to 15%) and Cyperaceae pollen (up to 36%), which represent the main vegetation from the EHF.

Table 6.1 Modern vegetation units on the Bragança Peninsula.

| Units | Main taxa | Area (km ²) | Altitude(m) above mean sea level | Substrat | Soil salinity in dry season | Inundation frequency (day/year) |
|--------------------------|--|-------------------------|--|----------|-----------------------------|---------------------------------|
| Amazon Coastal Forest | <i>Coccoloba latifolia</i> , <i>Himatanthus articulata</i> , <i>Anacardium occidentale</i> , <i>Protium heptaphyllum</i> , <i>Ouratea castanaefolia</i> , <i>Ouratea microdonta</i> , <i>Tapirira guianensis</i> , <i>Myrcia fallax</i> , <i>Myrcia sylvatica</i> , <i>Eugenia patrisii</i> . | <1 | > 3.0 (never flooded by tides) | sand | <36 | 0 |
| Restinga | <i>Chrysobalanus icaco</i> , <i>Anacardium occidentale</i> , <i>Byrsonima crassifolia</i> . (Menezes, unpublished data). | 2 | > 3.0 (developed near to wave dominated coast) | sand | <36 | 0 |
| Elevated Herbaceous Flat | <i>Sporobolus virginicus</i> (<i>Poaceae</i>) and the <i>Eleocharis geniculata</i> (<i>Cyperaceae</i>), (Menezes, unpublished data). | 7 | 2.4 to 3.0 (inundated only by maximal spring high tides) | mud-sand | 90-100 | <28 |
| Degraded mangroves | dead roots and trunks of <i>Avicennia</i> and <i>Rhizophora</i> | 3 | 2.2 to 2.5 (inundated only by spring high tides) | mud | 80-100 | 20 to 51 |
| Mangroves | <i>Rhizophora mangle</i> , <i>Avicennia germinans</i> and <i>Laguncularia racemosa</i> . | 168 | 1.0 to 2.4 (located between spring high and mean tide levels) | mud | 36-90 | 28 to 233 |

Unit B

Radiocarbon data from 3 cores from the base of unit B give an age of 5115 ± 35 yr BP, 2170 yr B.P. (extrapolated) and 1437 ± 35 yr BP. (about 1.4 m amsl, 4 and 0,1 m below the mean sea-level, respectively). The ages of 1018 ± 26 yr BP (1.8 m amsl), 1830 ± 23 yr B.P. (0 m, m.s.l.) and 1265 ± 25 yr BP (0,5m, a.m.s.l.) were obtained from the middle part of the cores, and 373 ± 25 yr BP (2.4 m amsl) was obtained from the top of this deposit (Fig. 2). The pollen record of this unit is characterized throughout by the dominance of mangrove pollen, primarily by the high pollen producer *Rhizophora* (80-

97%). The low pollen producers *Avicennia* (2-7%) and *Laguncularia* (1-3%) are represented by low values (Behling, et al., 2001).

6.4.3 Model of Bragança mangrove development

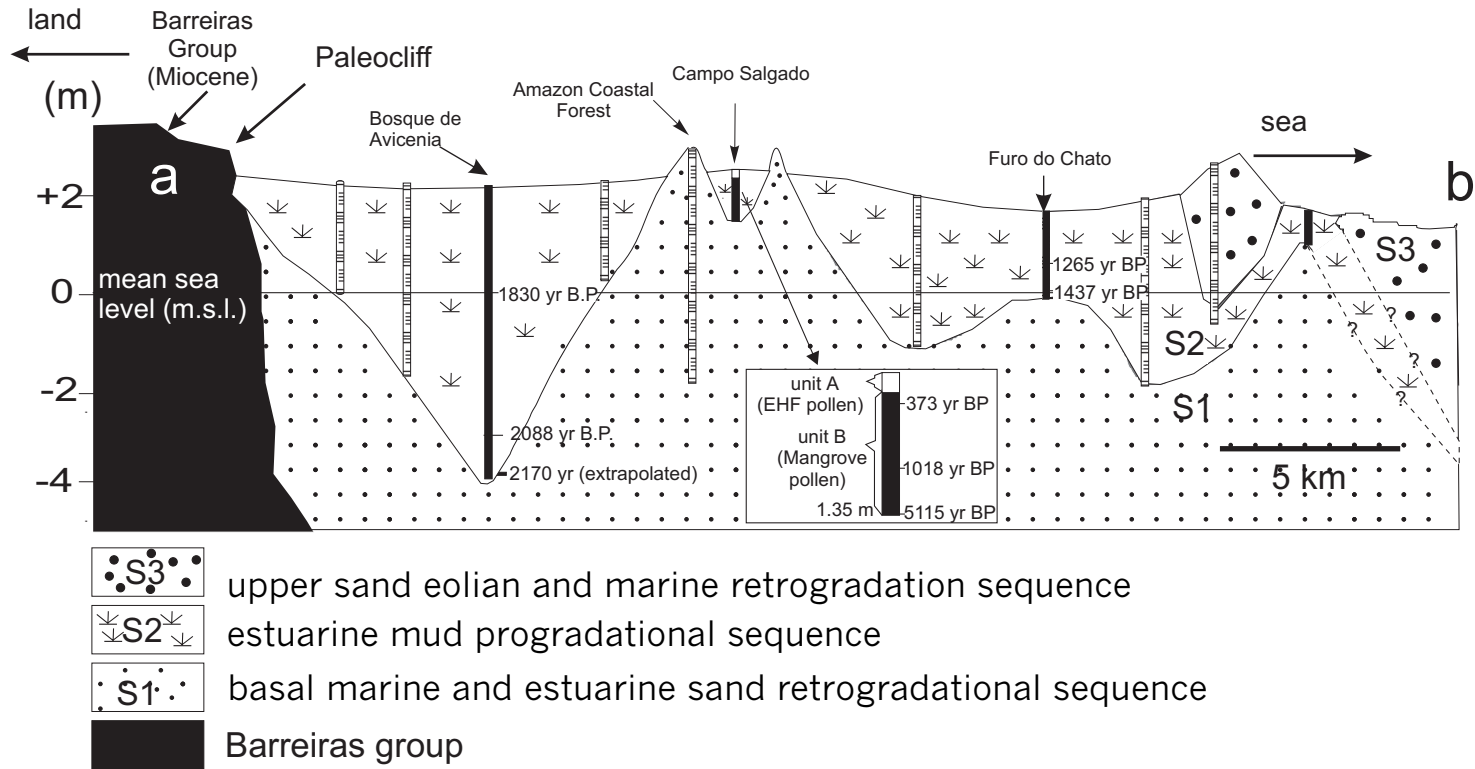
Phase 1

The phase 1 occurred when the prior valleys were flooded by a rapidly rising postglacial sea-level. The stabilization of the sea-level around 5100 yr BP resulted in one of the firsts mangroves in this region. This phase is represented by the mangrove sediments from “Campo Salgado” core bottom, which reaches 1.4 m above the present mean sea-level. These sediments overlay a marine basal sands that include shell fragments, indicating that the shallow sea ground changed to a tidal flat suitable for a mangrove development. Regarding that the present Bragança mangroves developed between 1 and 2.4 m a.m.s.l. during the Holocene, the RSL during the mid Holocene, probably was close to the modern sea-level. Mangrove forests were probably restricted to the “Campo Salgado” area and to the channels landward, which probably developed mangroves fringes on the Barreiras Group. The Amazon coastal forest probably was limited to the highest part of the “Campo Salgado” area (Fig. 6.3).

Phase 2

Palynological data indicate the presence of mangroves at the “Bosque de *Avicennia*” site during the last 2170 yr BP (Behling et al., 2001). At this area, around 2170 yr BP, is documented mud sediments with mangrove pollen (unit A) that overlies a marine sand layer (4 m below m.s.l.).

Two hypotheses can be proposed to interpret this data: 1) the mud with mangrove pollen would have only deposited in mangrove area. This would imply that the sea-level was at least 5 m below the current msl, and the whole sequence would have deposited by vertical accretion, or 2) the mud with mangrove pollen would have deposited mainly in the lower part of the tidal plain and in tidal channel by lateral accretion, which would not imply in a sea-level fall during this phase. To accept this hypothesis means recognize that the sediments with mangrove pollen not always are deposited under mangrove conditions.



This second hypotheses is supported by the elevated sedimentation rates (1.16 cm/yr) found between 2170 and 1830 yr BP in the “Bosque de *Avicennia*” compared to “Campo Salgado” (0.011 cm/yr). Therefore, probably, the mangrove vegetation in this time was topographically restrict to higher zones (Fig 6.3).

Palynological data suggest the uninterrupted presence of mangroves since 5100 until 1000 yr BP on the “Campo Salgado” area (Behling et al. 2001), and regarding the current mangrove development zone (1-2.4 m a.m.s.l), the RSL should not have been significantly modified during this time interval in this region, or otherwise, another vegetation type (EHF or Coastal Forest) would have occurred on “Campo Salgado” site. Therefore, is improbable that mangroves have existed simultaneously on the “Campo Salgado” and on the “Bosque de *Avicennia*” area, due to the topographical difference of around 6 meters in that time.

Phase 3

From 1800 until 420 yr BP, the mud progressively filled the estuaries and mangrove forests expanded. The change in sedimentation rate in “Bosque de *Avicennia*” from 1.16 to 0.1 cm/yr suggest a transition time on the mangrove sediments deposition from lateral to vertical accretion. According to this situation, between 1800 and 1400 yr BP is probable a low RSL to justify the appearance of mangrove on the “Furo do Chato” (0.1 m a.m.s.l.). Its relatively low sedimentation rate (0.18 cm/yr) and topographic position suggest vertical deposition instead of lateral accretion in this area. During that time, following the topographic mangrove development zone and the mangrove presence in “Campo Salgado”, probably the RSL was not lower than 1 m below the current (Fig. 6.4).

Phase 4

On the “Campo Salgado” site, pollen assemblages indicate at 420 ¹⁴C yr BP a transition between mangrove dominated by *Avicennia* to herbaceous vegetation mainly occupied by Poaceae. The site changed to Cyperaceae after 200 ¹⁴C yr BP (Phase 5), under continuously low inundation frequency. In the last 400 yr BP, based on the habitat salinity zone (Table 6.1), this vegetation change suggests a gradual RSL fall or a vertical accretion of mangrove sediments that gradually eliminated the mangroves in this area.

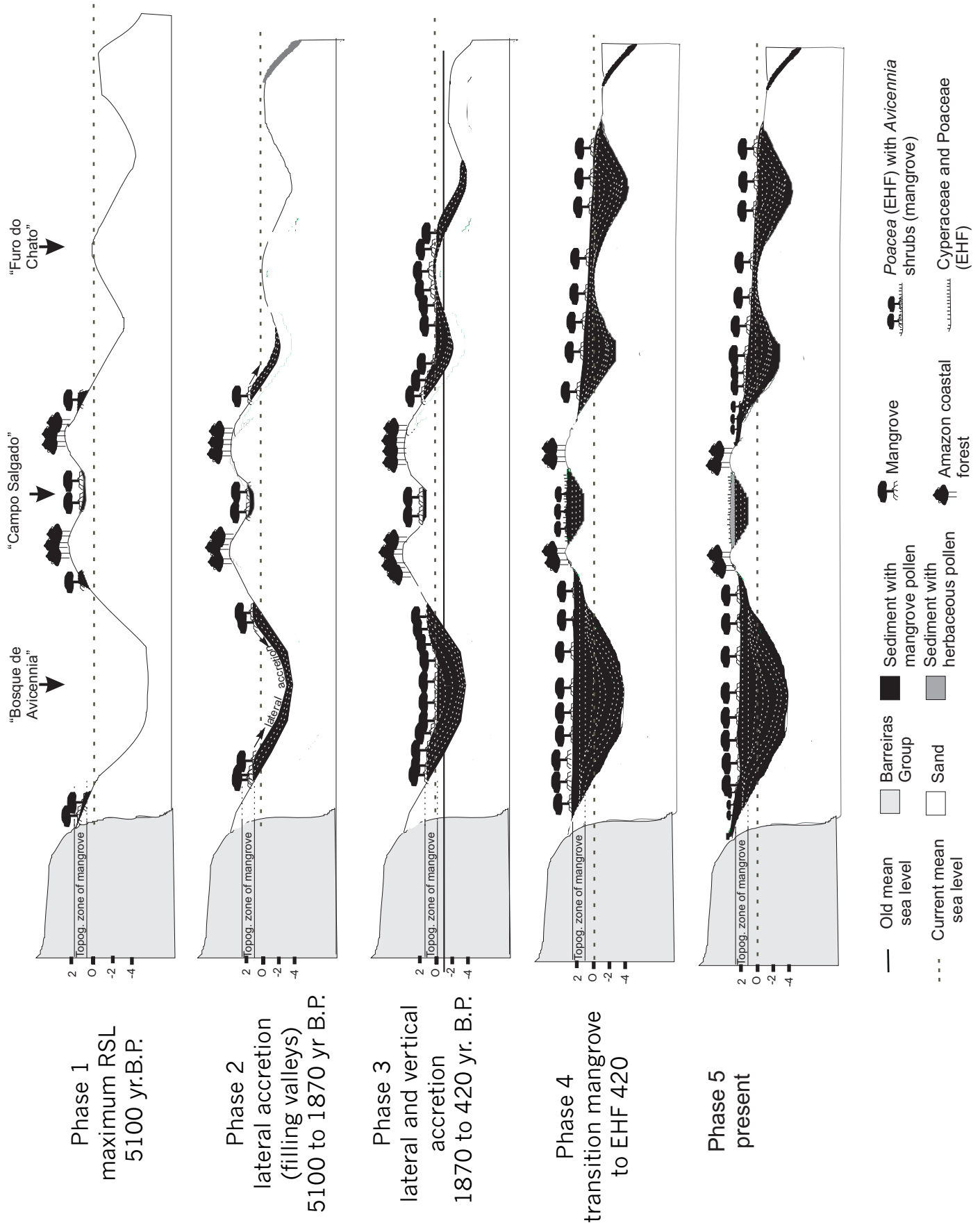


Figure 6.3- Mangrove development of the Bragança Peninsula.

The absence of mud layers in the 5 m long core of the Amazon coastal forest area, which currently is positioned 3 m a.m.s.l. (Fig. 6.2 and Table 6.1), suggests a uninterrupted presence of this vegetation during the last 5115 yr B.P (Fig. 6.3). Therefore, the tidal floods were not high enough for mangrove development in this area.

6.7 Discussions

6.7.1 Sea-level indicated by mangrove sediments

Mangrove deposits have advantages in the reconstruction of sea-level. They are generally deposited intertidally and may be directly related to the position of the sea at their time of deposition, and the sediments may contain large amounts of organic carbon suitable for radiocarbon dating (Woodroffe, 1981). Pollen analysis of radiocarbon-dated drill hole sediments shows that ecologically uniform mangrove occurred throughout the South Alligator plains (Australia) when sea-level was rising, 7000 to 6000 years ago, which suggests that the substrate rose uniformly as sea-level rose (Woodroffe et al., 1986; Chappell, 1990).

Several studies (e.g. Scholl, 1964; Fujimoto et al., 1996; Beaman et al., 1994; Woodroffe et al. 1993; Fujimoto and Miyagi, 1993; Bryant et al., 1992; Chappell, 1993; Caratini and Fontugne, 1992; Clark and Guppy, 1988 and Mildenhall and Brown, 1987) admitted the mangroves distribution around mean sea-level to reconstruct the ancient sea-level. However, the erosion, accretion or other disturbances may cause variation of the order of ± 1 m (Bunt et al., 1985). Therefore, the topographical distribution of the mangroves in relation to mean sea-level is variable and may at times results in sea-level curve being displaced (Larcomb et al., 1995).

In Grand Cayman (Indies) the substrate of the marine mangrove was generally 15-30 cm a.m.s.l (Woodroffe, 1981), and in Florida (USA) at 0-12 cm a.m.s.l (Scholl and Stuiver, 1967). In the Townsville coastal plain (Australia), mangroves are found from 1.5 to 3.0 m a.m.s.l. (Belperio, 1979), while in Coral and Cocoa creek, northern Australia, the lower part of mangrove is between 0 and 1 m a.m.s.l. (Aucan and Ridd, 2000).

In order to reconstruct the sea-level based on mangrove sediments deposits, it is necessary to make certain assumptions. Firstly, the elevation range within which mangrove peat from the study site can form must be known, and that this only applies to areas identified as marine mangrove (Woodroffe, 1981). Also, palynological studies

may be able to indicate local palaeo-tidal levels to a relatively high precision (e.g. Grindrod and Rhodes, 1984; Gagan et al., 1994).

Regarding the autocompaction of older marsh peats, as described by Kaye and Barghoorn (1964), which the mud layer tend to sink lower than the depth at which it formed in relation to a former sea-level, reliable record of vertical growth of the marsh as result of rising sea levels could be obtained by analyzing the lateral accretion of the marsh (Redfield, 1972). In this approach, only the basal peat in contact with the old upland surface is dated, and the dated levels that are not in contact with the sandy substratum, just indicate the lowest level of the RSL for that time.

Generally, mud deposition on the Bragança Peninsula takes place within the tidal range and is largely due to mangrove, which according to Furukawa and Wolanski (1996), actively capture mud to create their own environments. Although the tidal range along this coast averages about of 3 to 4 m (Cohen et al., 1999), the current topographical extension of the Bragança mangrove is restricted to 1 and 2.4 m a.m.s.l. (Cohen et al., 2001).

Therefore, it would be reasonable to admit that the sediments, represented mainly by mud and composed by a pollen assemblage from mangrove, have deposited under mangrove conditions and within of the tide zone where the current mangrove are developed. Despite of a certain amount of pollen grains can be transported by wind and occur in another environment, the pollen traps, which record the modern pollen rain from the ‘Campo Salgado’ site with a herbaceous vegetation, and located at least 1 km distant from the closest *Rhizophora* trees and 100 m distant from *Avicennia* shrubs, document an average 2.3% of the mangrove pollens accumulation rates from a mangrove area (Behling, et al., 2001). Therefore, the mangrove pollen that occur in sediments deposited on no mangrove area, probably, have low accumulation rate, and would be easily distinguished from the mangrove area.

However, valleys near to mangroves can be filled by Holocene estuarine mud, which is vertically continuous only near valley margins. In central part of the valley, the sediments are deposited by lateral accretion (Woodroffe et al., 1989), and probably the mangrove pollen accumulation would be close to the concentration found in mangrove area. Therefore, mangrove sediments, deposited on bottom of the valleys and channels, could be used erroneously as paleo sea-level indicators, since they were not deposited immediately below the mangrove forest.

Based on the sediment cores sampled from this mangrove, the mangrove sediment deposits below the current mangrove forest have a thickness between 2.5 and 6 m (Fig. 6.2). Therefore, it would be necessary use the model of lateral accretion to justify all the mangrove sediments found in a depth that suggest a relative sea-level below the current, and the vertical accretion model when this sediments are within the current topographical zone of mangrove development. This simplification is very convenient to explain the evolution of this mangrove without relative sea-level changes.

However, it is possible that the relative sea-level between 5100 and 1000 yr BP has oscillated between 0.6 m above the msl (topographical limit of the Amazon Coastal Forest, which is never flooded) and 1.0 m below the msl (minimum tolerance of tidal inundation to the palaeo mangrove from “Campo Salgado” site, see Fig. 6.4).

Thus, the sedimentation rate, mangrove pollen accumulation, and topographic position suggest vertical deposition to the “Furo do Chato” site between 1800 and 1400 yr. BP, and within this msl oscillation limit, a probable low RSL (Figs 6.3 and 6.4).

On the other hand, the mangrove deposit of “Bosque de *Avicennia*” site possess a mangrove pollen accumulation typical to a mangrove region, but the high sedimentation rate suggests a fluvial valley with sediment accumulation by lateral accretion, followed by a transition to vertical accretion to complete the fulfill this valley. So, probably, the base of this core should not to be used as indicator of palaeo relative sea-level.

In every cases, the data presented in this work should be considered as preliminaries, so requiring another evidences of palaeo sea-level oscillation for the composition of a palaeo relative sea-level curve for the northern Brazilian.

6.7.2 RSL changes from Bragança compared with data from the eastern Brazilian coast

The existing RSL curves for Brazil present two distinct patterns for the late Holocene. The first one, proposed by Suguio et al. (1985a) for the States from Bahia until Santa Catarina (Fig. 6.4a) suggest RSL fall in the last 5100 yr BP with two oscillations. However, Angulo and Lessa (1997) disagree with the low RSL between 4100-3800 yr B.P. and 3000-2700 yr BP (Fig. 6.4b). The third curve, proposed by Tomazelli (1990), suggests an RSL rise in the last 1000 years in Rio Grande do Sul State (Fig. 6.4c). The comparison of the paleo sea-level data from Bragança mangrove region (Fig. 6.4d) with other published shows the following:

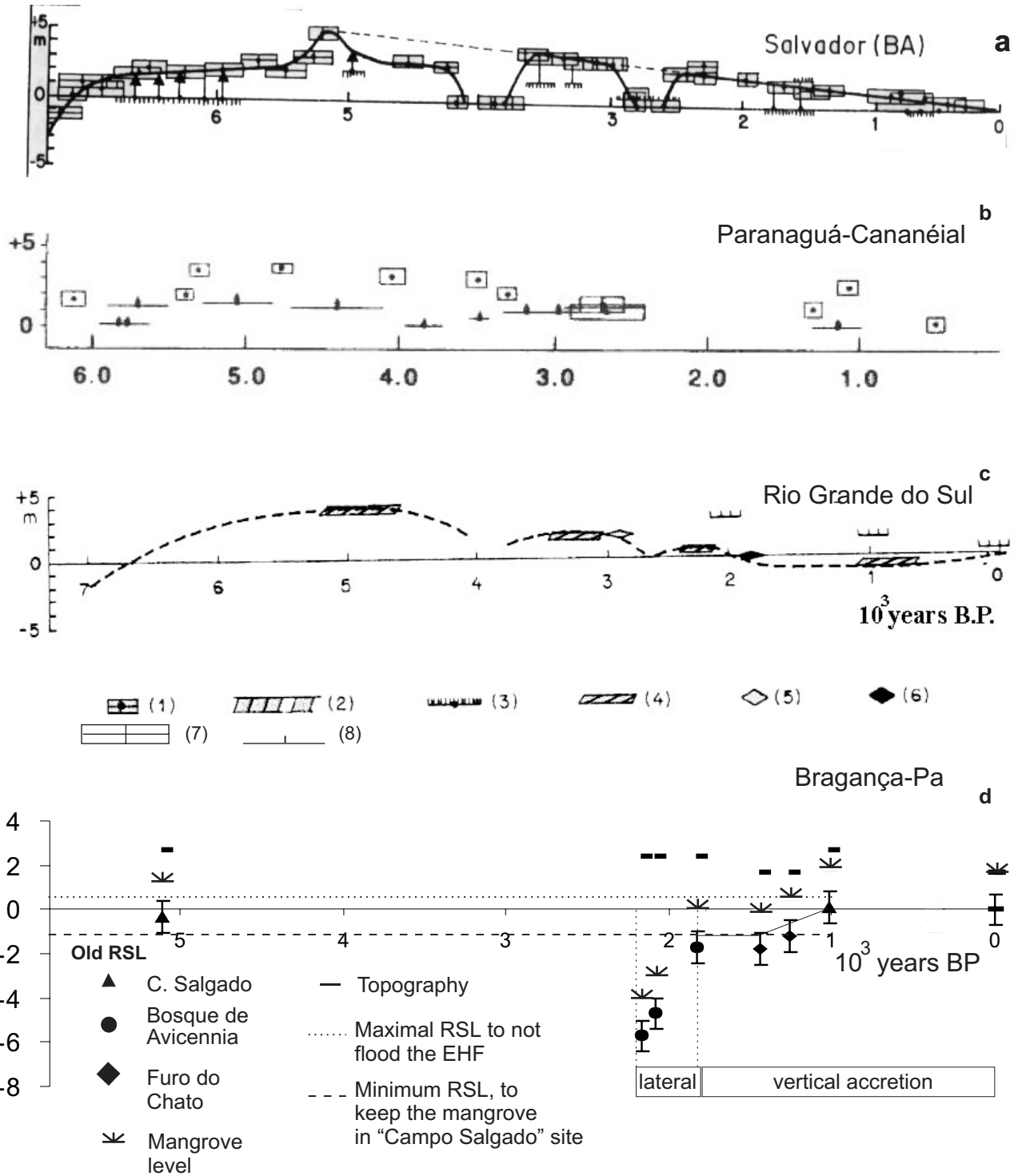


Figure 6.4 Comparison between Holocene RSL curves from northeast to south Brazil.

- the data presented here corroborate to the existence of a RSL rise until 5100 yr BP proposed by Suguio et al. (1985); Angulo and Lessa (1997) and Tomazelli (1990). However, our dates to that time suggest that the RSL stabilized close to the current;
- probably, between 1800 and 1400 yrs BP occurred a maximum fall of about 1 m below the modern RSL, following a gradual RSL rise until 1000 years B.P; when was re-established the current RSL, which reveal a particular evolution to the North Brazilian coast during the late Holocene, driving to geomorphological features (muddy coast) significantly contrasting with the South Brazil (sandy coast);
- between 5100 and 1000 yr B.P. the RSL at the Bragança coastline probably was never higher than 0.6 m above the current, as suggested by Suguio et al., (1985) for the states of Bahia, Rio de Janeiro, São Paulo, Paraná and Santa Catarina, and by Angulo et al. (1999) in the Santa Catarina State. According to Behling and Costa (2001), results from the site Lago do Crispim in the northeastern Pará State, which is located next to the modern coastline and only 1 m a.m.s.l, suggest that this region was never flooded during the last 8000 years.

6.8 Conclusions

Probably, the sedimentary deposits from Bragança mangroves were formed according to a models combination of lateral with vertical accretion (e.g. Woodroffe et al., 1989), following the topographic zone of mangrove development related to the RSL.

Therefore, the first mangrove habitats on the Bragança Peninsula probably began to develop at 5100 yr B.P. originated on the “Campo Salgado” area close at the current RSL. Probably, this littoral between 1800 and 1400 yr BP suffered a maximal RSL fall of 1 meter below the modern mean sea-level, following a gradual RSL rise until 1000 yrs BP; when was reached the modern RSL. Between 5100 and 1000 yr BP, the RSL at the Bragança coastline probably was never higher than 0.6 m above the current.

The first mangrove forest developed at 5100 yr BP disappeared from the plains as vertical accretion continued and/or a RSL fall, and were replaced by herbaceous vegetation at about 400 yr BP. Hence, the current 168 km² of mangrove area on the Bragança Peninsula were developed starting from the middle of the peninsula, where currently is mainly colonized by Cyperaceae and Poaceae.

Chapter 7
LATE HOLOCENE MANGROVE DYNAMICS ON
THE BRAGANÇA PENINSULA (NORTHERN
BRAZIL): THE RELATIVE SEA-LEVEL AND THE
LITTLE ICE AGE⁶

⁶ Cohen, M. C. L., Behling, H., Lara, R.J. Late Holocene mangrove dynamics on the Bragança Peninsula (northern Brazil): The relative sea-level and the Little Ice Age. In preparation

Abstract

The integration of stratigraphic and palynological data with radiocarbon dating, allowed identifying two periods with low inundation frequency during the last 1000 years, in the mangroves on the Bragança Peninsula in northern Brazil. The first event extended over a period of 500 years and took place between 880 and 370 ¹⁴C yr BP. The second one started at 200 ¹⁴C yr BP and probably finished 100 ¹⁴C yr BP. These two dry events are temporally correlated with the so called “Little Ice Age” period, and may reflect a sea-level regression and/or less rainfall. The study also indicates that mangroves on the Bragança Peninsula have been migrating to higher elevated zones during the last decades, suggesting a relative sea-level rise. This increase can be associated with the global tendency of eustatic sea-level rise, due to the increase in temperature and glaciers melting around the world during the last 150 years.

Keywords: Amazon region, Late Holocene, Little Ice Age, mangroves, palynology, sea-level

7.1 Introduction

The sea-level has increased since the end of the Little Ice Age (LIA) to present-day, characterized by melting of glaciers (Ekman, 1999). The global mean sea-level rise of about 18 cm during the last century (Gornitz, 1995) has produced displacements of coastal ecosystem (Chappell, 1990; IPCC, 1996; Crooks and Turner, 1999). On the Pacific margin of Canada, the relative sea-level rose of up to 40 cm, assuming a sea-level rise of 6 mm/yr, resulted in as much as 12 m of coastal retreat (Barrie and Conway, in press). The estuaries could migrate landwards at rates of around 10 m/yr and open-coast landforms can exhibit long-shore migration rates of 50 m/yr (Pethick, 2001). In Brazil, tidal records obtained over the last 50 years show a general rise in relative sea-level (Pirazolli, 1986; Mesquita and Harari, 1983; Mesquita and Leite, 1985; Silva and Neves, 1991; Silva, 1992; Aubrey et al. 1988).

The effects of sea-level increase can be observed in the tropical regions by mangrove net losses as a result of the coastal erosions (e.g. Senegal, Benin, Côte d’Ivoire, Colombia, Venezuela and Brazil; in Blasco et al., 1996). This trend has been also recognized for the Brazilian coastline, reflected in shore erosion (Muehe and Neves, 1995). Partly of the Pará State coastline, located southeast of the Amazon river

mouth, has been observed loss of mangrove cover at least for the last 25 years, occurring at about 42% along this coastline with a net loss of mangrove coverage area of about 3.2%. On the other hand, mangroves invaded elevated herbaceous flats, in the highest portions during same period (Cohen and Lara, in press).

Increasing greenhouse gas concentrations are thought to provide the dominant forcing of climate change over the last decades (IPCC, 1995), driving to temperatures of unprecedented levels (Bradley, 2000), resulting in predicted rates of sea-level rise of +15 cm by the year 2050 and of +35 cm by 2100 (Titus and Narayanan, 1995). However, more recent predictions indicate a sea-level rise between 60 and 100 cm until the end of this century (Douglas et al., 2000).

While increases in greenhouse gas concentrations are widely assumed to be the primary cause of recent climate change, surface temperatures varied significantly during pre-industrial periods, provoked by fluctuation of solar activity levels, which produced relatively cold periods during the LIA (Lean and Rind, 1999).

The term “Little Ice Age” does not refer directly to climate but to the most recent period during which glaciers extended globally and remained enlarged (Grove, 2001), e.g. in Switzerland (Röthlisberger et al., 1980), Alaska (Calkin et al., 2001), Canadian Rockies (Luckman, 2000) and in the Andes (Iriondo and Kröhling., 1995). Based on glacial advances, the LIA occurred during the last six or seven centuries, and ending somewhere between 1850 and 1890 (Bradley and Jones., 1992). This cold period was recognized in South America by several authors (e.g. Heusser, 1961; Politis, 1984; Hurtado et al., 1985, away), causing glacier advances in the Andes (Malagnino and Strelin, 1996) and aridity in the lowlands of Argentina (Cioccale, 1999) and Venezuela (Iriondo, 1999). In Argentina, this dry period provoked a recession of the fluvial systems (Furlong Cardiff, 1937). For example during the year AD 1752 the discharge of the Paraná River was so small that the small ships (with less than 5 ft draft) could not navigate on this river at that time. Today, the Paraná River is navigated by oversea trade ships (up to 18 ft draft) as far as Asunción in Paraguay. This indicates that the dry climate of the LIA had an influence across the whole Paraná basin, including the upper sector in Brazil and Paraguay (Iriondo, 1999).

The LIA effects have not been hitherto described for Brazilian ecosystems, only in the southern region, changes of vegetation patterns coincided with the LIA period (Behling et al. submitted). In northern Brazil, the LIA effects should be recorded on the costal zones, since over 80% of sediments of the Amazon River discharge has been

derived from this mountain range (Gibbs, 1977). Changes are reflected in the Amazon shelf sedimentation, which recorded a depositional conditions from >1800 to 700 yr B.P. and a erosional phase from 700 to 100 ¹⁴C yr BP (Sommerfield et al., 1995).

The sediment transport of the Amazon River produced the longest mud coastline in the world (Kjerve and Lacerda, 1993). This coastline is colonized by mangroves, which are considered highly susceptible to sea-level fluctuations and climatic changes (Gornitz, 1991). Recently, well established sea-level histories based on coastal sequences have become important in the study and prediction of global climatic, oceanographic and tectonic fluctuations (Pirazzoli, 1988; Shennan, 1989).

The purpose of this paper is to study the environmental history of the Bragança Peninsula during the late Holocene (<1000 yrs.), focusing on the vegetation development in the central part of the peninsula, where boundaries of mangrove and salt marshes occur, and sensitive vegetation changes related to sea-level changes can be expected. This study uses the methods of stratigraphy analysis, pollen analysis and radiocarbon dating, to understand the environmental changes and its timing.

7.2 Study area

The study site is located on the Bragança Peninsula, in the eastern Amazon region, between the Maiaú and Caeté bays (00° 46' 00" - 1° 00' 00" S and 46° 36' 00" – 46° 44' 00" W, Fig. 1). The mangroves of the Bragança peninsula occur between 1 and 2.4 m above the mean sea-level (Cohen et al., 2001).

The vegetation of Bragança Peninsula is represented by the following units: Amazon coastal forest, elevated herbaceous flats (EHF), mangroves, degraded mangroves and restinga (shrub and herbs vegetation that occurs on sand plains and on dunes close to the shore line). These units are pounded on specific topographic ranges (Table 7.1 and Fig. 7.1).

7.3 Methods

7.3.1 Sampling and sample processing

Nine sediment cores of one meter depth were collected on the Bragança Peninsula (Fig.1) using a vibracore equipment. The geographic position of the sediment cores was acquired by GPS, and the topographic data were taken by hydrographic devices as described in Cohen et al. (2001). Sediment color was classified according to the Rock-Color Chart (1984).

The cores of the southern (M1, M2, M3 and M4) and northern (M5, M6, M7 and M8) part of the studied transect of 3.2 km length (Fig.7.1) were sampled from areas colonized by mangroves, at elevations between 1.7-2.0 m and 2.1-2.3 m above the mean sea-level (amsl), respectively. Integrating this transect is the M9 core, positioned 3 km to the northwest. These parts are separated by the elevated herbaceous flat (EHF) with topographical quotas reaching 2.7 m amsl. (Cohen and Lara, in press).

For pollen analysis, 0.5 cm³ samples were taken at 2.5-cm intervals along the cores. Prior to processing sediment, one tablet of exotic *Lycopodium* spores was added to each sample for calculation of pollen concentration (grains/cm³) and pollen accumulation rate (grains/cm²/yr). All samples were prepared using standard pollen analytical techniques including acetolysis (Faegri and Iversen, 1989). Sample residues were mounted in a glycerin gelatin medium. For identification of pollen grains and spores published pollen morphological descriptions were consulted (Behling, 1993; Herrera and Urrego, 1996; Roubik and Moreno, 1991). A minimum of 300 pollen grains were counted for each sample. In a few cases only 200 grains were counted. The total pollen sum excludes fern spores, fungal spores, algae and micro-foraminifers. Pollen and spore data are presented in pollen diagrams as percentages of the total pollen sum. Taxa were grouped into mangrove, herbs and forest. The software TILIA and TILIAGRAF were used for calculation and to plot the pollen diagrams (Grimm, 1987).

7.3.2 Radiocarbon dating

Based on stratigraphic contacts, which can suggest changes in tidal inundation regime, seven bulk samples of 1 cm³ were selected for radiocarbon dating by Accelerator Mass Spectrometry (AMS) in the Leibniz Laboratory of Isotopic Research at the Christian-Albrechts University in Kiel (Germany). Seeking the age comparison, the radiocarbon dates of the Campo Salgado (CS) sediment core were obtained by the Van der Graaff Laboratory at the Utrecht University (Netherlands).

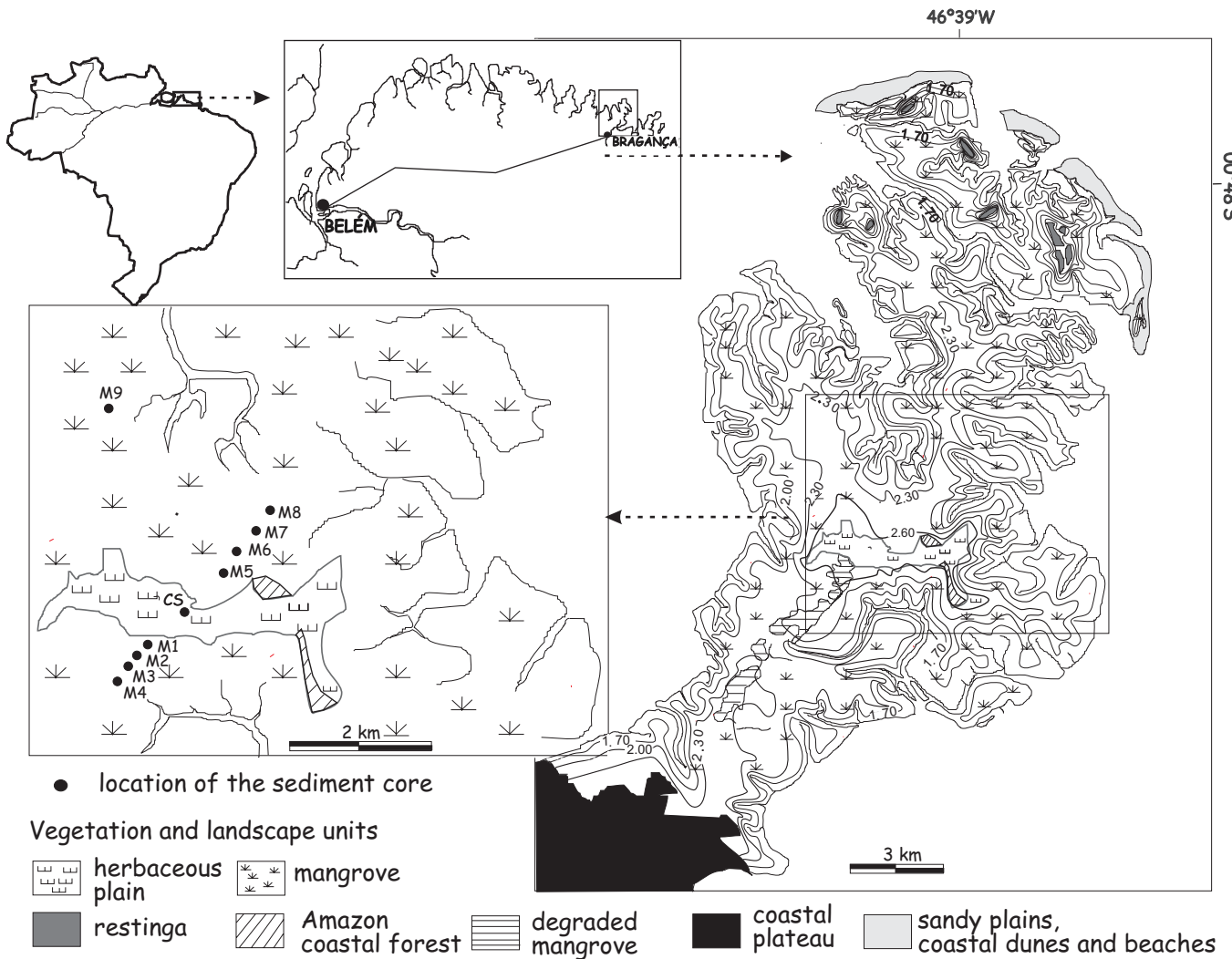


Fig. 7.1 Topographic map from Bragança Peninsula with the sediment core position and vegetation units.

Table 7.1- Topographic distribution of vegetation units on the Bragança Peninsula.

| Vegetation Units | Area | Topography and Tide | Sediment |
|-----------------------|---------------------|---|----------|
| Amazon coastal Forest | 1 km ² | 3.0 m above the mean sea-level, never inundated by the tide | Sand |
| Restinga | 2 km ² | 3.0 m , close to the littoral | Sand |
| Herbaceous plan | 7 km ² | 2.4-3.0 m, supra-tidal | Mud-sand |
| Degraded mangrove | 3 km ² | 2.2 – 2.5 m inundated only in spring tide | Mud |
| Mangrove | 168 km ² | 1.0 – 2.4 m occurs between the mean sea-level and the mean high tide of spring tide | Mud |

7.4 Results

7.4.1 Stratigraphy

The cores from northern and southern part of the studied transect (Fig.7.1) show significant stratigraphic differences (Fig. 7.3). Only the base most of the sediment cores have common layers (C1 and C2). The core base from the northern and southern part contain gray (N8) fine sand, well sorted, with sand waves inserted with mm- and cm-thick gray (N5) mud lens, composing the C1 layer. This grain size alternation can be related to tidal actions (Reineck and Wunderlich, 1967; 1968). The unit C1 contains a gradational contact to the upper layer (C2), which is mainly constituted by gray (N5) sandy mud. The next layer (C5) is constituted by organic gray (N5) mud, and occurs in all sediment cores from the southern part of the transect, except in the M1 core. Above this unit occurs an oxidized mud layer (C8), with dark yellow color (5Y 6/4), and brown spots (5 YR 5/6). This sedimentary sequence is completed by a non-oxidized thin sandy mud layer on the core top (C9). Some cores (CS and M9) reveal an organic mud layer (C7), with root fragments. Besides the described units, the sediment cores from the northern part present also a gray (N5) sandy layer (C3), between the C5 and C2 layers to the south, which is characterized by a dark yellow (5Y 6/4) oxidized sandy mud.

7.4.2 Radiocarbon age and sedimentation rates

The radiocarbon dates (Table 7.2) indicate that the sediment deposits accumulated relatively undisturbed (Fig. 7.3). The calculated sedimentation rates are about 0.66 (M5), 0.66 (M6), 0.75 (M2), 0.8 (M9) and 0.95 mm/yr (M3), which is in the range of previously sedimentation rate published by Behling et al. (2001) for upper part of the Campo Salgado core (0.9 mm/yr). The radiocarbon date of the M1/10 cm sample indicates that the non-oxidized C9 layer probably was deposited over the last 50 years.

7.4.3 Pollen data

Based on the pollen analyses of the nine sediment cores (Fig. 7.2) was composed a pollen profile, which shows the zones of different paleo-vegetation types (Fig. 7.4). The cores M5 and M6 from the northern sector contain mangrove pollen in the sediments above the C1 sandy layer, primarily represented by *Rhizophora* (88-98%) and *Avicennia* (0.8-3.5%) (Fig. 7.2). The pollen composition suggests a frequently flooded zone colonized by mangrove (see Table 1). In the upper part of this layer, mangrove pollen become progressively less frequent until the layer, which contains non-pollen (P1, Figs.

2 and 4). This layer present few pollens and spores, and they are mostly destroyed. Then, they are not included in the pollen diagram. For more details about this unit see Behling et al. (2001).

Table 7.2- Radiocarbon dates (AMS) and the topographic position of the samples.

| Sample | Depth below sediment (cm) | Depth related to the mean sea-level (cm) | Radiocarbon dates (years BP) | Cal yr BP |
|---------------------------------|---------------------------|--|------------------------------|-----------|
| M1/10 cm | 10 | +18 | >1950 AD | >1950 AD |
| M3/30 cm | 30 | -25 | 315 ± 25 | 390 ± 50 |
| M2/27,5 cm | 27.5 | -10 | 365 ± 25 | 420 ± 70 |
| CS/30 cm (Behling et al., 2001) | 30 | +70 | 373 ± 25 | 420 ± 70 |
| M9/32 cm | 32 | +28 | 400 ± 30 | 440 ± 70 |
| M5/15 cm | 15 | -65 | 450 ± 30 | 510 ± 20 |
| RKS3/351 cm (Koch, unp.data) | 351 | -251 | 756 ± 20 | 690 ± 20 |
| M5/57.5 cm | 57 | -07 | 860 ± 40 | 800 ± 70 |
| M6/57.5 cm | 57.5 | -20 | 875 ± 35 | 820 ± 70 |
| CS/90 cm (Behling et al., 2001) | 90 | +10 | 1018 ± 26 | 950 ± 20 |

Above the non-pollen layer (P1) occurs a sedimentary unit, found in the M9, M6, M7 and M8 core, with mangrove pollen marked by *Rhizophora* (M6: 68-80%; M7:~65%; M8: 72-90% and M9: 64-88%) and *Avicennia* (M6: 4-10%; M7:~15%; M8: 4-10% and M9: 4-7%). This zone contains also a significant amount of herbaceous pollen (M6: 7-18%; M7:~10%; M8: 3-8% and M9: 8-27%). These pollen assemblages characterize the upper limit of mangrove area with a relatively low tidal inundation frequency (Table 1) according to results obtained by modern pollen rain studies (Behling et al., 2001).

The following zone (P2), found in the M9, M5, M6 and M7 cores, is characterized by abundant herbaceous pollen, represented by Cyperaceae (M5: 27-39%; M6: 23-65% and M9: 34-71%) and Poaceae (M5: 1-27%; M6: 4-11%; M7: 5-25% and M9: 0-5%).

Mangrove pollen are less frequent, but *Avicennia* (M5: 4-13%; M6: 5-12%; M7: 9-15% and M9: 5-10%) is proportionally more abundant in relation to *Rhizophora* (M5: 38-65%; M6: 24-47; M7: 59-65% and M9: 20-55%) than in the mangrove layer before. The CS core, sampled from a relatively high elevated area, contains herbaceous pollen up to the surface, but cores from the southern and northern sector show a mangrove pollen layer above the herbaceous pollen layer (Fig. 7.4).

The southern sector is characterized by a horizontal limit of the herbaceous pollen layer (Fig. 7.4, P2). The P2 layer in this sector is represented by Cyperaceae (M1: 17% and M4: 62-61%) and Poaceae (M1: 9,4% and M4: 0-5,7%). Despite of the P2 layer, observed only in the M1 and M4 core, the non-pollen layer (P1) occurs in the M1, M2 and M3 cores from the southern sector.

In the upper part of the southern sector a mangrove layer occurs, characterized by pollen of *Rhizophora* (M1: 81-95%, M2: 87-96%, M3: 88-98% and M4: 73-95%) and *Avicennia* (M1: 1-5%; M2: 1-3; M3: 0-4% and M4: 1-5%).

7.5 Interpretation and discussion

7.5.1 Climate change/Relative sea-level relation

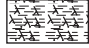

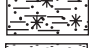



The coastal relative sea-level acts as an integrator of the forces (Plang and Tsimplis, 1999), e.g. interacting isostatic, eustatic, tectonic and climatic (rainfall-river discharge, air temperature and air pressure). Palyno-chronostratigraphic records suggest that warm climate is related to a high sea-level (e.g. Molodkov and Bolikhovskaya, 2002). Therefore, disregarding the tectonic activity, sea-level regression corresponds to climatic cold phases and sea-level transgressions to climatic warm phases due basically to the glacial eustasy (e.g. Fairbridge, 1961 and Oerlemans, 2001).

During the Late Holocene, the sea-level was affected by other forces, such as precipitation that strongly influence the run-off, and the river discharge which have significant effects on sea-level, resulting in a local “eustatic” variations (e.g. Mörner, 1996). Therefore at regional level, rapid regressions may be caused by short (a century, or so) regional dry events (Mörner, 1999). Even season variability such as air pressure (Loon et al., 1993) or air temperature (Thompson, 1995) can result in relative sea-level changes (Plang and Tsimplis, 1999).





In this context, the data from the Bragança Peninsula allow to propose periods with different tidal inundation frequencies. However, vegetation changes may also be related to climate provoked exclusively by the precipitation changes, which would be sufficient to cause adjustments in porewater salinity (Sylla et al., 1995) and displace the wetlands (Baltzer, 1970).



Stratigraphic units

-  organic mud bio-turbated
-  gray organic mud
-  oxidized sandy-mud, dark yellow with light brown spots
-  gray sandy sediments
-  gray sandy-mud
-  sand waves alternating with mud lenses.

Palaeo-environmental units

-  mangrove
-  herbaceous plain
-  hypersaline tidal flat (non-pollen)
-  sandy flood plain

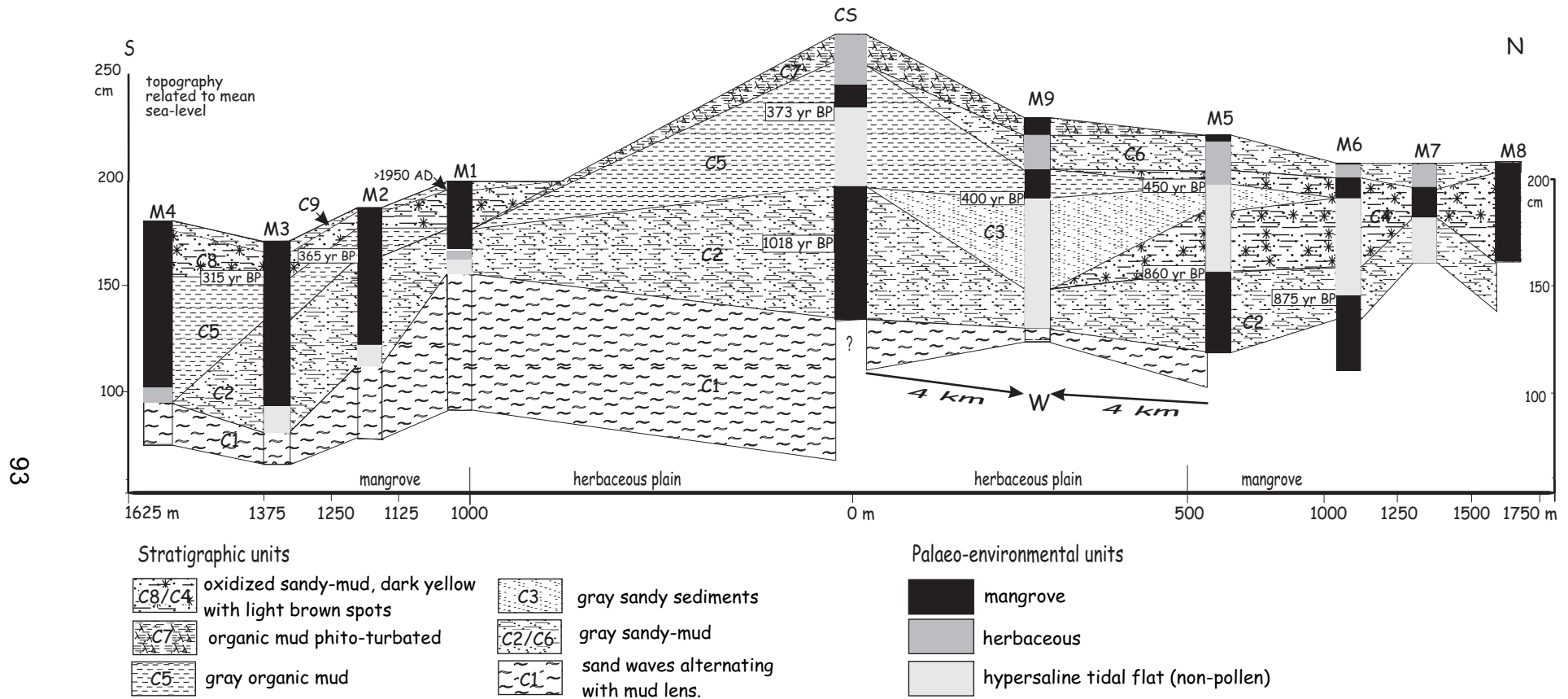


Fig. 7.3- Integration of stratigraphy and pollen profile. The sediment cores are named as M1 to M9 and CS. The sediment layers are C1 to C8.

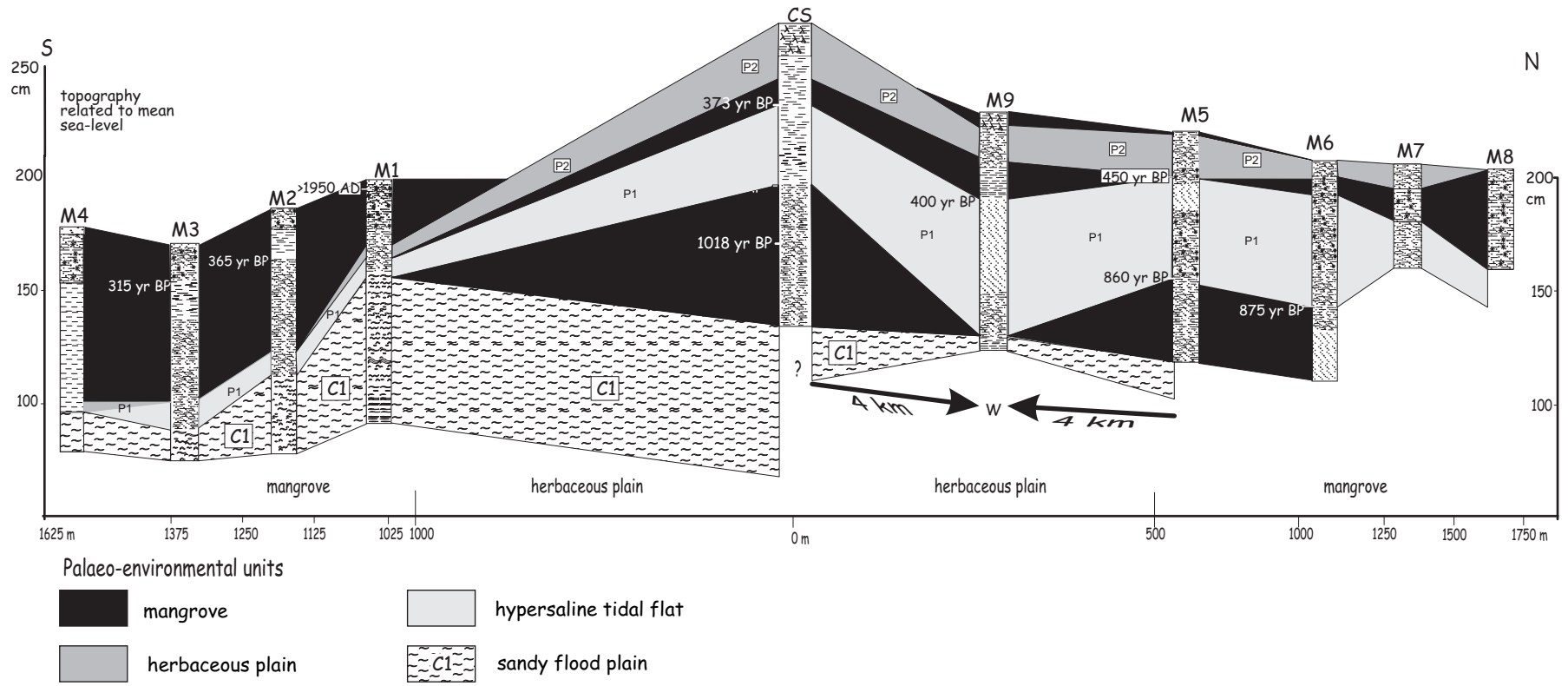


Fig. 7.4- Composition of pollen profile from study site.

The combination of stratigraphic sequences and pollen records obtained from mangrove deposits (Fig. 7.4) suggests the possibility to discuss the interaction between climate and inundation regime changes. Since, changes in the sediment grain-size, probably imply an adjustment in the sediment transport energy in mangroves (Furukawa and Wolanski, 1996), while the pollen assemblage may indicate annual rainfall rates and/or inundation frequency changes in mangroves.

According to these parameters, the base of sediment cores sampled from Bragança Peninsula are characterized by sediments and structures (sand waves alternating with mud lens, see stratigraphy) that indicate a sandy plain (C1) with a relatively high inundation frequency (Figs. 7.3 and 7.4). In its upper limit is found a decrease in grain-size, and mangrove pollen occur. Probably, this concomitant change of pollen assemblages and grain-size evidences a decrease of tidal inundation frequency. Mangrove occurred until about 860 and 875 yr BP in the M5 and M6 sites. These ages also mark the lower limit of a mud layer in the CS core and an oxidized sandy mud layer in the M5 core (Fig. 7.3). Above the layer with mangrove pollen occurs a sediment deposit with non-pollen content (Fig. 7.4), which probably is related also to a decreasing trend of inundation frequency. This suggests a period (P1) of low flooding frequency until approximately 370, 400, and 450 yr BP in CS, M9, and M5 cores, respectively. This layer may have deposited under conditions of a hypersaline tidal flat, which are devoid of vegetation and occurs along arid coastlines. This habitat is characterized by a low tidal inundation frequency and/or insufficient rainfall to dilute the extreme hypersalinity that arises due to the high evaporation (Spenceley, 1976; Sommenfield, 1984; Tomlinson, 1986; Semeniuk, 1996).

The uppermost zone is covered by a mangrove layer, which is registered in the cores M9, CS, M6, M7 and M8, with 10, 7, 7.5, 10 and 40 cm thickness, respectively. In the M9 core, the palynological evidence of mangrove occurs together with a grain-size decrease, which suggests changes in the flooding regime. However, in the CS and M6 cores were not found any significant changes in sediment characteristic for this transition (Fig. 7.3). It may suggest climate factors (e.g. increase in annual rainfall rates) simultaneously acting with the increase of inundation frequency to develop this mangrove.

Probably, after this short mangrove phase, the hydrologic situation changed again. Palynological and sediment grain-size data evidence a low inundation frequency phase

(P2) that favored the development of a herbaceous plain mainly represented by Cyperaceae and Poaceae (Fig. 7.4).

Nowadays, a similar vegetation unit occurs only on topographically elevated areas of the Bragança Peninsula. In the M1, M9, M5, M6 and M7 cores this herbaceous zone is found, but covered by a new layer characterized by mangrove pollen. The stratigraphical relation between these cores indicates that the Bragança Peninsula mangroves are migrating to topographically elevated areas (Fig. 7.4).

Temporal analysis of satellite images covering a period of 25 years, also indicated a mangrove migration to elevated sectors of this peninsula. On the other side, the mangrove ecosystem is losing area at the coast. This vegetational dynamic suggests that the mangroves are reacting according to increases in tidal inundation frequency, which is probably associated to relative sea-level rise (Cohen and Lara, in press). This increase may be related to the trend of global sea-level rise, according to the temperature increase and to the glaciers retreat around the world during the last 150 years (Oerlemans, 2001).

7.5.2 Relative sea-level changes at the Bragança Peninsula during the Little Ice Age chronozone

Atlantic sea-level fluctuation was probably the major factor in palaeoenvironmental changes in the Amazon Basin during the Holocene. High water levels in the Amazon Basin might also partly related to climate change, resulting in higher annual rainfall rates (Behling, 2002). The pollen and stratigraphic records from the Bragança Peninsula indicate two little flooded periods, which may be resulted of a relative sea-level fall associated, or not, to lower annual rainfall rates. The first event (P1), with a duration of 500 years, occurred between 880 and 370 ^{14}C yr BP. The second one (P2) started about 200 ^{14}C yr BP ago. The end of this period is still indefinite due to the dating limit of the ^{14}C , but it may have finished about 100 yr BP, due to the current trend of global sea-level rise.

The presence of oxidized layers may also indicate hydrologic changes as suggested by palynological results, since generally the oxidation of sulfides in the sediment can be due to the water table drop and/or low rainfall (Clark et al., 1998; Brown and Cohen, 1995). The radiocarbon dates obtained from the base of two oxidized layers indicate that they were oxidized between 860 (C4 layer) and 315 yr BP (C8 layer, Fig.7.3). Since the water table in many parts of the study area fluctuates with changing climatic conditions,

the stratigraphic position of the upper redox transition is not constant (Clark et al., 1998). Therefore, it is probable that these oxidized zones are relics of the two dry periods registered in the pollen profiles.

Although the dated samples are not a definitive indicator of the eustatic sea-level changes, they may be used to construct the local history of its relative oscillations (Gardner and Porter, 2001). The contacts between intertidal sandy plains and mangroves provide data to trace the relative sea-level changes in tropical regions (Scholl, 1964; Fujimoto and Miyagi, 1993; Woodroffe et al., 1993; Beaman et al., 1994; Fujimoto et al., 1996 and Belperio et al., 2002). Therefore, the relationship between the topography vegetation and the mean sea-level (Cohen et al., 2001) allow to suggest a relative sea-level trend over the last 1000 yr BP for the Bragança Peninsula (Fig. 7.5).

Therefore, for the period between 1000 and 860 yr BP, the relative sea-level (RSL) was similar to the current, and during the following four centuries, the RSL was below the modern (756 ¹⁴C yr BP -2.5 meters below the mean sea-level (bmsl); and 450 ¹⁴C yr BP -0.65 m bmsl). A RSL fall of about 2.5 m, about 750 yr BP, seems improbable for a time interval of ~100 years. Factors involving autocompaction (Kaye and Barghoorn, 1964) and/or lateral accretion (Woodroffe, et al., 1989) may results in sea-level curve being displaced (Larcomb et al., 1995). However, the other RSL of about 0.65 m bmsl at 450 ¹⁴C yr BP, and the pollen assemblages suggest in fact that the RSL was below the present during this time interval (880 to 400 yr BP).

A RSL close to the current probably occurred about 370 ¹⁴C yr BP. Later, this region may have suffered a small RSL fall, and again a rise until to the current level (Fig. 7.5).

7.5.3 Climate change during the last 1000 years

Pollen record from lowland Amazonian Ecuador indicate that the last 1000 yr BP were relatively dry (Weng et al., 2002). The first and second dry periods on the Bragança Peninsula are temporally synchronized with dry periods registered in Venezuela (Iriando, 1999) and Argentina (Cioccale, 1999). Besides, the glaciers advance in Alaska (Calkin et al., 2001), Canada (Luckman, 2000), Switzerland (Röthlisberger et al., 1980) and mainly in the Andes (Malagnino and Strelin, 1996) also support the existence of two relatively colds periods, close to the time intervals found on the Bragança Peninsula (Fig. 7.5). However, it should be considered whether the model of the “Little Ice Age” derived from the northern hemisphere is applicable to the southern (Grove, 2001).

Apparently, the climate in South America has been controlled by different factors, e.g. El Niño/Southern Oscillation (ENSO) and the decadal variations of the interhemispheric sea surface temperature (SST) gradient across the Equator in the Atlantic, which is also called the tropical Atlantic SST dipole (TAD) (e.g. Shulmeister, 1999; Trauth, et al., 2000; Kogan, 2000). However, the connection among events registered in different parts of this continent can also be attributed to fluvial system, since the rivers discharge affects the mangrove distribution (Kjerve and Lacerda, 1993), and the Amazon River has 80% of its sediments derived from Andes (Gibbs, 1977). Data from the Colombian Andes indicate wet and dry periods during the last 800 yr BP (Van der Hammen, 1986), which may have produced changes in the discharge of the Amazon River (Vital and Stattegger, 2000).

Geological studies of the Amazon shelf show changes in the dispersal of Amazon River sediments during the late Holocene (Alexander et al., 1986; Eisma et al., 1991). The relict-mud depositional phase occurred at least from 1800 to 700 ^{14}C yr BP. Erosion of deposits probably occurred between about 700 and 100 ^{14}C yr BP, when the modern phase of accumulation began, indicating a maximum hiatus of about 600 yr. This depositional and erosional phase is due to the interactions of river discharge with oceanographical and meteorological processes (Sommerfield et al., 1995). More specifically, Eisma et al. (1991) suggest that dry climatic periods in the Colombian Andes from 900 to 600 ^{14}C yr BP and 400 to 200 ^{14}C yr BP reduced the supply of Amazon sediment and water to the shelf, resulting in erosion or non-deposition.

Therefore, ahead of the presented evidences (Fig. 7.5), we believe that the causes to these events should be analyzed together. Although, certain synchronization lack among the cited events occur, which can have several causes (e.g. insufficient dating, sediment type, see Bartlein et al., 1995), apparently, two cold/dry events occurred over the last 1000 ^{14}C yr BP, and the first one was temporally larger than the second.

7.6 Conclusion

The integration of pollen and sediment analyses, including AMS-radiocarbon dating, was used to identify the inundation regime characteristics on the Bragança Peninsula in northern Brazil during the last 1000 yr BP. This study suggests two periods of low inundation frequency (P1 and P2), which probably occurred between 875 and 370 ^{14}C yr

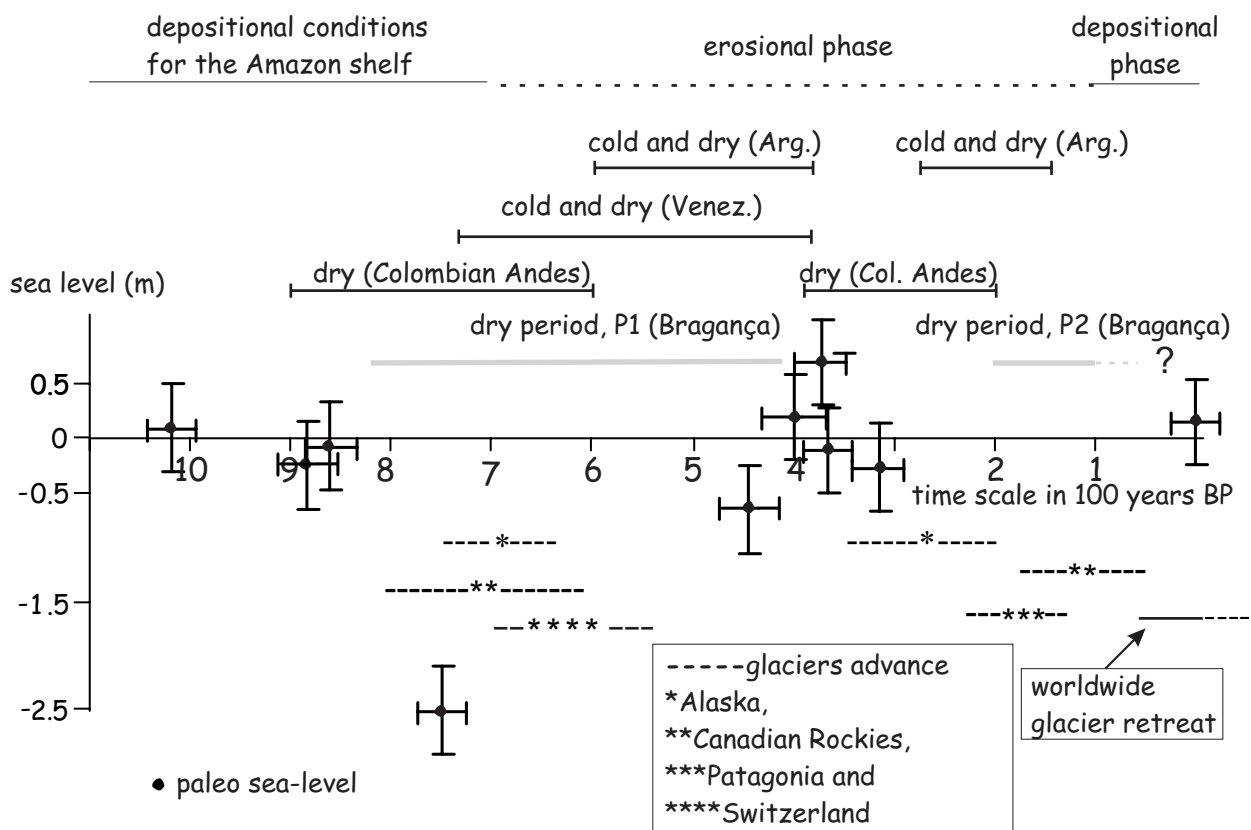


Fig. 7.5 Comparative diagram between some LIA records, and the hydrologic and paleovegetation characteristics from Bragança Peninsula over the last 1000 years BP.

BP; and 200 and 100 yr BP. This alternation of dry and wet periods is coupled with relative sea-level changes. The pollen records also indicates that mangroves on the Bragança peninsula migrate to higher elevated zones during the last decades, suggesting a relative sea-level rise.

The data presented in this work allowed to discuss the possible links between these two dry periods at the Bragança Peninsula and global climatic changes that occurred during the last 1000 years. The P1 and P2 events may be temporally correlated to an erosional period in the Amazon shelf, dry climate in South America and glacier advances in Europe, North America and Andes. The present mangrove migration can be associated to the global tendency of eustatic sea-level rise, due to the increase in temperature and glaciers melting around the world during the last 150 years.

References

- Alexander, C.R., Nitrouer, C.A., DeMaster, D.J., 1986. High resolution seismic stratigraphy and its sedimentological interpretation on the Amazon continental shelf. *Continental Shelf Research* 6, 337-357.
- Alongi, D.M., Boto, K.G., Robertson, A.I., 1992. Nitrogen and Phosphorus Cycles. pp. 251-292. In: Robertson A.I., Alongi D.M. (eds), *Tropical Mangrove Ecosystems*. American Geophysical Union, Washington, DC.
- Angulo, R.J., Lessa, G.C., 1998. The Brazilian sea-level curves: a critical review with emphasis on the curves from the Paranaguá and Cananéia regions. *Marine Geology* 140, 141-166.
- Angulo, R.J., Giannini, P.C.F., Suguio, K., Pessenda, L.C.R., 1999. Relative sea-level changes in the last 5500 years in southern Brazil Laguna–Imbituba region, Santa Catarina State based on vermetid ¹⁴C ages. *Marine Geology* 159, 323–339.
- Angulo, R.J., Lessa, G., 1997. The Brazilian sea level curves: a critical review with emphasis on the curves from Paranaguá and Cananéia regions. *Marine Geology* 140, 141-166.
- Arai, M., Truckenbrodt, W., Nogueira, A.C.R., Góes, A..M. Rosseti, D.F., 1994. Novos dados sobre a estratigrafia e ambiente deposicional dos sedimentos barreiras, NE do Pará. In: *Simpósio de Geologia da Amazônia*, 4., Belém. SBG-Núcleo Norte. pp.185-187.
- Argento, M.S.F., 1989. The Paraíba do Sul retrogradation and the Atafona environmental impact. In: Neves, C.F., Magoon, O.T. (eds.), *Coastline of Brazil*, New York: American Society of Civil Engineers. pp. 267-277.
- Aubrey, D.G., Emery, K.O., Uchupi, E., 1988. Changing coastal levels of south america and the Caribbean region from tide-gauge records. *Tectonophysics* 154, 269-284.
- Aucan, J., Ridd, P.V., 2000. Tidal asymmetry in creeks surrounded by saltflats and mangroves with small swamp slopes. *Wetlands Ecology and Management* 4, 233-231.
- Augustinus, P.G.E.F., 1980. Actual development of the chenier coast of Suriname (South America). *Sedimentary Geology* 26, 91-113.
- Baltzer, F., 1970. Etude sédimentologique du marais de Mara (Côte ouest de la Nouvelle Calédonie) et de formations quaternaires voisines. *Mémoires expédition française sur les récifs coralliens de la Nouvelle Calédonie*, Foundation Singer-Polignac 4, 146–169.
- Barrie, J.V., Conway, K.W. Rapid sea-level change and coastal evolution on the pacific margin of Canada. *Sedimentary Geology*, (in press).
- Bartlein, P.J., Edwards, M.E., Shafer, S.L., Barker Jr. E.D., 1995. Calibration of Radiocarbon Ages and the Interpretation of Paleoenvironmental Records. *Quaternary Research* 44, 417-424.
- Beaman, R., Larcombe, P., Carter, R.M., 1994. New evidence for the Holocene sea-level high from the inner shelf, Central Great Barrier Reef, Australia. *Journal of Sedimentary Research. A Sedimentary Petrology Process* 4, 881-885.
- Behling, H., 1993. Untersuchungen zur spätpleistozänen und holozänen Vegetations- und Klimageschichte der tropischen Küstenwälder und der Araukarienwälder in Santa Catarina (Südbrasilien). *Dissertationes Botanicae* 206, J. Cramer, Berlin Stuttgart, pp.149.

- Behling, H., 1996. First report on new evidence for the occurrence of *Podocarpus* and possible human presence at the mouth of the Amazon during the Late-glacial. *Vegetation History and Archaeobotany* 5, 241-246.
- Behling, H., da Costa, M.L., 1997. Studies on Holocene tropical vegetation, mangrove and coast environments in the state of Maranhão, NE Brazil. *Quaternary of South America and Antarctic Peninsula* 10, 93-118.
- Behling, H., da Costa, M.L., 2000. Holocene environmental changes from the Rio Curuá record in the Caxiuana region (eastern Amazon Basin). *Quaternary Research* 53, 369-377.
- Behling, H., da Costa, M.L., 2001. Holocene vegetation and coastal environmental changes from Lago Crispim in northeastern Pará State, northern Brazil. *Review of Palaeobotany and Palynology* 114, 145-155.
- Behling, H., Pillar, V.D., Orlóci, L., Bauermann, S.G. Late Quaternary *Araucaria* forest, grassland (Campos), fire and climate dynamics, studied by high resolution pollen, charcoal and multivariate analysis of the Cambará do Sul core in southern Brazil. *Palaeogeography, Palaeoclimatology, Palaeoecology* (submitted).
- Behling, H., Cohen, M.C.L., Lara, R.J., 2001. Studies on Holocene mangrove ecosystem dynamics of the Bragança Peninsula in north-eastern Pará, Brazil. *Palaeogeography, Palaeoclimatology, Palaeoecology* 167, 225-242.
- Behling, H., 2002. Impact of the Holocene sea-level changes in coastal, eastern and central Amazonia. *Amazoniana* 17, 41-52.
- Belperio, A.P., Harvey, N., Bourman, R.P., 2002. Spatial and temporal variability in the Holocene sea-level record of the South Australian coastline. *Sedimentary Geology* 150, 153-169.
- Belperio, A.P., 1979. Negative evidence for a mid-Holocene high sea level along the coastal plain of the Great Barrier Reef Province. *Marine Geology*, M1-M9.
- Bijlsma, L., 1996. Coastal zones and small islands. In: Watson, R. Zinyowera, M., Moss, R. (eds.), *Climate Change 1995: Impacts, Adaptations and Mitigation of Climate Change: Scientific-Technical Analyses. Contribution of Working Group II to the Second Assessment Report of the Intergovernmental Panel on Climate Change*, Cambridge University Press, Cambridge: pp. 289-324
- Blasco, F., Saenger, P., Janodet, E., 1996. Mangroves as indicators of coastal change. *Catena* 27, 167-178.
- Boto, K.G., Wellington, J.T., 1983. Phosphorus and nitrogen nutritional status of a northern Australian mangrove forest. *Marine Ecology Progress Series* 11, 63-69.
- Bradley, R.S., 2000. Past global changes and their significance for the future. *Quaternary Science Reviews* 19, 391-402.
- Bradley, R.S., Jones, P.D., 1992. When was the "Little Ice Age", in Mikami, T. (ed.), *Proceedings of the International Symposium on the "Little Ice Age" Climate*, Department of Geography, Tokyo Metropolitan University, 1-4.
- Bromfield, S.M., 1960. Some factors affecting the solubility of phosphates during the microbial decomposition of plant material. *Australian Journal Agriculture Research* 11, 304-316.
- Brown, K.E., Cohen, A.D., 1995. Stratigraphic and micropetrographic occurrences of pyrite in sediments at the confluence of carbonate and peat-forming depositional systems, southern Florida, U.S.A. *Org. Geochemical* 22, 105-126.
- Bryant, E.A., Young, R.W., Price, D.M., Short, S.A., 1992. Evidence for Pleistocene and Holocene raised marine deposits, Sandon Point, New South Wales. *Australian Journal* 39, 481-493.

- Bunt, J.S., Williams, W.T., Bunt, E.D., 1985. Mangrove species distribution in relation to tide at the seafront and up rivers. *Australian Journal of Marine Freshwater Research* 36, 481-492.
- Burrough, P.A., 1986. Principles of Geographical Information Systems for Land Resources Assessment. Monographs on Soil and Resources Survey. Clarendon Press, Oxford, pp.193.
- Calkin, P.E., Wiles, G.C., Barclay., D.J., 2001. Holocene coastal glaciation of Alaska. *Quaternary Science Reviews* 20, 449-461.
- Caratini, C., Fontugne, M., 1992. A high sea level stand assigned to c. 125,000 years BP on the western coast of India. In: *Oceanography of the Indian Ocean*. Desai, B.N. (ed). New Delhi India Oxford and IBH. pp. 439-445.
- Carlson, P.R., Yarbrow, L.A., Zimmermann, C.F., Montgomery, J.R., 1983. Pore water chemistry of an overwash mangrove island. In: Taylor, W.K. and Whittier, H.O. (eds), *Future of the Indian River System*. First Symposium, Melbourne, FL, USA, pp. 239-250.
- Chapman, V.J., 1960. *Salt Marshes and Salt Deserts of the World*. New York, Interscience Publishers, pp. 382.
- Chappell, J. 1990. Some effects of sea-level rise on riverine and coastal lowlands. In: P. Bishop (ed), *Lessons for Human Survival: Nature's Record from the Quaternary*. Geological Society Australian Symposium 1, 37-49.
- Chappell, J., 1993. Contrasting Holocene sedimentary geologies of lower Daly River, northern Australia, and lower Sepik-Ramu, Papua New Guinea. *Sedimentary Geology* 83, 339-358.
- Chappell, J., 1990. Some effects of sea level rise in marine and coastal. *Geological Society Australian., Special Publication* 1, 37-45.
- Chappell, J., Polach, H., 1991. Post-glacial sea-level rise from a coral record at Huon Peninsular, Papua New Guinea. *Nature* 349, 147-149.
- Cioccale, M.A., 1999. Climatic fluctuations in the Central Region of Argentina in the last 1000 years. *Quaternary International* 62, 35-47.
- Clark, R.L., Guppy, J.C., 1988. A transition from mangrove forest to freshwater wetland in the monsoon tropics of Australia. *Journal of Biogeography* 15, 665-684.
- Clark, M.W., McConchie, D. Lewis, D.W., Saenger, P., 1998. Redox stratification and heavy metal partitioning in *Avicennia*-dominated mangrove sediments: a geochemical model. *Chemical Geology* 149, 147-171.
- Cohen, M.C.L., Lara, R.J., Ramos, J.F.F., Dittmar, T., 1999. Factors influencing the variability of magnesium, calcium and potassium in waters of a mangrove creek in Bragança, North Brazil. *Mangroves and Salt Marshes* 3, 9-15.
- Cohen, M.C.L., Lara, R.J., Szlafsztein, C.F., Dittmar, T., 2001. Digital Elevation Model applied to Mangrove Coast Analysis, Amazon Region, Brazil. *Journal of International Environment Creation* 4, 1-8.
- Cohen, M.C.L., Lara, R.J., Szlafsztein, C. F., Dittmar. Mangrove inundation and nutrient dynamics under a gis perspective. *Wetlands Ecology and Management*, (in press).
- Cohen, M.C.L., Lara, R.J. Temporal changes of mangrove vegetation boundaries in Amazônia: application of GIS and remote sensing techniques. *Wetlands Ecology and Management*, (in press).
- Cohen, M.C.L., Lara, R.J., Szlafsztein, C.F., Dittmar, T., 2000. Analysis of mangrove inundation by GIS techniques. *Symposium Mangroves 2000*. Recife, Brazil.CD.

- Costa, J.B.S., Borges, M.S., Bemerguy, R.L., Fernandes, J.M.G., Costa Jr., P.S. Costa, M.L., 1993. Evolução cenozóica da região de Salinópolis, Nordeste do Estado do Pará. *Geociências* 12, 353-372.
- Costa, J.B.S., Bemerguy, R.L., Hasui, Y., Borges, M. S., Fereira Júnior, C.R.P., Bezerra, P.E.L., Costa, M.L., Fernandes, J.M.G., 1996. Neotectônica da Região Amazônica: Aspectos tectônicos, geomorfológicos e deposicionais. *Geonomos* 4, 23-44.
- Crooks, S., Turner, R.K., 1999. Integrated coastal management: sustaining estuarine natural resources. *Ecology Research* 29, 241-289.
- DHN – Departamento de Hidrografia e Navegação, 1999. Tábuas de Marés para 1999. Costa do Brasil. Rio de Janeiro, DHN, 1-6.
- Dittmar, T., Lara, R.J., 2001. Driving forces behind nutrient and organic matter dynamics in a mangrove tidal creek in North Brazil. *Estuarine Coastal Shelf Science* 52, 249-259.
- Douglas, B.C., Kearney, M.S., Leatherman, S.P., 2000. Sea Level Rise, History and Consequences. Academic Press. Vol. 75, pp. 416.
- Eisma, D., Augustinus, P.G.E.F., Alexander, C.R., 1991. Recent and subrecent changes in the dispersal of Amazon mud. *Neth. Journal Sea Research* 28, 181-192
- Ekman, M., 1999. Climate changes detected through the world's longest sea level series. *Global and Planetary Change* 21, 215-224.
- Fabre, A.C., 1992. Inorganic phosphate in exposed sediments of the river Goronne. *Hydrobiologia* 228, 37-42.
- Faegri, K., Iversen, J., 1989. *Textbook of Pollen Analysis*. 4th ed. Wiley, Chichester, pp. 328.
- Fairbridge, R.W., 1961. Eustatic changes in sea level. *Physics and Chemistry of the Earth* 4, 99-185.
- Fisher, P.F., 1991. Spatial data sources and data problems. In: Maguire, D.J., Goodchild, M. and Rhind, D. (eds.), *Geographical Information Systems: Principles and Applications*. Longman, London 1, 175-189.
- Flessa, K.W., Constantine, K.J., Cushman, M.K., 1977. Sedimentation rates in a coastal marsh determined from historical records. *Chesapeake Science* 18, 172-176.
- Fletcher III, C.H., Pizzuto, J.E., John, S., van Pelt, J.E., 1993. Sea-level rise acceleration and the drowning of the Delaware Bay coast at 1.8 ka. *Geology* 21, 121-124.
- Franzinelli, E., 1982. Contribuição à geologia da costa do Estado do Pará (entre a baía de Curaça e Maiau). In: *Atlas IV Simpósio do Quaternário no Brasil*, (K. Suguio, M.R.M. De Meis and M.G. Tessler, eds). Rio do Janeiro, pp. 305-322.
- Frey, R.W., Basan, P.B., 1985. Coastal salt marshes. *Coastal Sedimentary Environments*. Davis, R. A. Jr. (ed.) pp. 225-302.
- Fujimoto, K., Miyagi, T., 1993. Development process of tidal-flat type mangrove habitats and their zonation in the Pacific Ocean. A geomorphology study. *Vegetation* 106, 137-146.
- Fujimoto, K., Miyagi, T., Kikuchi, T., Kawana, T., 1996. Mangrove habitat formation and response to Holocene sea-level changes on Kosrae Island, Micronesia. *Mangroves and Salt Marshes* 1, 47-57.
- Furlong Cardiff, G., 1937. *Cartografia Jesuítica del Rio de La Plata*. Buenos Aires. Publicaciones del Instituto de Investigaciones Históricas LXXXI, pp.125.
- Furukawa, K., Wolanski, E., 1996. Sedimentation in mangrove forest. *Mangroves and Salt Marshes* 1, 3-10.
- Gable, F.J., Aubrey, D.G., Gentile, J.H., 1991. Global environmental change issues in the Western Indian Ocean region. *Geoforum* 22, 401-419.

- Gagan, M.K., Johnson, D.P., Crowley, G.M., 1994. Sea level control of stacked late Quaternary coastal sequences, central Great Barrier Reef. *Sedimentology* 41, 329-351.
- Gardner, L.R., Porter, D.E., 2001. Stratigraphy and geologic history of a southeastern salt marsh basin, North Inlet, South Carolina, USA. *Wetlands Ecology and Management* 9, 371-385.
- Gayes, P.T., Scott, D.B., Collins, E.S., Nelson, D.D., 1992. A late Holocene sea-level fluctuation in South Carolina. In: C.H. Fletcher and J.F. Wehmiller (eds.), *Quaternary Coasts of the United States: Marine and Lacustrine Systems*, SEPM Special Publication 48, 155-160.
- Grove, J.M., 2001. The initiation of the "Little Ice Age" in regions round the North Atlantic. *Climatic Change* 48, 53-82
- Gibbs, R.J., 1977. Clay mineral segregation in the marine environment. *Journal Sedimentary Petrology* 47, 237-243.
- Gleason, M.L., Elmer, D.A., Pien, N.C., Fisher, J.S., 1979. Effects of stem density upon sediment retention by salt marsh cordgrass, *Spartina alterniflora*, Loisel. *Estuaries* 2, 271-273.
- Gomes, F.C., Jr., 1987. Inferência sobre a migração de ilhas barreira na região da Lagoa da Conceição, Ilha de Santa Catarina. *Anais I Congresso Associação Brasileira para Estudos do Quaternário*, Porto Alegre, RS, July 6-12, pp.277-295.
- Gornitz, V., 1991. Global coastal hazards from future sea level Rise. *Palaeogeography, Palaeoclimatology, Palaeoecology* 89, 379-398.
- Gornitz, V., 1995. Sea-level RSC: a review of recent past and near future trends. *Earth Surface Processes and Landforms* 20, 7-20.
- Grimm, E.C., 1987. Coniss: a Fortran 77 program for stratigraphically constrained cluster analysis by the method of the incremental sum of squares. *Computer and Geosciences* 13, 13-35.
- Grindrod, J., Rhodes, E.G., 1984. Holocene sea-level history of a tropical estuary: Missionary Bay, North Queensland. In: Thom, B. G. (ed.), *Coastal Geomorphology in Australia*. New York: Academic Press, pp. 151-178.
- Gusmão, L.A.B., Cassar, J.C.M., Neves, C.F., 1993. The Northern Coast of the State of Rio de Janeiro. *Proceedings Coastal Zone 93*, New York: American Society of Civil Engineers, pp.106-120.
- Herrera, L.F., Urrego, L.E., 1996. Atlas de polen de plantas úteis y cultivadas de la Amazonia colombiana (Pollen atlas of useful and cultivated plants in the Colombian Amazon region). *Estudios en la Amazonia Colombiana*, XI. Tropenbos-Colombia, Bogota, pp. 462.
- Heusser, C., 1961. Some comparisons between climatic changes in northwestern North America and Patagonia. *Annals of the New York Academy of Sciences* 95, 642-757.
- Hurtado, M., Dillon, A., Castillo, R., 1985. Incidencia de factores pedogenéticos en suelos del partido de Carlos Tejedor. 1º *Jornal Geology Province Buenos Aires Actas*, 23-35.
- IPCC (Intergovernmental Panel on Climate Change), 1996. *Second Assessment Report: Climate change: The Science of Climate Change*. Cambridge University Press, Cambridge, UK.
- Iriondo, M., Kröhling, D., 1995. El Sistema Eólico Pampeano. *Com. Museo Prov. Ciências Naturales* 5, 1-80.
- Iriondo, M., 1999. Climatic changes in the South American plains: Records of a continent-scale oscillation. *Quaternary International* 57/58, 93-112.

- Jackson, M.J., Woodsford, P.A., 1991. GIS data capture hardware and software. In: Maguire, D.J., Goodchild, M. and Rhind, D. (eds.), *Geographical Information Systems: Principles and Applications*. Longman, London 1, 239-249.
- Jenson, S.K., Dominguez, J.O., 1988. Extracting topographic structure from digital elevation data for geographic information system analysis. *Photogrammetric Engineering and Remote Sensing* 54, 1593-1600.
- Jennings, J.N., 1975. Desert dunes and estuarine fill in the Fitzroy estuary, north-western Australia. *Catena* 2, 215-262.
- Jennings, J.N., Coventry, R.J., 1973. Structure and texture of a gravelly barrier island in the Fitzroy Estuary, Western Australia, and the role of mangroves in the shore dynamics. *Marine Geology* 15, 145-167.
- Kaye, C.A., Barghoorn, E.S., 1964. Late Quaternary sea-level change and crustal rise at Boston, Mass., with notes on the autocompaction of peat. *Geology Society Bulletin* 75, 63-80.
- Kjerfve, B., Lacerda, L.D., 1993. Mangroves of Brazil. In: *Conservation and Sustainable Utilization of mangrove Forests in Latin America and Africa Regions. Part I - Latin America*. L. D. Lacerda (ed.). ITTO/International Society for Mangrove Ecosystems. Okinawa, Japan, pp. 245-272.
- Kogan, F.N., 2000. Satellite observed sensitivity of world land ecosystems to El Niño/La Niña. *Remote Sensing Environment* 74, 445-462.
- Lara, R.J., Dittmar, T., 1999. Nutrient dynamics in a mangrove creek (North Brazil) during the dry season. *Mangroves and Salt Marshes* 3, 185-195.
- Larcomb, P., Carter, R.M., Dye, J., Gagan, M.K., Johnson, D.P., 1995. New evidence for episodic post-glacial sea-level rise, central Great Barrier Reef, *Australian Marine Geology* 127, 1-44.
- Lean, J., Rind, D., 1999. Evaluating sun-climate relationships since the Little Ice Age. *Journal of Atmospheric and Solar Terrestrial Physics* 61, 25-36.
- Loon, H., Kidson, J.W., Mullan, A.B., 1993. Decadal variation of the annual cycle in the Australian dataset. *Journal Climate* 6, 1227-1231.
- Luckman, B.H., 2000. The Little Ice Age in the Canadian Rockies. *Geomorphology* 32, 357-384.
- Lugo, A.E., Snedaker, S.C., 1974. The ecology of mangroves. *Annual Review of Ecology and Systematics* 5, 39-64.
- Maine, M.A., Hammerly, J.A., Leguizamon, M.S., Pizarro, M.J., 1992. Influence of the pH and redox potential on phosphate activity in the Paraná Medio system. *Hydrobiologia* 228, 83-90.
- Malagnino, E. D., Strelin, J., 1996. Oscilaciones del englazamiento en el brazo Norte del Lago Argentino y península Herminita desde el Holoceno Tardío hasta la actualidad. XIII Congr. Geol. Arg., Actas IV, pp. 290-308.
- Mandelbrot, B.B., 1982. *The Fractal Geometry of Nature*. Freeman, San Francisco.
- Martin, L., Suguio, K., Flexor, J.M., Azevedo, A.E.G., 1988. Mapa geológico do quaternário costeiro dos estados do Paraná e Santa Catarina. *Série Geologia* 28, Seção Geologia Básica 18, 1-40.
- Martin, L., Flexor, J.M., Boas, G.S.V., Bittencourt, A.C.S.P., Guimaraes, M.M.M., 1979. Courbe de variation du niveau relatif de la mer au cours des 7000 dernières années sur un secteur homogène du littoral brésilien nord de Salvador- Bahia. *International Symposium on Coastal Evolution in the Quaternary, Sao Paulo, 1978. Proceedings, Sao Paulo, IGCP Project 61, Instituto de Geociencias, Universidade de Sao Paulo*, pp. 296-331.

- Martin, L., Suguio, K., 1978. Excursion rout along the coastline between the town of Cananéia (state of São Paulo) and Guaratiba outlet (state of Rio de Janeiro). Int. Symp. on Coastal Evolution, São Paulo, 1978. Spec. Publ. No. 2, São Paulo, IG, USP, SBG, 98 p.
- Menezes, M.P.M., 1997. Mecanismo de pollinisation du palétuvier, *Rhizophora mangle*, dans des mangroves en Amazonie, Brésil. Masters thesis, Université du Quebec Montreal, Canada, pp 127.
- Mesquita, A.R., Harari, J., 1983. Tides and tide gauges of Ubatuba and Cananéia. Relatório Instituto Oceanográfico. Universidade de São Paulo, pp. 225.
- Mesquita, A.R., Leite J.B.A., 1985. Sobre a variabilidade do nível médio do mar na costa sudeste do Brasil. I Encontro Regional de Geofísica, São José dos Campos, pp. 27-29.
- Mildenhall, D.C., Brown, L.J., 1987. An early Holocene occurrence of the mangrove *Avicennia marina* in Poverty Bay, North Island, New Zealand: Its climatic and geological implications. *Journal Botanic* 25, 281-294.
- Molodkov, A.N., Bolikhovskaya, N.S., 2002. Eustatic sea-level and climate changes over the last 600 ka as derived from mollusk-based ERS-chronostratigraphy and pollen evidence in Northern Eurasia. *Sedimentary Geology* 150, 185-201.
- Mörner, N.-A., 1996. Global change and interaction of earth rotation, ocean circulation and paleoclimate. *Anais da Academia Brasileira de Ciências* 68, 77-94.
- Mörner, N.-A., 1999. Sea level and climate: rapid regressions at local warm phases. *Quaternary International* 60, 75-82.
- Muehe, D., Caruso Jr., F., 1989. Batimetria e algumas considerações sobre a evolução geológica da Lagoa da Conceição, Ilha de Santa Catarina. *Geosul*, 7, 32-44.
- Muehe, D., Correa, C.H.T., 1989. The coastline between Rio de Janeiro and Cabo Frio. In: Neves, C.F. and Magoon, O.T. (eds.), *Coastline of Brazil*. New York: American Society of Civil Engineers, pp.110-123.
- Muehe, D., Neves, C.F., 1995. The implications of Sea-level Rise on the Brazilian Coast: A Preliminary Assessment. *Journal of Coastal Research* 14, 54-78
- Muehe, D., Neves, C.F., 1990. Potential impacts of sea-level rise on the coast of Brazil. In: *Changing climate and the coast*, U. S. Environmental Protection Agency, (Titus, J.G. ed.). Washington D.C., pp. 311-340.
- Nittrouer, C. A., Kuehl, S.A., Rhine, J.M., Figueiredo, A.G., Faria. L.E.C., Dias, G.T.M., Silva, M.A.M., Allison, M.A., Pacioni, T.D., Segall, M.P., Underkoffler, E.C., Borges, H.V., 1991. Sedimentology and stratigraphy of the Amazon continental shelf. *Oceanography* 25, 33-38.
- Oerlemans, J., 2001. *Glaciers and Climate Change*. Library of Congress Cataloging-in-Publication Data, pp.123.
- Pernetta, J.C., 1993. Mangrove forests, climate change and sea-level rise: hydrological influences on community structure and survival, with examples from the Indo-West Pacific. A Marine Conservation and Development Report. IUCN, Gland (Switzerland), 46 pp.
- Peuquet, D.J., 1984. A conceptual framework and comparison of spatial data models. *Cartographica* 21, 66-113.
- Pethick, J., 2001. Coastal management and sea-level rise. *Catena* 42, 307-322.
- Pirazolli, P.A., 1986. Secular trends of relative sea levels (RSL) changes indicated by tide-gauge records. *Journal of Coastal Research*, Special Issue 1, 1-26.
- Pirazolli, P.A., 1988. Sea-level correlations: applying IGCP results. *Episodes* 11, 111-116.

- Plang, H.P., Tsimplis, M.N., 1999. Temporal variability of the seasonal sea-level cycle in the North Sea and Baltic Sea in relation to climate variability. *Global and Planetary Change* 20, 173-203.
- Politis, G., 1984. Climatic variations during historical times in eastern Buenos Aires Pampas, Argentina. *Quaternary of South America and Antarctic Peninsula* 2, 133-161.
- Price, W.A., 1955. Environment and formation of the chenier plain. *Quaternaria* 2, 75-86.
- Prost, M.T., Lintier, M., Barthes, B., 1988. Evolution cotière en Guyane Française: la zone de Sinnamary. *Congresso Brasileiro de Geologia e 7 Congresso Latinoamericano de Geologia, Abstracts, Belém, Brazil*, pp. 406-407.
- Rademacher, V., 1998. Ernährungsökologie, habitatbeschreibung und populationsstruktur der mangrovenkrabbe *Ucides cordatus*(Linnaeus, 1763) im Caeté-mangrovenästuar, Nordbrasilien. Diplomarbeit, Universität Bremen/ZMT.
- Redfield, A.C., 1972. Development of a New England salt marsh. *Ecological Monographs* 42, 210-237.
- Reineck, H. E., Wunderlich, H. G., 1967. A new method to measure rate of deposition of single lamina on tidal flats and shelf bottoms. *7th International Sedimentological Congress (abstract)*, pp.32.
- Reineck, H. E., Wunderlich, H. G., 1968. Classification and origin of flaser and lenticular bedding. *Sedimentology* 11, 99-104.
- Röthlisberger, F., Hass, P., Holzhauser, H., Keller, W., Bircher, W., Renner, F., 1980. "Holocene climatic fluctuations – radiocarbon dating of fossil soils (fAh) and woods from moraines and glaciers in the Alps", in *Geography in Switzerland, Geographica Helvetica* 35, 21-52.
- Roubik, D.W., Moreno, J.E., 1991. Pollen and Spores of Barro Colorado Island. *Missouri Botanical Garden, St. Louis*. 36, pp.268.
- Rock-Color Chart Committee. 1984. Rock-color chart. Netherlands, Huyskes-Enschade.
- Rossetti, D.F., Truckenbrodt, W., Góes, A.M., 1989. Estudo paleoambiental e estratigráfico dos sedimentos barreiras e Pós-Barreiras na Região Bragantina, Nordeste do Pará. *Boletim do Museu Paraense Emílio Goeldi* 1, 25-74.
- Salomons, W., Gerritse, R.G., 1981. Some observations on the occurrence of phosphorus in recent sediments from Western Europe. *Science Total Environmental* 17, 37-49.
- Santos, J.V.M., Rosário, C. S., 1988. Levantamento da vegetação fixadora das dunas de Algodual-PA. *Boletim do Museu Paraense Emílio Goeldi (Sér. Bot.)* 4, 133-154.
- Santos, M.C.F.V., Zieman, J.C., Cohen, R.R.H. 1997. Interpreting the upper mid-littoral zonation patterns of mangroves in Maranhão (Brazil) in response to microtopography and hidrology. In: Kjerfve, B., Lacerda, L. D. and Diop, El Hadji (eds.). *Mangroves Ecosystem studies in Latin America and Africa*. pp.127-144.
- Scholl, D.W., 1964. Recent Sedimentary Record in Mangrove Swamps and Rise in Sea Level Over the Southwestern Coast of Florida: Part 1. *Marine Geology* 1, 344-366.
- Scholl, D.W., Stuiver, A., 1967. Recent submergence of southern Florida: A comparison with adjacent coasts and other eustatic data. *Geological Society of America Bulletin* 78, 437-454.
- Schwendenmann, L., 1998. Tidal and seasonal variations of soil and water properties in a Brazilian mangrove ecosystem. M.Sc. Thesis, University of Karlsruhe, pp.138.
- Semeniuk, V., 1980. Mangrove zonation along an eroding coastline in King Sound, North-western Australia. *Journal of Ecology* 68, 789-812.
- Semeniuk, V., 1981. Long-term erosion of the tidal flats, King Sound, North-western Australia, *Marine Geology* 43, 21-48.

- Semeniuk, V., 1996. Coastal form and Quaternary process along the arid Pilbara coast of northwestern Australia. *Palaeogeography, Palaeoclimatology, Palaeoecology* 123, 49-84.
- Shackleton, N.J., Opdyke, N.D., 1973. Oxygen isotope and paleomagnetic stratigraphy of equatorial Pacific core V 28-238: Oxygen isotope temperatures and ice volumes on a 105 and 106 year scale. *Quaternary Research* 3, 39-55.
- Shennan, I., 1989. Late Quaternary Sea-level changes: measurement, correlation, and future applications the international significance of IGCP Project 200. *Journal Quaternary Science* 4, 3-5.
- Shulmeister, J., 1999. Australasian evidence for mid-holocene climate change implies precessional control of Walker Circulation in the Pacific. *Quaternary International* 57/58, 81-91.
- Silva, G.N., 1992. *Variação do Nível Médio do Mar: Causas Causas, Consequências e Metodologia de Análise*. M.Sc. Thesis. Programa de Engenharia Oceânica, COOPE. Universidade Federal do Rio de Janeiro, pp.93.
- Silva, G.N. Neves, C.F., 1991. *Variação do nível médio do mar na Ilha Fiscal entre 1965-1986*. Anais IX Simpósio Brasileiro de Recursos Hídricos e 5º Simpósio Brasileiro de Hidráulica e Recursos Hídricos, November 11-14,1991, Rio de Janeiro. Brazilian Water Resources Association (ABRH) 3, 568-577.
- Silva, C.A.R., Sampaio, L.S., 1998. Speciation of phosphorus in a tidal floodplain forest in the Amazon estuary. *Mangroves and Salt Marshes* 2, 51-57.
- Slavich, P.G., Walker, G.R., Jolly, I.D., 1999. A flood history weighted index of average root-zone salinity for assessing flood impacts on health of vegetation on a saline floodplain. *Agriculture Water Management* 39, 135-151.
- Snedaker., 1978. Mangroves: their value and perpetuation. *Nature Resource* 14, 6-13.
- Snedaker, S.C., 1993. Impact on mangroves. In: G.A. Maul (ed.), *Climatic change in the Intra-Americas Sea*. Edward Arnold, London, pp. 282-305
- Sommenfield, P., 1984. *Briness and Evaporites*. Academic Press, London, 613 pp.
- Sommerfield, K.C., Nittrouer, C.A., Figueiredo., 1995. Stratigraphic evidence of changes in Amazon shelf sedimentation during the late Holocene. *Marine Geology* 125, 351-371.
- Souza Filho, P.W.M., El-Robrini, M., 1996. Morfologia, processos de sedimentação e litofácies dos ambientes morfo-sedimentares da planície costeira bragantina, nordeste do Pará, Brasil. *Geonomos* 4, 1-16.
- Souza Filho, P.W.M., 1995. *A planície costeira bragantina (NE do Pará): Influência das variações do nível do mar na Morfoestratigrafia costeira durante o Holoceno*. Federal University of Pará. Center of Geosciences. *Geology and Geochemistry Course*. Master Thesis, pp. 123.
- Souza Filho, P.W.M., El-Robrini, M., 1998. As variações de nível relativo do mar e a estratigrafia de seqüências da Planície Costeira Bragantina, Nordeste do Pará, Brasil. *Boletim Museu Paraense Emílio Goeldi, Ciências da Terra* 10, 45-78.
- Spenceley, A.P., 1976. Unvegetated saline tidal flats in norrrth Queensland. *Journal Tropical Geography* 42, 78-85.
- Star, J.L., Estes, J.E., 1990. *Geographic Information Systems: An Introduction*. Prentice Hall, Englewood Cliffs, NJ, pp. 220.
- Suguió, K., Martin, L., Bittencourt, A.C.S.P, dominguez, J.M.L, Flexor, J.M., Azevedo, A.E.G., 1985. Flutuações do Nível do Mar durante o Quaternário Superior ao longo do Litoral Brasileiro e suas Implicações na Sedimentação Costeira. *Revista Brasileira de Geociências* 15, 273-286.

- Suguio, K., Martin, L., 1978. Quaternary marine Formations on the States of São Paulo and southern Rio de Janeiro. In: International Symposium on Coastal Evolution in the Quaternary, São Paulo, Spec. Publ. 1, São Paulo, IGPC, Project 61, pp. 55.
- Suguio, K., Martin, L., Flexor, J.M., 1980. Sea level fluctuations during the past 6000 years along the coast of the state of São Paulo, Brzil. In: Mörner, N.A.(Ed.), Earth reology, isostasy and eustasy. Chichester, Wiley, pp. 471-486.
- Sylla, M., Stein, A., van Breemen, N., Fresco, L.O., 1995. Spatial variability of soil salinity at different scales in the mangrove rice agro-ecosystem in West Africa. *Agriculture Ecosystems and Environment* 54, 1-15.
- Szlafsztein, C., Lara, R.J., Cohen, M.C.L., 2000. Coastal Management: some studies of the past and present of the Bragança region (Pará, Brazil). The MADAM project. *Journal of International Environmental Creation* 2, 132-139.
- Thompson, D.J., 1995. The seasons, global temperature, and precession. *Science* 268, 59-68.
- Thüllen, N., Berger, U., 2000. A comparative examination of environmental factors at patchy mangrove seedling stands on the peninsula of Bragança, northern Brazil *Ecotropica* 6, 1-12.
- Titus, J.G., Narayanan, V.K., 1995. The probability of sea level rise. United States Environmental Protection Agency, Office of Policy, Planning, and Evaluation (2122), EPA 230-R-95-008, Washington, DC, pp. 186.
- Tomazelli, L.J., 1990. Contribuição ao estudo dos sistemas deposicionais holocênicos do Nordeste da Província Costeira do Rio Grande do Sul, com ênfase no sistema eólico, PhD Thesis. Porto Alegre, Universidade Federal do Rio Grande do Sul, pp. 270.
- Tomlinson, P.B., 1986. *The Botany of Mangroves*. Cambridge Univ. Press, pp. 413.
- Townsend, P.A., Walsh, S.J., 1998. Modeling floodplain inundation using an integrated GIS with radar and optical remote sensing. *Geomorphology* 21, 295-312.
- Trauth, M.H., Alonso, R.A., Haselton, K.R., Hermanns, R.L., Strecker, M.R., 2000. Climate change and mass movements in the NW Argentine Andes. *Earth and Planetary Science Letters* 179, 243-256.
- Van der Hammen, T., 1986. Fluctuaciones holocénicas del nivel de inundaciones en la cuenca del Bajo Magdalena Cauca-San Jorge (Colombia). *Geología Norandina* 10, 11-18.
- Van de Plassche, O., 1986. Sea level research: A manual for the collection and evaluation of data. *Geobooks Norwich*, 615 pp.
- Vegas Vilarrúbia, T., 2000. Zonation pattern of an isolated mangrove community at Playa Medina, Venezuela. *Wetlands Ecology and Management* 8, 9-17.
- Vetter, R.E., Botosso, P.C. 1989. El Niño may affect growth behaviour of Amazonian trees. *GeoJournal* 19, 419-421.
- Vital, H., Statterger, K., 2000. Lowermost Amazon River: evidence of late Quaternary sea-level fluctuations in a complex hydrodynamic system. *Quaternary International* 72, 53-60.
- Walter, H., Lieth, H., 1967. *Klimadiagramm-Weltatlas*. Gustav Fischer, Jena.
- Weng, C., Bush, M.B., Athens, J.S., 2002. Holocene climate change and hydrarch succession in lowland Amazonian Ecuador. *Review of Palaeobotany and Palynology* 120, 73-90.
- Woodroffe, C.D., 1981. Mangrove swamp stratigraphy and Holocene transgression, Grand Cayman Island, West Indies. *Marine Geology* 41, 271-294.
- Woodroffe, C.D., 1982. Geomorphology and development of mangrove swamps, Grand Cayman Island, West Indies. *Bulletin Marine Science* 32, 381-398.

- Woodroffe, C.D., Chappell, J., Thom, B.G., Wallensky, E., 1986. Geomorphological dynamics and evolution of the South Alligator River and Plains, Northern Territory. Australia National University, North Australia Research Unit. Mangrove Monograph, pp. 190.
- Woodroffe, C.D., Thom, B.G., Chappell, J., Wallensky, E., Grindrod, J., Head, J., 1987. Relative sea-level in South Alligator River Region, North Australia, during the Holocene. *Search*, 18, 198-200.
- Woodroffe, C.D., Chappell, J., Thom, B.G., Wallensky, E., 1989. Depositional model of a macrotidal estuary and floodplains, South Alligator River, Northern Australia. *Sedimentology* 36, 737-756.
- Woodroffe, C., 1992. Mangrove sediments and geomorphology. In: *Tropical Mangrove Ecosystems, Coastal and Estuarine Studies*, (A.I. Robertson and D.M. Alongi, eds.). American Geophysical Union, Washington DC 41, 7-43.
- Woodroffe, C.D., Mulrennan, M.E., Chappell, J., 1993. Estuarine infill and coastal progradation, southern van Diemen Gulf, northern Australia. *Sedimentary Geology* 83, 257-275.
- Woodroffe, C.D., Mulrennan, M.E., Chappell, J., 1993. Estuarine infill and coastal progradation, southern van Diemen Gulf, Northern Australia *Sedimentary Geology* 83, 257-275.